Coordinated Control and Spectrum Management for 5G Heterogeneous Radio Access Networks

Grant Agreement No. : 671639

Call: H2020-ICT-2014-2

Deliverable D4.2

Final report on flexible spectrum management

Version:	8
Due date:	30.11.2017
Delivered date:	13.12.2017
Dissemination level:	PU

The project is co-funded by

Authors

Adrian Kliks (Editor-in-Chief), Bartosz Bossy, Łukasz Kułacz, Paweł Kryszkiewicz, Hanna Bogucka (PUT), Tapio Suihko, Miia Mustonen, Tao Chen, (VTT); Shah Nawaz Khan, Roberto Riggio, Leonardo Goratti (CNET); Sergio Lembo, Sewda Biza, Olav Tirkkonen (AALTO); Karol Kowalik, Michał Kołodziejski (INEA); Heikki Kokkinen, Jaakko Ojaniemi, Arto Kivinen (FS)

Coordinator

Dr. Tao Chen

VTT Technical Research Centre of Finland Ltd
Tietotie 3
02150, Espoo
Finland
Email: tao.chen@vtt.fi

Disclaimer

Acknowledgement

This report is funded under the EC H2020 5G-PPP project COHERENT, Grant Agreement No. 671639.

Version history

Version	Date	Remarks
1	04.07.2017	First version of ToC was created.
2	04.10.2017	First contribution included; report showed at the project meeting
3	20.10.2017	First complete report released to WP4
4	27.10.2017	Second version of the complete report released to WP4
5	03.11.2017	Third complete version send to WP4 partners
6	30.11.2017	First pre-complete version after Review
7	08.12.2017	Final version sent for last check before submission to EC/PO
8	13.12.2017	Final version submitted to PO

Executive Summary

The work within the WP4 of the COHERENT project was focused on development of new solutions for flexible spectrum sharing and management, particularly considering their application in virtualized wireless networks. Practical realization of the virtualization concept in the context of radio access networks must take into account various limitations and restrictions originated from the spectrum management domain. As the key goal of the Work Package was to concentrate the work around the effective spectrum utilization and management in a virtualized scenario, other WP4 targets pointed the need for development of new spectrum sharing paradigms for future wireless networks. This document is the final report of WP4, which presents the overall results achieved during the second part of the COHERENT project in the field of flexible spectrum management. In particular, it includes new findings on various spectrum sharing schemes like Licensed Shared Access (LSA) and Licensed Assisted Access (LAA), intra- and inter-operator spectrum management, FDD flexible duplexing, and the algorithms for the spectrum coordinator.

The whole research work in WP4 was built on four pillars as graphically presented in Figure 1. The first one is constituted by the investigation of the final architecture for flexible spectrum management as part of the COHERENT architecture and as the prospective solution for future wireless networks. The second pillar contains the discussion on the framework for spectrum abstraction as the basis for SDK implementation. The third pillar is formed by the rich set of research achievements in the field of spectrum management and sharing, conducted simultaneously in parallel but with association to the proposed spectrum management architecture. Finally, the last fourth one represents the effort on trials and experimental works on flexible spectrum management. Thus, this document is split logically into four parts corresponding to those four pillars.

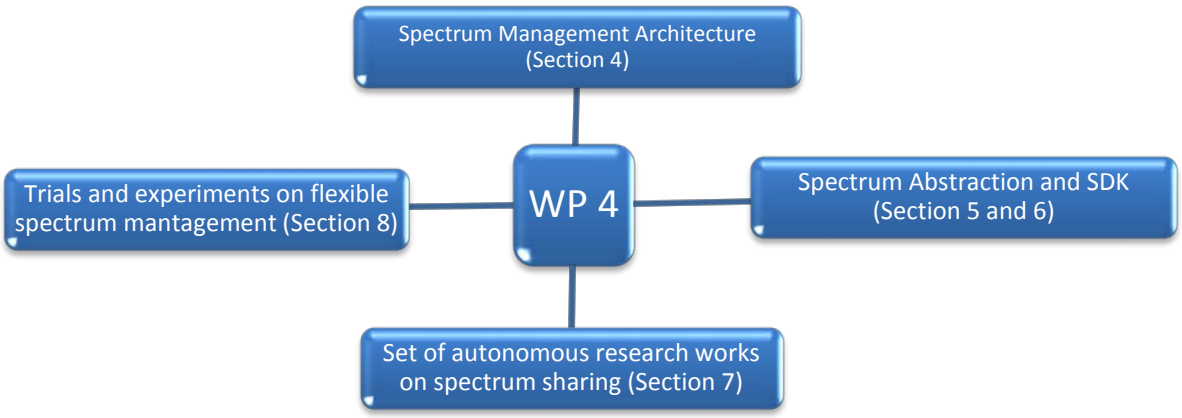

Figure 1. Four research pillars of WP4

In the **first logical part** of the deliverable (consisting of Sections from 2 to 4, and corresponding the first pillar of WP4), we discuss the recent advances in spectrum management in the context of 5G networks and provide the final COHERENT proposal for spectrum management architecture. Thus, we have started with a short recap on WP4 findings with regard to the most promising spectrum sharing strategies. Next, we discuss the recent decision towards definition of the so-called pioneering bands for 5G networks. After that we overview the most significant regulatory decisions and standardization activities which are related to spectrum management. These sections reveal that flexible access to the spectrum is being more and more considered as the reliable solution for future use; the regulatory decisions seem to open wider the doors for dynamic spectrum utilization in the upcoming years. Once the regulatory and standardization aspects are summarized, we provide the final COHERENT vision on the spectrum management architecture for the highly virtualized wireless communication systems. It has been identified that the entire spectrum management functionality may be realized by means of the Spectrum Management Application (being part of the Service Plane) and the Central Coordinator and Controller (C3) entity, controlling the underlying hardware. Based on that, a method of creation of

the annotated spectrum management network graphs (or policy-graphs) has been proposed and the ways how the policies may be represented have been discussed.

In the **second logical part** of this document (consisting of Sections 5 and 6, and corresponding the second pillar of WP4), the discussion on the framework for low-layer abstraction for spectrum sharing is conducted. It starts from the analysis of the existing ways for communicating spectrum availability and is followed by an overview of the requirements for low-layer abstraction in spectrum sharing and management. Once the way of abstracting the spectrum is presented, the discussion on north-, south- and east/west-bound flows is performed jointly with the identification of key programming aspects concerning flexible spectrum management. As the result of this discussion, the system level simulation model is presented.

The **third logical part** of the document (corresponding the third pillar of WP4) is constituted by the set of various research activities undertaken with reference to spectrum management architecture. The results of this research effort are collected and presented in a unified form in Section 7 – each subsection starts with a short lead where the key goals of the investigation are provided jointly with the mapping to the entities of the spectrum management architecture. Several research topics have been considered, as listed below:

- *Inter-tier resource allocation problem for HetNets* – where the problem of sharing frequency resources in the context of intra-operator spectrum sharing was verified.
- *Fine-Grained Spectrum Sharing in Multi-Tenant RAN* – where the spectrum management architecture to enable very fine-grained time and frequency domain spectrum sharing was tested. A multi-tenant RAN scenario is considered.
- *Fine-Grained Scheduling of Co-Primary Shared Spectrum* – it is the continuation of the previous work towards co-primary spectrum sharing with emphasis on scheduling policies for the common/shared radio resources.
- *Management of coexistence between LTE and Wi-Fi in unlicensed bands* – here the goal was to study the possibilities of enabling an improved coexistence between LTE and Wi-Fi networks when operating over the 5 GHz unlicensed band by means of the COHERENT SMA and C3.
- *Location-Based Spectrum Sharing* – where a coordination protocol for co-primary spectrum sharing between coexisting mobile network operators is investigated.
- *FDD Flexible duplexing* – in this section the guideline to determine the downlink transmit power of a FDD flexible duplexing cell is presented.
- *Multi-user simultaneous flexible duplexing* – where the idea was to consider simultaneous FDD flexible duplexing in multi-user scenario.
- *Multi-User Small-Scale Spectrum Aggregation* – where the concept of small-scale spectrum aggregation (where the leased spectrum may have a width of several subcarriers) is discussed and investigated in single-user and multi-user scenarios.

The last, fourth pillar of WP4 is formed by the practical implementation and verification of certain flexible spectrum management algorithms, and is presented in the **last logical part** of this document (see Section 8). In this context, two evaluation platforms have been used, OpenAirInterface by EURECOM and EmPOWER by CNET. In WP4, the possibilities of implementation of the spectrum management application on these platforms have been verified and the set of routines have been prepared constituting the SDK for flexible spectrum management. Finally, one of the key undertaken activities was the preparation and execution of the spectrum trials, where the proposed advanced flexible spectrum management techniques have been tested on real wireless networks. Initial laboratory experiments have been followed by field trials and drive tests, where three networks (access technologies) have been controlled in a softwerized way by means of the dedicated databases. These spectrum trials have proved the great possibilities opened by an elastic approach of spectrum access and utilization.

List of Abbreviations

3GPP	3rd Generation Partnership Project
ACLR	Adjacent Channel Leakage power Ratio
ACI	Adjacent Channel Interference
ACIR	Adjacent Channel Interference Ratio
ACS	Adjacent Channel Selectivity
AI	Agenda Item
AMBR	Aggregate Maximum Bit Rate
ANDSF	Access Network Discovery and Selection Function
API	Application Programming Interface
BEREC	Body of European Regulators for Electronic Communications
BRS	Broadband Radio Service
BS	Base Station
C3	Central Coordinator and Controller
CBRS	Citizen Broadband Radio Service
CBSD	Citizens Broadband radio Service Devices
CC	Carrier components
CCA	Clear Channel Assessment *and* Combinatorial Clock Auction
CDF	Cumulative Distribution Function
CEPT	Conférence européenne des administrations des postes et des télécommunications (European Conference of Postal and Telecommunications Administrations)
CPE	Customer Premises Equipment
CQI	Channel Quality Indicator
CSG	Closed Subscriber Group
CRE	Cell Range Extension
CUS	Collective Use of Spectrum
DA-RR	Demand Aware Round Robin
D2D	Device to Device
DL	Downlink
DSM	Digital Single Market
EBI	East Bound Interface
EC	European Commission
ECC	Electronic Communications Committee
ED	Energy Detection
EIRP	Equivalent/Effective Isotropic Radiated Power
eMBB	enhanced Mobile BroadBand
eNodeB	evolved Node B
eNB	evolved Node B

EPC	Evolved Packet Core
ESC	Environmental Sensing Capability
ETSI	European Telecommunications Standards Institute
E-UTRA	Evolved UMTS Terrestrial Radio Access
FAP	Femtocell Access Points
FCC	Federal Communications Commission
FD	Flexible Duplexing
FDD	Frequency Division Duplex
GAA	General Authorized Access
GBR	Guaranteed Bit Rate
HetNet	Heterogeneous Network
HMN	Heterogeneous Mobile Network
ICT	Information and Communications Technologies
IEEE	Institute of Electrical and Electronics Engineers
IMT	International Mobile Telecommunications
ISD	Inter-Site Distance
ISM	Industrial, Scientific and Medical
ITS	Intelligent Transport System
ITU	International Telecommunications Union
ITU-R	ITU Radiocommunication Sector
LA-RR	Load-Aware Round Robin
LAA	Licensed Assisted Access
LBT	Listen Before Talk
LC	LSA Controller
LPWAN	Low-Power Wide-Area Network
LR	LSA Repository
LSRAI	Spectrum Resource Availability Information
LSA	Licensed Shared Access
LTE	Long Term Evolution
LTE-A	LTE Advanced
LTE-U	LTE in Unlicensed Spectrum
MAC	Medium Access Control
MCS	Modulation and Coding Scheme
MFCN	Mobile/Fixed Communications Networks
MNO	Mobile Network Operator
MTC	Machine-Type Communications
MVNO	Mobile Virtual Network Operator
NBI	North Bound Interface

NC-FBMC	Non-Contiguous FilterBank MultiCarrier
NC-MC	Non-Contiguous Multicarrier
NC-OFDM	Non-Contiguous Orthogonal Frequency Division Multiplexing
NED	**N**etwork Modelling Language
NFV	Network Functions Virtualisation
NRA	National Regulatory Authority
OAI	OpenAirInterface
OoB	Out of Band
OoBE	Out of Band Emission
PAL	Priority Access License *or* Phase Alternate Line
PAWS	Protocol to Access White-Space Databases
PFD	Power Flux Density
PHY	Physical
PL	Pluralistic Licensing
PL-RR	Pre-emptive Load Aware Round Robin
PR	Physical Resource
PRB	Physical Resource Block
PT	Project Team
PU	Primary User
PUCCH	Physical Uplink Control Channel
PUSCH	Physical Uplink Shared Channel
QCI	QoS Class Identifier
QoS	Quality of Service
RB	Resource Block
RAN	Radio Access Network
RAT	Radio Access Technology
REM	Radio Environment Map
RLAN	Radio Local Area Networks
RRM	Radio Resource Management
RSPG	Radio Spectrum Policy Group
RSSI	Received Signal Strength Indicator
RT	Radio Transceiver
RTC	Real Time Controller
SAS	Spectrum Access System
SBI	Southbound Interface
SCM	Spectrum Consumption Models
SDK	Software Development Kit
SDN	Software Defined Network

SDR	Software Defined Radio
SLA	Service Level Agreement
SMA	Spectrum Manager Application
SINR	Signal to Interference plus Noise Ratio
SM	Spectrum Management/Manager
SQL	Structured Query Language
SSA-ST	Shared Spectrum Access for Similar Technologies
SU	Secondary User
TDD	Time Division Duplex
TR	Technical Report
TTI	Transmit Time Interval
TVWS	TeleVision White Space
UE	User Equipment
UHF	Ultra-High Frequency
UL	UpLink
UMTS	Universal Mobile Telecommunications System
URC	Ultra-Reliable Communication
VMNO	Virtual Mobile Network Operator
VoIP	Voice over IP
WRC	World Radiocommunication conference
WiMAX	Worldwide Interoperability for Microwave Access

Table of Contents

List of Figures

List of Tables

1. Introduction

Flexible yet effective spectrum management is one of the promising key enablers for the success of 5G networks. The benefits that can be achieved by dense deployment of Heterogeneous Mobile Networks (HMNs) in 5G networks can be further enhanced by advanced spectrum sharing.

Given that the spectrum is allocated to different operators, and also due to the very high deployment density, the classical coexistence solutions within the licensed as well as unlicensed spectrum may not provide required isolation anymore. Also, classical approaches based on orthogonal spectrum sharing among operators in licensed bands may be inefficient in small-cell scenarios with changing numbers of users, variable area coverage of operators, and variable load. A new vision for spectrum utilization is required. It is then worth noticing that - similarly to previous cellular system generations - also the 5G network deals not only with new innovations in PHY/MAC layers, but also new spectrum sharing paradigms, together with efficient spectrum access techniques. Various approaches are possible as alternatives for licensed-only solutions, such as licensed shared access (LSA), license exempt, co-primary sharing, and pluralistic licensing, among others.

1.1. COHERENT Goals

The COHERENT project aims to design, develop and showcase a novel control framework for 5G heterogeneous mobile networks, which leverages the proper abstraction of physical and MAC layer in the network and a novel programmable control framework, to offer operators a powerful means to dynamically and efficiently control spectrum and radio network resources in their increasingly complex HMN.

COHERENT proposes proper abstractions of physical and MAC layer states, behaviours and functions in order to enable a centralized network view of the underlying radio networks with significantly reduced signalling overhead. The centralized network view with sufficient but abstracted information on spectrum, radio links, interference, network topology, load information, and physical layer reality is essential to enable optimal resource allocation in the network.

One of the key goals of the WP4 within the COHERENT project is to investigate the true benefits that can be gained by the network operator and end-users through the application of the wireless network virtualization concepts and based on the recent achievements in the area of radio-environment-map design, practical conclusions from cognitive radio, legal regulations and field experiments (e.g., [Monserrat_2015], [Kliks_2016], [Liang_2015_1], [Liang_2015_2]). In WP4, we envisage the application of an advanced spectrum management and coordination system, which provides tools for wireless network virtualization.

1.2. Document Structure and Relation with Other WPs in COHERENT

This document is Deliverable D4.2 “Final report on flexible spectrum management” for Work Package 4 “Flexible Spectrum Management”. It is split into four logical parts corresponding to four pillars of WP4. As already mentioned in the executive summary, the first one deals with the investigation of the final architecture for flexible spectrum management as part of the COHERENT architecture. The second pillar is constituted by the discussion on the framework for spectrum abstraction as the basis for SDK implementation. The third pillar is formed by the rich set of research achievements in the field of spectrum management and sharing. These research activities have been carried out simultaneously in parallel and have been realized with association to the proposed spectrum management architecture. The last, fourth pillar is represented by the work on trials and experimental works on flexible spectrum management. Following this approach, the report is structured as follows:

Introduction

- **Chapter 1** – it is the current chapter, it contains the introduction to this deliverable.

Logical part corresponding to the activities associated with first pillar:

- **Chapter 2** presents the recent advances in the spectrum management, and consists of three subchapters: first one is a summary of the discussion made in the first phase of WP4 in

COHERENT project, where the problem of identification of most promising spectrum sharing schemes was covered; second summarizes the latest agreements on the pioneering bands for 5G networks; and finally the third subchapter provides an update on the achievements made in other European Research Projects;

- **Chapter 3** overviews in a concise way the recent regulatory and standardization decisions related to spectrum management;
- **Chapter 4** provides the final structure of the spectrum management application being a part of the entire COHERENT architecture; moreover, it reflects the idea of policy network graph, which represents the specificity of the dynamic spectrum management.

Logical part corresponding to the activities associated with second pillar:

- **Chapter 5** reflects the outcomes on the investigation on dedicated framework for low-layer abstraction of spectrum related aspects of wireless networks; in particular it overviews existing interfaces for communicating spectrum-related data, it tackles the requirements for low layer abstraction and discusses the prospective spectrum management operations.
- **Chapter 6** is devoted for Software Development Kit (SDK) implementation; it also provides the guidelines for system level simulation model for analysing multi-tenant radio-access technologies and spectrum sharing.

Logical part corresponding to the activities associated with third pillar:

- **Chapter 7** presents in a concise form the key research activities undertaken during the project lifetime; it consists of 8 autonomous subchapters which deal with various spectrum sharing issues:
  - *Inter-tier resource allocation problem for HetNets* – where the problem of sharing frequency resources in the context of intra-operator spectrum sharing was verified.
  - *Fine-Grained Spectrum Sharing in Multi-Tenant RAN* – where the spectrum management architecture to enable very fine-grained time and frequency domain spectrum sharing was tested. A multi-tenant RAN scenario is considered.
  - *Fine-Grained Scheduling of Co-Primary Shared Spectrum* – it is the continuation of the previous work towards co-primary spectrum sharing with emphasis on scheduling policies for the common/shared radio resources.
  - *Management of coexistence between LTE and Wi-Fi in unlicensed bands* – here the goal was to study the possibilities of enabling an improved coexistence between LTE and Wi-Fi networks when operating over the 5 GHz unlicensed band by means of the COHERENT SMA and C3.
  - *Location-Based Spectrum Sharing* – where a coordination protocol for co-primary spectrum sharing between coexisting mobile network operators is investigated.
  - *FDD Flexible duplexing* – in this part the guideline to determine the downlink transmit power of a FDD flexible duplexing cell is presented.
  - *Multi-user simultaneous flexible duplexing* – where the idea was to consider simultaneous FDD flexible duplexing in multi-user scenario.
  - *Multi-User Small-Scale Spectrum Aggregation* – where the concept of small-scale spectrum aggregation (where the leased spectrum may have a width of several subcarriers) is discussed and investigated in single-user and multi-user scenarios.

Logical part corresponding to the activities associated with fourth pillar:

- **Chapter 8** provides the brief description of the considered evaluation platforms, as well as the way, how spectrum management can be included in final evaluation; moreover it constitutes the summary of the long-term trials performed during the lifetime of the project; the trials are the inter-WP activity which connects WP4 and WP6; in this report we deal with the input that WP4 provides to WP6 to perform the trials; the results from these trials will be examined in the final report of WP6.

Summary

- **Chapter 9** concludes the report.

1.3. Summary of Key Results Towards/From Other Activities

Although numerous joint activities have been undertaken during the whole project lifetime, let us identify the key-relation between the particular WPs.

1.3.1. Towards/From WP2

- Towards: Spectrum Management Application has been proposed and its position in the COHERENT architecture has been defined jointly with communication interfaces.

- From: WP2 has delivered the overall definition of the COHERENT architecture as well as numerous uses cases what allows the researchers in WP4 to define the role of spectrum management in the entire system

1.3.2. Towards/From WP3

- Towards: Methods for spectrum abstraction and virtualization have been proposed.

- Towards: The policy network graph has been identified which may be a part of the overall COHERENT network graph.

- From: WP3 has indicated the detailed ways of wireless network abstraction, what in turn allows for precise definition of network graphs applied for spectrum management.

1.3.3. Towards/From WP5 and WP6

- Towards: Spectrum Management Application has been developed in both experimentation platforms, OAI and EmPOWER.

- Towards: The overall setup and algorithms for the COHERENT spectrum trials have been defined.

- From: the work on SDK and hardware implementation done within WP5 and WP6 has defined the detailed guidelines for the research activities undertaken in WP4 from the perspective of practical application of the developed solutions.

1.3.4. Towards Standardization (WP7)

- COHERENT has submitted a contribution to ECC PT1 meeting from 12-16/09/2016 in Budapest. The contribution presented the simulation results on Flexible duplex, detailed in D4.1.

2. Recent Advances in Spectrum Management

2.1. Reminder on Identified Most Promising Spectrum Sharing Strategies

One of the key aspects covered by the COHERENT project lays in defining new ways for advanced and flexible spectrum management for future wireless networks, and in particular in the context of wireless network virtualization. Proposed generic model for spectrum management, its position in the whole COHERENT ecosystem, respective interfaces and communication methods, would be applicable for any considered spectrum sharing scheme.

For further detailed discussions, we have identified the following strategies:

1. The popularity of exclusive spectrum use and its counterpart - license exempt approach – will not decrease in the nearest future. Thus the traditional solutions will be considered as the reference.
2. From the European point of view, the selection of LSA is somehow natural mainly due to the popularity of such a solution in operators and service providers; on the other hand, the Spectrum Access System (SAS) solution is under practical tests now in US, thus it should not be neglected.
3. The Licensed Assisted Access (LAA) approach is gaining popularity, thus the coexistence of licensed and unlicensed services is envisaged.
4. An interesting option is the co-primary sharing scheme, as this approach gives new degrees of freedom for operators.

Clearly, from the perspective of real implementation, the above solutions can be applied in various contexts (e.g., for TV White Spaces (TVWS), or with the use of dedicated databases supported by sensing function), however we think that more flexible approaches to spectrum sharing (such as innovative pluralistic licensing or various cognitive radio oriented schemes) may require further investigation.

2.2. Update on the Pioneering Bands for 5G

The European Commission (EC) Radio Spectrum Policy Group (RSPG) released an opinion [RSPG_2016] about the 5G spectrum bands for Europe in November 2016. According to RSPG opinion, 5G will be deployed in bands already harmonized for International Mobile Telecommunications (IMT) below 1 GHz, especially in the 694-790 MHz band. 3.4-3.8 GHz is named as the primary band suitable for the introduction of 5G-based services in Europe. 24.25-27.5 GHz is selected as the pioneer band above 24 GHz is band. Further bands in the opinion paper identified for 5G are: 31.8-33.4 GHz and 40.5-43.5 GHz.

The main lines for 5G spectrum allocations are decided in the World Radio Conference (WRC) of the International Telecommunication Union (ITU) [JRC 5G]. The previous meeting was in Geneva in November 2015 and the next one will take place from October 28 to November 22 in 2019. In WRC-15, there was no change in respect to 470-694 MHz; a review will be considered in WRC-19. The frequency band 3.4-3.8 GHz was already harmonized in Europe under Radio Spectrum Decision [EU/2014/276] before WRC-15. The agenda item 1.13 of WRC-19 contains studies for the following frequency bands: 24.25-27.5 GHz, 31.8-33.4 GHz, 37-40.5 GHz, 40.5-42.5 GHz, 42.5-43.5 GHz, 45.5-47 GHz, 47-47.2 GHz, 47.2-50.2 GHz, 50.4-52.6 GHz, 66-71 GHz, 71-76 GHz, and 81-86 GHz [ITU-R WRC-19], [DigitalEurope]. The agenda item 1.16 considers Radio Local Area Network (RLAN) and additional allocation to the mobile service in the frequency band between 5.150 and 5.925 GHz.

The European Commission targets to promote preliminary 5G trials, which take place from 2017 onwards, to carry out pre-commercial trials including EU cross-border issues in 2018, to identify at least one major city to be "5G-enabled" by the end of 2018, and to have uninterrupted 5G coverage in all urban areas and major terrestrial transport paths by 2025 [COM(2016) 588]. 700 MHz band, which in most cases is taken into LTE use rather than 5G, has a status of committed, completed, underway, or planned in Austria, Finland, Czech Republic, Denmark, Estonia, Finland, France, Germany, Iceland,

Liechtenstein, Luxemburg, Malta, Moldova, Norway, Portugal, Slovenia, Sweden, Switzerland, and the UK [ECC/DEC/(15)01] in Oct 2017.

A part or whole 3.4-3.8 GHz band is allocated in Czech Republic, Hungary, Ireland, and Romania in 2017. It is planned to be auctioned in two parts in the UK in 2017 and 2018, in Sweden in 2017-2018, in Germany, Spain, and Italy in 2018, in Belgium, Austria, Finland, and Switzerland in 2018-2019 [DigitalEurope].

26 GHz band is expected to be released in Germany and Italy in 2018, and in Finland and Sweden in 2019. France, Spain, and the UK have plans to release the 26 GHz band, as well. [DigitalEurope]

2.3. Update on Achievements on Spectrum Management from 5GPPP – METIS-II Project

Metis-II project [MET_DEL] defines that the main challenge of 5G spectrum deployment in mobile networks and devices is to integrate the several frequency bands, having various bandwidths over a large frequency range and containing different certainty of availability, like exclusively licensed, shared, or licence-exempt. On regulative level, the successful 5G spectrum allocation contains several contiguous, wide and globally harmonized spectrum bands from 600/700 MHz up to 86 GHz. The flexible spectrum management concept should support, in addition to the mobile network operator requirements, the potential new 5G user groups, including vertical industry applications, Intelligent Traffic System, and Public Protection and Disaster Recovery. The recommended way to increase flexibility in spectrum management is Licensed Shared Access. Spectrum Assignment Coordination, which takes the assignment decisions, supported by a number of further entities, is proposed for mobile network operator domain.

3. Current Status of Undertaken Regulatory and Standardization Activities

Preparatory studies are ongoing for the World radio Conference 2019 (WRC-19) in both ITU-R and CEPT. Agenda items (AIs) of WRC-19 that relate to 5G and COHERENT project are listed in Table 1 together with responsible groups in both ITU-R and the Electronic Communications Committee (ECC) of the European Conference of Postal and Telecommunications Administrations (CEPT). Some AIs have direct impact on the enhanced mobile broadband (eMBB), whereas others are related to verticals that are envisaged to be a part of 5G ecosystem. The most direct impact on the eMBB is naturally the quest for new frequency bands for International Mobile Telecommunications (IMT) under AI 1.13. New bands for IMT for WRC-19 are 24.25-27.5 GHz, 31.8-33.4 GHz, 37-43.5 GHz, 45.5-50.2 GHz, 50.4-52.6 GHz, 66-76 GHz and 81-86 GHz, on which sharing and compatibility studies are ongoing in ITU-R and CEPT [ITU-R_2015]. These studies address the compatibility with and protection of all existing services, including their future deployments, in the same and adjacent frequency bands. The focus in Europe is on the frequency bands 24.25-27.5 GHz, 31.8-33.4 GHz, 40.5-43.5 GHz and 66-71 GHz. The highest priority is given for the 24.25-27.5 GHz band, which is a targeted to be harmonised for 5G in Europe already prior to 2020 [RSPG_2016].

In WRC-19, there are several AIs that consider so called vertical industries associated with 5G. AI 1.11 of the WRC-19 considers the spectrum needs, technical and operational characteristics and implementation of railway communications systems between train and trackside [ITU-R_2015_2]. AI 1.12 of the WRC-19 considers possible harmonization of frequency bands for Intelligent Transport Systems (ITS), car communications, globally or regionally [ITU-R_2015_3]. The current requirements for ITS operations have been developed under the existing primary mobile allocation and they address sharing and compatibility issues. AI 9.1.8 considers technical and operational aspects of radio networks and systems, as well as spectrum needed, including possible harmonized use of spectrum to support the implementation of narrowband and broadband machine-type communication (MTC) infrastructures [ITU-R_2015_4]. In ITU-R, studies on MTC are led by WP 5D which considers IMT technologies, supporting groups are WPs 1B and 5A which deal with non-IMT technologies.

AI 1.16 for WRC-19 considers issues related to wireless access systems, including radio local area networks (also known as Wireless LANs (WLANs)), in the 5 150-5 925 MHz band [ITU-R_2015_5]. Currently, mobile frequency bands designated for implementation of RLANs are 5150-5350 MHz and 5470-5725 MHz. Within this AI, studies are conducted to find the appropriate regulatory actions, including possibly additional spectrum allocations to the mobile service and for RLANs. On the other hand, in accordance to some difficulties that have been experienced in the sharing and compatibility between RLANs and other existing usage, additional restrictions (e.g. power level limitations) could be introduced to the current RLAN usage. It should be noted that some of the considered RLAN frequency overlaps in Europe with the existing applications under the mobile service, such as ITS.

Table 1. 5G-related agenda items in WRC-19 and responsible groups in ITU-R and CEPT.

WRC-19 AI	ITU-R WP	ECC PT	Description
AI 1.11	WP 5A	PT D	**TRAIN AND TRACKSIDE** to take necessary actions, as appropriate, to facilitate global or regional harmonized frequency bands to support railway radiocommunication systems between train and trackside within existing mobile service allocations, in accordance with Resolution 236 (WRC-15)
AI 1.12	WP 5A	PT D	**ITS** to consider possible global or regional harmonized frequency bands, to the maximum extent possible, for the implementation of evolving Intelligent Transport

WRC-19 AI	ITU-R WP	ECC PT	Description
			Systems (ITS) under existing mobile-service allocations, in accordance with Resolution 237 (WRC-15)
AI 1.13	TG5/1	PT 1	**IMT-2020** to consider identification of frequency bands for the future development of International Mobile Telecommunications (IMT), including possible additional allocations to the mobile service on a primary basis, in accordance with Resolution 238 (WRC-15)
AI 1.16	WP 5A	PT D	**RLAN 5GHz** to consider issues related to wireless access systems, including radio local area networks (WAS/RLAN), in the frequency bands between 5 150 MHz and 5 925 MHz, and take the appropriate regulatory actions, including additional spectrum allocations to the mobile service, in accordance with Resolution 239 (WRC-15)
AI 9.1.8	WP5D	PT 1	**MTC** to study the technical and operational aspects of radio networks and systems, as well as spectrum needed, including possible harmonized use of spectrum to support the implementation of narrowband and broadband machine-type communication infrastructures, in order to develop Recommendations, Reports and/or Handbooks, as appropriate, and to take appropriate actions within the ITU Radiocommunication Sector (ITU-R) scope of work.

3.1. Spectrum Sharing Related Activities in ITU-R

ITU-R WP 1B has finalized two spectrum sharing related reports in June 2017. The first report is a description of regulatory tools that support enhanced shared use of the spectrum [ITU-R_2017] which was developed within the framework of an ITU-R Question 208-1/1 [ITU-R_2015_6] “Alternative methods of national spectrum management”. The purpose of the report was to provide a collection of national regulatory mechanisms for spectrum management. The report introduces two concepts: Licensed Shared Access (LSA) and Shared Spectrum Access for Similar Technologies (SSA-ST). LSA has been described using the European regulation and standardization framework as a baseline. SSA-ST refers to sharing between operators that provide same radio service or use the same radio technology for example two mobile operators. The second report is about spectrum management principles, challenges and issues related to dynamic access to frequency bands by radio systems with cognitive capabilities [ITU-R_2017_2] and it was developed in response to ITU-R Resolution 58 [ITU-R_2012]. Unlike the previous service-specific technical reports from various WPs of ITU-R, see for example [ITU-R_2011] [ITU-R_2011_2] [ITU-R_2014], this report aims to provide a wider perspective throughout different radiocommunication services, by studying the general framework and highlighting

some challenges related to CRS techniques, including the means to ensure the protection of incumbent services on the same band or adjacent bands.

3.2. Electronic Communications Committee

In addition to the ongoing studies for AIs of WRC-19, ECC of CEPT is conducting studies on the use of C-band, more specifically 3.4-3.8 GHz band, in response to the study Mandate from EC [EC_2016_2]. The EC has identified this band as the primary band for 5G and it has already been harmonised within Europe for mobile use through ECC decision [ECC_2014]. The aim of the studies currently conducted in Project Team (PT) 1 of the ECC is to assess the suitability of the existing harmonised technical conditions for 5G. In addition, the aim is to develop guidelines to help administrations to defragment the band, as well as to develop plans and timescale for its future use.

3.3. European Commission

In Europe, common framework is needed to achieve economies of scale. European Commission (EC) and its radio Spectrum Policy Group (RSPG) has been actively promoting shared use of spectrum and regional harmonization for several years already for example by

- Publishing a report on cognitive radio technologies in 2010 [RSPG_2011],
- Publishing a report on infrastructure and spectrum sharing in mobile networks together with Body of European Regulators for Electronic Communications (BEREC) [RSPG_BEREC_2011],
- Founding of the Radio Spectrum Policy Program (RSPP) in 2012 with a mission to enable a common digital market [EU_2012],
- Publishing a communication to promote shared use of spectrum and highlighted the importance of identifying beneficial sharing opportunities in both licensed and license-exempt frequency bands [EU_2014],
- Identifying two dynamic sharing approaches that relate spectrum availability into time and geographical area; namely Collective Use of Spectrum (CUS) [RSPG_2011_2] and Licensed Shared Access (LSA) [RSPG_2013],
- Initiating work on LSA with Mandates to CEPT [EC_2014] and ETSI [EC_2012], and
- Initiating Digital Single Market (DSM), which includes for example more effective spectrum co-ordination and common EU-wide criteria for spectrum assignment at national level [EC_2015].

The 5G Action plan for Europe published in 2016 states that the potential for spectrum sharing, including under license-exempt use, should be maximized as it supports innovation and market entry [EC_2016]. It also states unlocking spectrum assets for 5G as one of the key actions to support innovation and market entry, and calls for national 5G deployment roadmaps already by the end of 2017. RSPG published an early opinion on spectrum aspects for 5G in 2016 providing a strategic roadmap towards 5G for Europe [RSPG_2016]. In this opinion, the pioneer bands for 5G launch were highlighted. These included so called coverage bands below 1GHz as well as capacity bands both at 3.6 GHz and above 24 GHz as identified for WRC-19. EC initiated further technical studies on these bands in CEPT by issuing a study Mandate [EC_2016_2]. A subsequent opinion from the RSPG is expected to identify and analyse spectrum related challenges, such as spectrum sharing, usage and license conditions. A communication from the EC in 2016 towards a gigabit society promotes shared use of spectrum, either on the basis of general authorisation or individual rights of use, as it can enable more efficient and intensive exploitation of spectrum especially in the new mmw spectrum bands foreseen for 5G communications [EC_2016_3].

3.4. Federal Communications Commission

In the US, the Citizens Broadband Radio Service (CBRS) is the sharing framework developed by the Federal Communications Commission (FCC) for the 3.55-3.7 GHz band [FCC_2016]. In CBRS, the incumbent access, consisting of for example fixed satellite service and radars, is complemented with both licensed Priority Access License (PAL) usage and unlicensed General Authorized Access (GAA) usage. Spectrum Access System (SAS) is the new spectrum management component enabling shared use and coordinating between the three tiers of users. In the case of governmental incumbent usage, thus naval radars, an Environmental Sensing Capability (ESC) is used for detecting transmissions. The FCC has finalized the rules governing the use of this band including licensing, technical, and service rules.

During 2017 the FCC also allowed broadcasting companies to return their usage rights on the lower UHF band (600 MHz band) to FCC to be auctioned in so called incentive auctions [FCC_2012]. The incentive auctions closed in March 2017 and as an outcome 84 MHz of spectrum was repurposed, mainly to new licenses but some of it also to unlicensed usage.

4. Spectrum Management System – Final COHERENT Approach

4.1. Considered Spectrum Management Architecture for Virtualized Wireless Networks

One of the key objectives of the COHERENT project is to propose the architecture for efficient virtualization of the 5G systems. Below we provide the description of the considered spectrum management and control framework, where we concentrate on both high level architectural aspects and on the lower level spectrum coordination and monitoring functions.

In our analysis of the spectrum management, coordination and control system we consider three groups of users:

- *spectrum regulators* – such as National Regulatory Authorities (NRAs), which are responsible for the high level regulation of spectrum management rules, and monitoring of its execution,
- *spectrum usage right holders or licensees* – such as mobile network operator (MNO), or a virtual mobile network operator (VMNO), incumbents, etc. which benefit from usage of the spectrum,
- *mobile users (mobile terminals)* – the end users or more generally clients of, e.g., the network operators.

In the context of spectrum management, coordination and control, the last group can be omitted as they only utilize the spectrum assigned to them by the spectrum usage right holder. On the other hand, the main role of spectrum regulators is to provide guidelines for spectrum usage, thus they are key players in spectrum management. Finally, MNOs possess the rights for spectrum control and coordination within bands licensed to them. Clearly, these two roles can overlap, i.e., it is possible that MNOs will possess their own, local/private spectrum management systems for the whole set of frequencies assigned to them.

Having these observations in mind, as well as the key investigation subject of COHERENT project being the wireless network virtualization, the whole proposed structure can, in general, be divided into three planes: spectrum management system plane (or equivalently spectrum manager application), spectrum control and coordination plane (realized by means of COHERENT central controller and coordinator; in terms of network virtualization this plane corresponds to the spectrum control function and includes network graphs) and infrastructure plane (please note that the infrastructure plane includes also such physical resources as spectrum). The key idea is illustrated in Figure 2.

The proposed Spectrum Manager Application (SMA) exemplifies the application of the so-called cognitive engine (discussed in first deliverable in WP4, mainly [COHERENT_D41]). It can exploit various abstraction models representing the status of the underlying network, so the cognitive algorithms and predictive models can be executed. A particular abstraction model is the interference map, which utilizes the SINR measurement reports. The reports are obtained from monitoring physical and virtual devices. Furthermore, the SMA will rely also on different databases, including the Radio Environment Maps (REMs) and a repository where national and international regulations are stored and maintained. The abstraction models are used for short-term spectrum management, whereas the REM and the repository of regulations for long-term usage (see next section for more details on short- and long-term usage). Thus, we enable two different REMs which operate over different time scales and that together become the enabler for efficient spectrum management.

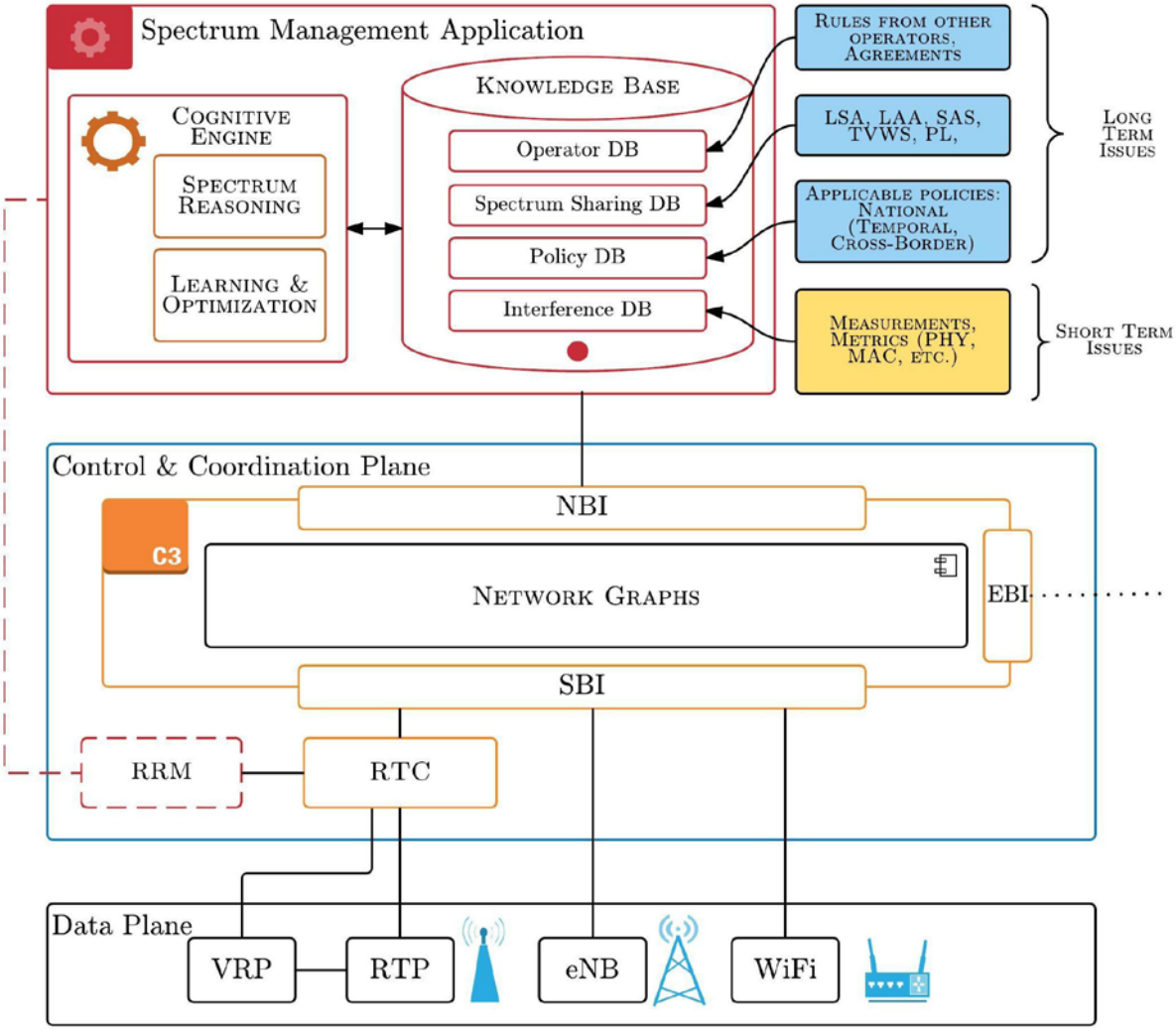

Figure 2. COHERENT spectrum management, coordination and control system

4.2. Role of Centralized Coordination and Control in Spectrum Management

The role of the C3 entity in the COHERENT architecture ([COHERENT_D22]) is to coordinate and control the underlying radio access networks. From the perspective of spectrum management two types of operations can be envisaged, mainly related to the long-term and short-term spectrum usage. As the former one is related to the long-term decisions regarding the best transmit opportunities (e.g., the selection of best frequency band or the best transmit policy), the latter deals with immediate changes of spectrum usage (e.g., related to execution of radio resource management issues). Below we concisely characterize both groups of spectrum-usage schemes [Kliks_2016].

4.2.1. Long-Term Aspects of Dynamic Spectrum Usage

- *Spectrum sharing policies* – these type of policies define ways for long-term spectrum sharing between various stakeholders; beside the traditional exclusive use of spectrum (also referred to as command and control) and license-exempt usage (in which any system is allowed to use the spectrum provided that it complies with technical specifications), solutions such as LSA, LAA, SAS for CBRS or many others can be proposed. Once the operator goes for the spectrum sharing policy, it entails several requirements on its practical implementation. The rules and policies need to be stored and updated on demand in a dedicated database; these spectrum usage rules will have an impact on the coordination and control algorithms implemented in C3 engine.
- *Mutual inter-operator agreements* – beside long-term spectrum sharing policies, which are open to any interested stakeholder, mobile network operators can decide to share not only the infrastructure, but to extend this concept to spectrum sharing. Such agreements are strictly

related to dedicated players. Long-term detailed agreements, stored in a dedicated repository, pave the way also for short-term coexistence rules.

- *National and regional regulations* – these simply defines the general rules for spectrum usage at specific location and time; all spectrum sharing models must be compliant with the national regional regulations. An illustrative example would be the implementation of SAS or any other hierarchical approach.
- *Cross-border rules* – the spectrum management system has to be aware of the differences between different countries and national regulations, thus cross-border dependencies have to be further evaluated. This includes not only the consideration of rules coming from regulators, but also the mutual agreements between foreign operators and service providers.
- *History analysis* – C3 may benefits from the historic data; it may be beneficial to rely on the spectrum sharing decisions already made in the past in certain circumstances. Such an approach would require the presence of a dedicated cognitive engine for the analysis of data logs, as well as of databases and possibly large storage capacity. It can also be imagined that persons responsible for maintenance and traffic control would also be interested in data mining, thus dedicated interfaces serving the purpose should be developed.
- *Service license agreements (SLA) for certain users* – the dedicates set of rules for specific users may be stored in the databases to guarantee user-centric approach in the spectrum sharing scheme.

4.2.2. Short-Term Aspects of Dynamic Spectrum Usage

- *Spectrum monitoring and occupancy* – different wireless systems deployed over the same area require permanent real-time monitoring of the spectrum resource. This is crucial to verify that the generic, long and short time rules are fulfilled and that constraints are not violated. The parameters measured at Layer-1 could include values of the received power and interference levels, whereas at higher layers other metrics could be used to estimate spectrum occupancy. In the context of 5G the development of a monitoring function is necessary, which requires careful database design for efficient (big) data mining. In this case, specific machine-to-machine communication is required, as the controller (engine) will query and update the database automatically without human intervention.
- *Emergency situations* require that the monitoring function must be complemented with the strict rules characterizing emergency situations. Once an emergency starts, immediate actions have to be performed to adapt network behavior in order to fulfill the rules set in place during a specific crisis. These rules are derived from the long-term databases described previously but need also to be continuously updated and maintained. Human intervention should be limited in this case.
- *Requirements resulting from existing licenses granted to incumbents* implies that once the long-term rules for incumbent protection are set in place, they have to be monitored in real time. It may happen that under an existing licensing scheme a new service specific of a protected system will be initiated, and the whole network needs to be reconfigured and adapted. Interaction between the databases and monitoring function is foreseen.
- *Management of priorities* depends on the spectrum sharing strategies enforced in a specific geographical region. Different priorities can be defined, and the presence of high-priority users has to be detected, such information stored and service quality ought to be guaranteed. Hence, permanent monitoring of different metrics that pertain to different layers is needed.
- *Connection to other standardized databases and systems* is essential for future wireless networks based on the integration of different technologies. A good example is the mutual coexistence between cellular and Wi-Fi networks (we could indeed refer to advanced 3GPP Access Network Discovery and Selection Function (ANDSF), and to the Wi-Fi Passpoint concept). The role of the database would be to continuously exchange information between coexisting wireless systems for better spectrum utilization similar to the LAA approach.
- *Equipment databases* could also be envisaged since the presence of databases containing information on the registered or currently operating devices could be beneficial for spectrum management. For example, incumbents or prioritized users could register their devices and request full protection at the expense of some additional cost.

4.3. Spectrum Management Application Mapped to the COHERNT Architecture

As the role of the Spectrum Management Application has been identified, as well as the short- and long-term usage was discussed, let us now map the SMA into the COHERENT architecture (for more details on COHERENT architecture please go to [COHERENT_D22]). The SMA has been indicated by dashed edge-rounded rectangle in Figure 3. Clearly, as an application, SMA is a part of the service layer, and it is not – in general – a part of any slice or other application (although, one may envisage such a futuristic approach as well). Its goal is to analyse all transmit opportunities (i.e., identify the prospective spectrum bands jointly with the transmission rules and constrains), select the best one (based on some predefined criteria associated with, e.g., slice requirements), and deliver this information to the C3 entity. As discussed previously, the SMA is capable also to monitor, collect and process the information about utilization of the assigned resources, and – if necessary – to update the decision on the transmit opportunities [Khan_2017, Kliks_2016, Kliks_2016_3].

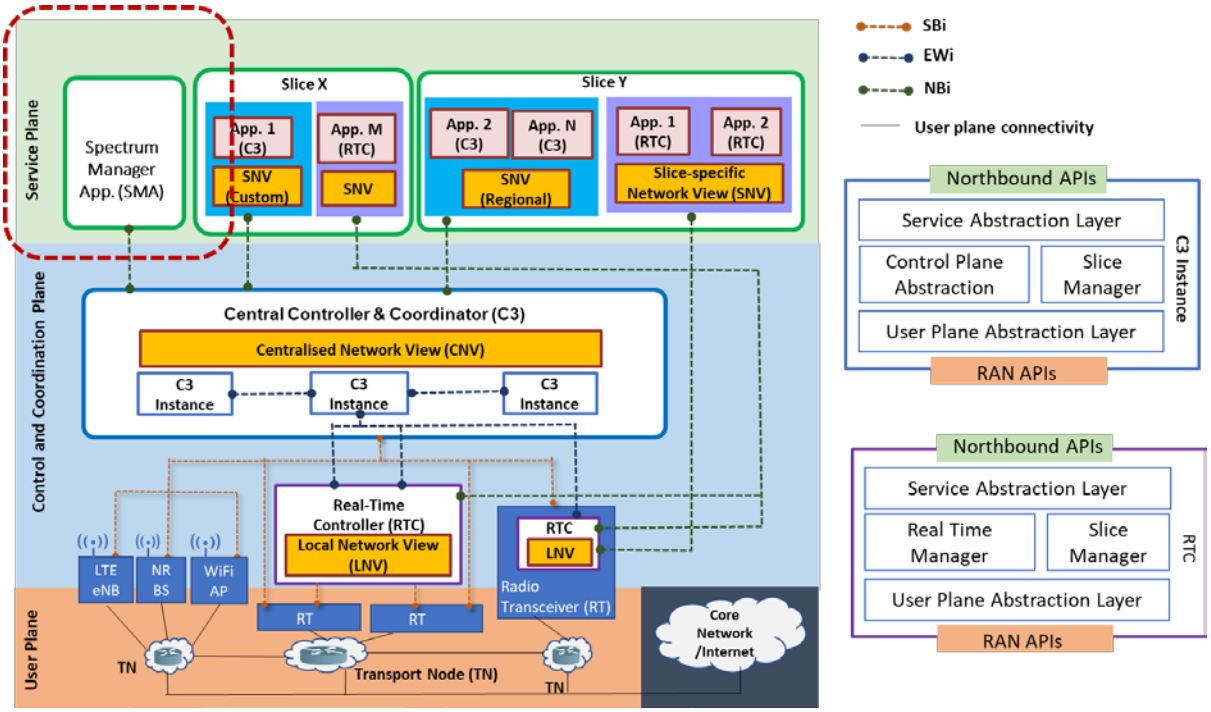

Figure 3. Identification of the SMA role in the final COHERENT architecture

4.4. Network Graphs Reflecting Spectrum Management Issues

In the first WP4 deliverable, i.e. [COHERENT_D41], initial discussion on the network graphs applied to reflect spectrum-related issues has been made. In this chapter, we provide the resultant analysis on how the spectrum changes may be reflected in form of a graph. This analysis will be made on a specific example (use case), in order to make it more specific. For that purpose, let us consider a situation shown in Figure 4, where the certain geographical area has been shown with the hexagonal-cell shapes and location of base stations. The dots' colours represent the mobile network operator (which this base station belongs to), whereas the cell-colours define the census tracts (which in a nutshell corresponds to some policies applied in the specific area and defined by, e.g., national regulatory authority, NRA). Please note that there is no relation between the operators coverage and the shape of the census tract. Obviously, the areas covered by the base stations belonging to different operators may overlap each other.

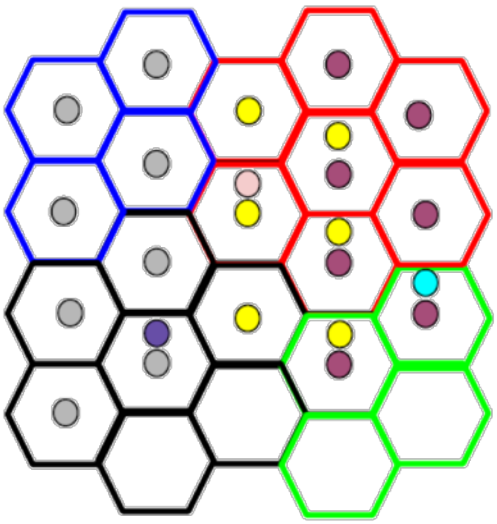

Figure 4. Use case under analysis: considered network structure for spectrum network graph analysis

The situation above may be represented in form of the following network graph Figure 5, which is at this stage complete. We call it a policy network graph, as it represents the relations between the nodes with regards to the rules of potential spectrum sharing between those nodes.

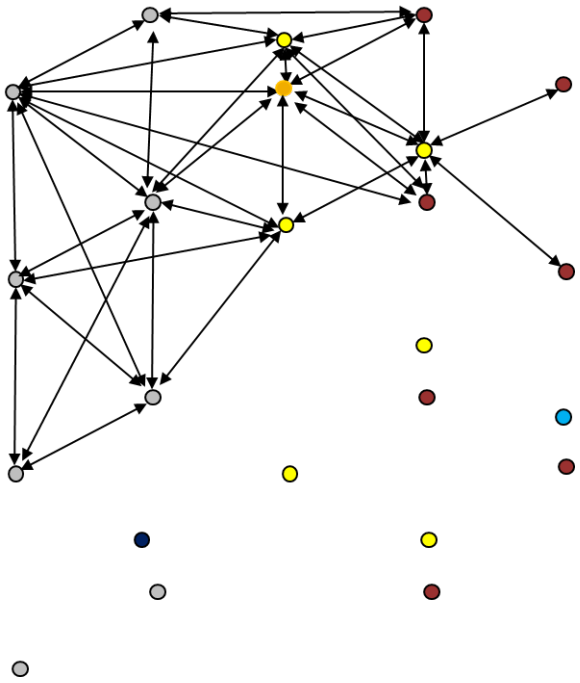

Figure 5. The fragment of complete policy network graphs corresponding to the considered use case

In this approach we agreed that the network node may be treated as either the access point (as in WLAN), base station (as eNB in cellular systems), or in general any Transmission Point. The edges between the nodes define the policies and agreements existing between the nodes, they also incorporate partially the guidelines originated from the census tracts from NRA. The edge may be represented in form of a tuple stored in, e.g., JSON format. Two exemplary tuples, $X_{A,B}$, defining the spectrum sharing rules between nodes A and B, are shown in Figure 6. In fact, the edges between the nodes may be oriented to show, who is a licence owner, and who only borrows the spectrum. One may observe that in the first case 17 resource blocks (RBs), numbered from 1 to 5, 8, and from 10 to 20, may be subject of leasing. For those resource blocks, there are some transmission constraints defined in form of

maximum transmit power on *i*-th resource block (P_i), transmission spectrum mask (M_i), sharing type (in our case for RB1 to RB5 the sharing type denoted as LSA1 is applied whereas LSA2 for the remaining resource blocks), and finally a price.

In the second example, the frequency resource granularity is not as high as in the previous example (we do not specify which resource blocks may be leased, but the exact frequency ranges are provided).

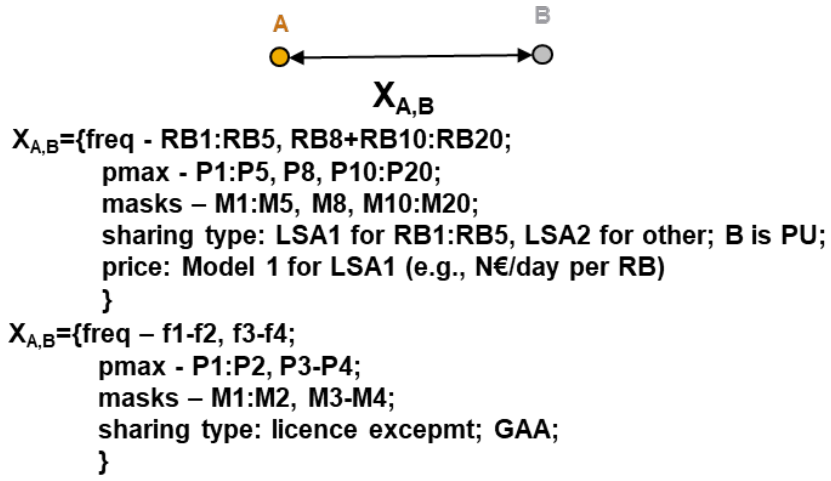

Figure 6. Exemplary generic tuples associated with the edge of policy network graph

Below we present the exemplary tuples for various sharing schemes, mainly for LSA, and for CBRS.

LSA policy Edge definition:

- **Simplified case – with predefined classes of LSA policies**
  {
  var: LSA_sharing_class;
  type: integer:
  }

  e.g., {LSA_sharing_class: 1}
- **Standard case**:
  - **Set of leased frequencies [Hz]**

    {freq: [{3.6e9, 3.64 e9}, {2.6e9, 2.61e9 }] }
  - **Minimum frequency gap to lease [Hz, RB]**

    {gap_min: [5; 4;]}
  - **Mask definition for each band [dB]**

    {mask: [{ {-30,-20} ,{-20, -30} }, { {-60, -40}, {-40, -50}} }]
  - **Time to borrow [s]**

    {time_to_borrow: [0, 50, 80]}
  - **Price to pay per minimum time unit per minimum frequency portion to lease** [€/$]:

    {price: [200, 500]}
  - **Time to leave** [ms]: {time_to_leave: [100, 50, 100]}
  - **Sensing sensitivity [dBm]:** {sensing_sens: [-90, -100]}

CBRS with SAS policy Edge definition (3550 – 3700 MHz)

- For Priority Access Licenses (PAL) mode as previously for LSA

- For GAA (sensing, possibly with dedicated database):
  - **Range of spectrum [Hz]** – {freq: [{3.55e9, 3.7e9}] }
  - **Interference temperature [dBm]** – {int_temp: -100}
  - **Time to leave** [ms]: {time_to_leave: [100, 50, 100]}
  - **Sensing sensitivity [dBm]:** {sensing_sens: [-90, -100]}

Obviously, the complete policy network graph may be optimized by reduction of unnecessary edges Figure 7. It may be achieved by:

- limiting the graph to the area controlled by one C3 (although some edges may exist also between such areas),
- limiting the graph due to the path loss influence,
- including only the real, existing relations between the operators,
- removing the edges between the same-operator nodes, as there is no need for definition of policies between the nodes of the same operator, at least within the census tracts, where the rules will be defined.

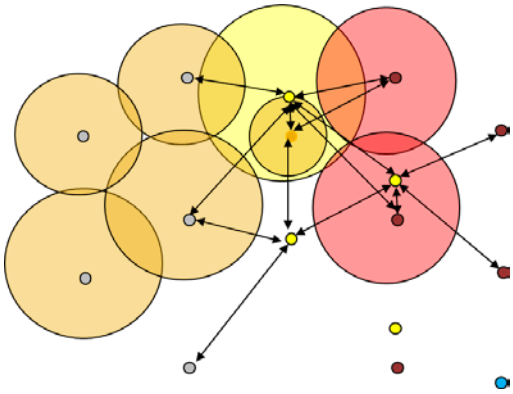

Figure 7. Optimized policy network graphs

This policy network graph may be further used jointly with classical but customized interference graph and request graph (see Figure 8). The request network graph (Figure 9) consists of the central node denoted here by means of star (and representing the mobile user), and the transmission points within its (users) transmission range. The green edges represent the exact transmission opportunities offered to this user. The C3 entity in the COHERENT architecture will be able to decide which node is the best to serve the user request. Once the node is selected, automatically the associated set of spectrum resources will be assigned to that user, causing interference to the other cells in the vicinity. This effect is reflected in the interference network graph (blue edges in Figure 8).

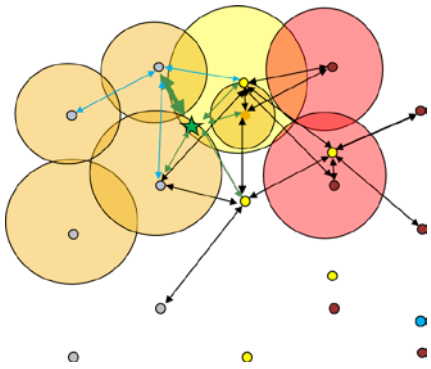

Figure 8. Policy network graphs jointly with customized requests- and interference-network graphs; the interference network graph is denoted by blue edges, whereas the requests-graph – by green edges. The bolded edge represents the selected node and associated transmission rules.

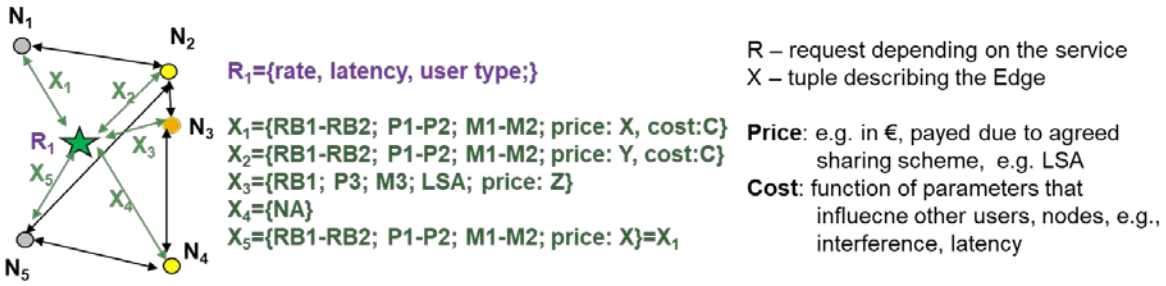

Figure 9. Definition of the tuples on the request network graph

The approach discussed above allows presenting in form of a network graph all of the changes appeared in the network due to the dynamic spectrum usage. The key aspect is the accurate definition of the policy network graph, as these graphs may be used for generation and further update of the customized interference network graphs. One may observe that in practice the changes in policy network graphs will be in most cases rather rare due to the following reasons. First, the changes in spectrum sharing policies (meaning the signed agreement etc.) are long-term processes, expressed even in days or weeks. Second, even in the case where the existing agreement allows for dynamic spectrum use (like in LSA scheme) the policy changes are not considered to be realized at millisecond level. Of course, there are research works that deal with extremely short term spectrum leasing, only in such a case, the change of the policy graph will be complicated. Knowing that, one may conclude that the policy network graph will define the fundamental rules for creation of the request network graph (which may be used for channel selection and assignment procedures) and interference network graphs. Finally, one may observe that the key impact of the spectrum-related issues on the network graphs (beyond creation of the policy network graph) is because the coverage area directly depends on the frequency. In other words, selection of a lower frequency band for data transmission will automatically result in much wider interference network graphs comparing to the case where higher frequencies are chosen.

5. Definition of the Framework for Low-Layer Abstraction for Spectrum Sharing

In this chapter we identify abstractions of radio access network state and configuration, and related operations, which are required for the purpose of supporting spectrum management in a MNO's network. Thus, the abstractions that relate to the sharing of the spectrum as such are not in the focus. Please let us remind that detailed discussions on the abstraction aspects have been included in WP3 deliverables, i.e., [COHERENT_D31] and [COHERENT_D32].

The abstracted view to the low-layer reality of the RAN infrastructure is constructed and maintained by COHERENT's central controller and coordinator (called "C3"). The abstractions are exposed to a Spectrum Management Application (SMA), also called as Spectrum Manager, at an interface between the Spectrum Manager and C3. This interface, here called as C3-SM interface, is in the focus of this study. In COHERENT architecture, local functions that operate in short time scales may be located in specific Real-Time Controllers (RTCs). The radio access nodes in the RAN infrastructure, like LTE eNBs or Wi-Fi APs, are commonly called as Radio Transceivers (RTs). The relationships between the components are illustrated in Figure 10.

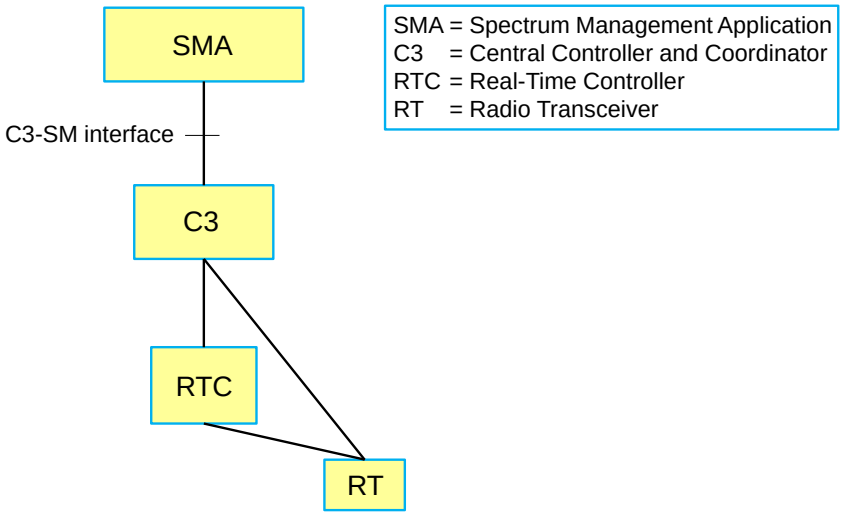

Figure 10. Interface between Spectrum Manager and C3

The Spectrum Manager may be part of the mobile network's OAM functionality, for example, or it may be a standalone application or it may even be a supervising controller within C3. Depending on the deployment model, the C3-SM interface may be defined as APIs, that is, northbound API at C3 and southbound API at the Spectrum Manager, or also as a control protocol (with APIs that implement the protocol).

The Spectrum Manager may also have interfaces to external functions and databases that represent different means of acquiring or relinquishing spectrum resources. Thus, the available of spectrum may originate from a mix of MNO's own individual licenses and on spectrum sharing arrangements with external entities.

In this report, the Spectrum Manager is assumed to hide the details of the various spectrum sharing schemes and their associated protocols and resource availability information models from C3. For example, spectrum sharing schemes typically build on the discovery of external spectrum repositories or other such entities and the establishment of a secure and continuous communication connection with those entities. The initial administrative phases of the communication (like registration procedures) and events in the state of this channel as such should not be directly visible to C3. However, the communicated spectrum sharing rules, policies and constraints have implications on what kind of actions/events and information flows need to be supported in the C3-SM interface.

In the following sections, we first (in subsection 5.2) examine existing models for expressing "spectrum availability information", with the aim of getting a "top-level" view to the spectrum management

concepts, which would be further mapped "down" to the low-layer abstractions. Next (in subsection 5.3), we analyse specific requirements for abstraction in selected spectrum sharing schemes, and then (in section 5.3) propose a set of low-layer functions and associated classes of information for the support of spectrum management. The identified abstractions are expected to provide a basis for further specification of the spectrum management interfaces between the components (in Figure 10). To that aim, we propose information and control flows for the spectrum management APIs, to be included in the COHERENT SDK (see later the subsection 6.5).

5.1. Examples of Models for Communicating Spectrum Availability Information

This section gives a brief review of some existing proposals about how to express constraints in using spectrum resources in general and with spectrum sharing schemes in particular. This section is not a part of the framework, but the intent is to give insights into how spectrum usage rules might be translated into network configuration constraints such that the radio transmission behaviour will be compliant with the rules.

5.1.1. LSA Spectrum Resource Availability Information

The LSA architecture [ETSI TS 103 379] defines an interface between LSA Controller (LC) and LSA Repository (LR). This interface, called LSA_1, carries Spectrum Resource Availability Information (LSRAI) from LR to LC.

LSRAI conveys information about the LSA spectrum resource that may be used by the Licensee, and the respective operational constraints. However, LSRAI does not necessarily contain descriptions of the spectrum resource that are static and already (a priori) included in the terms of the license.

The current ETSI specification outlines LSRAI as a container for the definitions of different types of geographical areas (e.g. circles or polygons), called "zones", in which there are constraints on the MNO's radio transmissions. The zone type, *protection*, *exclusion* or *restriction* zone defines the nature and levels of restrictions on causing harmful interference to the incumbent in a given frequency range and during given time frames. A protection zone sets limits on the maximum interference power or on the maximum Power Flux Density (PFD) at the incumbent location, whereas exclusion and restriction zones set constraints on the MNO's transmitters in the form of maximum Equivalent/Effective Isotropic Radiated Power (EIRP) limits and/or constraints on antenna parameters [CEPT 56], [CEPT 58]. These two basic types of incumbent protection have different implications on how flexibly a MNO is allowed to fulfil the constraints and what location information needs to be disclosed to each party (e.g., in order to derive the exclusion or restriction zones from the incumbent's protection requirements).

5.1.2. Spectrum Consumption Models

Spectrum Consumption Models (SCMs) represent spectral, spatial, and temporal consumption of spectrum by radio transmitters and receivers, and sets of systems formed of those [Stine_2015]. SCMs are being standardized in IEEE DySPAN-SC P1900.5.2 group.

There are two ways of consuming spectrum: transmission (emission) of RF signals and reception of RF signals. Accordingly, there are transmitter models, which convey the extent and strength of RF emissions; and receiver models, which convey what is harmful interference. The interaction between these two types of model between any two systems sets boundaries of spectrum use between the systems. That is, a system can consume spectrum as far as its transmitter model does not preclude the receivers of another system from operating and as far as its receiver model does not preclude the transmitters of another system from operating. When a party commits itself to an SCM it agrees to use spectrum within the bounds of the SCM.

The main constructs that are used to model spectrum consumption include [Stine_2015]:

- *total power*
  - power that drives antenna or received from antenna (reference for spectrum mask, underlay mask, and power map)
- *spectrum mask*
  - relative spectral power of emissions by frequency

- *underlay mask*
  - relative spectral power density of allowed interference
- *power map*
  - relative power flux density (PFD) per solid angle
- *propagation map*
  - path loss model per solid angle
- *start time / end time*
  - time when the model takes effect / no longer applies
- *location*
  - location where a component may be used (e.g., a volume, a trajectory or orbit)
- *minimum power spectral flux density*
  - power spectral flux density that, when used as part of a transmitter model, implies the geographical extent in which receivers in the system are protected
- *policy / protocol*
  - reference to system behaviour that enables inter-system coexistence in the same spectrum

The P1900.5.2 workgroup is standardizing an XML-based language for SCM, called Spectrum modelling Language (SCML).

5.1.3. Spectrum specification in PAWS

IETF RFC 7545 [IETF RFC 7545] defines PAWS (Protocol to Access White-Space Databases) which allows a device to consult a geospatial database in order to obtain a schedule of available spectrum at its location. The protocol is intended for use in the context of TVWS, but the spectrum data models are applicable also for other spectrum sharing schemes.

In the protocol, a device first registers with the spectrum database by giving information about the sets of rules that it complies with, its location, and antenna characteristics. Then the device may query from the database for available spectrum. The database responds with a set of available frequencies, permissible operating power levels, and a schedule of when they are available. The structure of the response is shown in Figure 11.

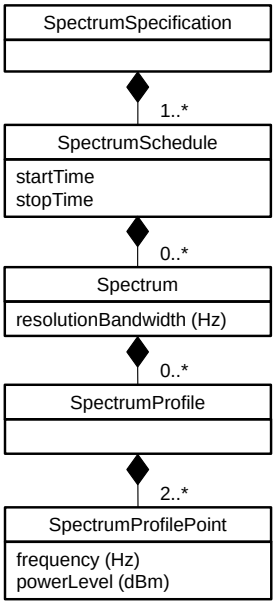

Figure 11. Spectrum specification in PAWS protocol

The requirements for the protocol operation and the data model have been specified in [IETF RFC 6953].

5.2. Requirements for Low-Layer Abstractions in Spectrum Sharing Use Cases

This section examines requirements for low-layer abstractions that stem from spectrum management in selected spectrum sharing schemes, including exclusive use of spectrum, license-exempt access, Licensed Shared Access (LSA), Licensed Assisted Access (LAA), and flexible duplexing.

The intent is to elicit ideas about how the "global" view to the network state information, provided by a centralised control entity could enable or facilitate efficient and effective spectrum management. Here, one of the key abstraction concepts is "network graph", including further derived graphs/maps. More information about COHERENT's abstraction framework can be found in [COHERENT_D31].

5.2.1. Exclusive Use of Spectrum

Exclusive use of spectrum with individual licenses represents a baseline scheme for spectrum management. The static allocation of spectrum resources allows long-term planning of frequency assignments among base stations, although the network topology may change frequently as Small Cells will need to be deployable in a plug-and-play fashion. Also carrier aggregation techniques call for agile spectrum mobility (within the bounds of the licensed static allocation). Here, spectrum management would assign sub-bands to cells according to the network's resource demands. On the other hand, "small-scale" resource allocation between different cell sites is coordinated by inter-cell RRM, especially in OFDMA systems with a frequency reuse of 1, such as LTE.

The obvious parameters for exclusive spectrum use relate to the spectrum definition by itself. This includes centre frequency and related normative constraints like band ranges; allowed resource granularity; and maximum allowed transmit power and requirements for spectrum masks on the spectrum blocks. Further, there are characteristics that associate a frequency band to a maximum theoretic rate or capacity according to the used radio technology. The license may limit the allowed transmit schemes (such as system type, e.g. GPRS, WCDMA, LTE, modulation formats, authorization types) at certain geographical area. The above-mentioned information about spectrum band characteristics is not necessarily contained in the network graph but it may be needed as part of input parameters in spectrum resource configurations.

The spectrum management needs to be aware of the network topology, cell configurations, and device properties and capabilities.

Further, there is a need to get statistics about network performance (e.g., spectrum occupancy, cell and backhaul load), radio conditions (e.g., interference, radio environment), traffic characteristics (e.g., temporal traffic variation, required QoS), and user behaviour (e.g., mobility).

Spectrum assignment is governed by MNO's optimization targets for the system operation, which may relate to QoS (e.g., probability of blockade), energy efficiency, monetary cost, for example.

5.2.2. License-Exempt Access

In spectrum management, awareness of spectrum resource usage is important, but in open access to spectrum, it is hard to estimate current spectrum occupancy or assess the remaining system capacity. Because the spectrum access is interference limited it may be is impossible to foresee the number of users trying to access the spectrum. Thus, the knowledge on the number of users and interference may mainly rely on some statistical derivations.

Licensed and license-exempt access schemes differ in their capability of supporting service guarantees to the users.

5.2.3. Licensed Shared Access

Licensed Shared Access is similar to the exclusive spectrum use case. However, it entails some distinguishing features: the temporal nature of spectrum usability and the constraints that originate from the need for protecting the incumbent from harmful interference (see section 8.1.1).

The possibility of non-planned evacuation of spectrum reduces the reliability (availability) of the resource and thus has on impact on QoS. But evacuation does not raise new major requirements for the

spectrum management functionality per se since the activation and cessation of spectrum usage are rather basic management operations anyway (e.g., turning on and off a transmitter for power saving).

The constraints on radio frequency emission may set limits to the maximum transmit power and to allowed antenna or beam direction (ranges of azimuth and elevation) and to maximum antenna height. The constraints may be defined for a single base station or for a group of them.

5.2.4. Licensed Assisted Access

Licensed Assisted Access can be seen as a mixture of the exclusive use and license exempt approaches. In spectrum management, there is a need to know all the details related to the usage of licensed part of spectrum, and in addition to that it will require information about the possibilities of unlicensed spectrum usage. Additionally in case of e.g. LTE-U when no channels are free, the Spectrum Manager should know the rules of spectrum sharing for unlicensed band.

5.2.5. Flexible Duplexing

In flexible duplexing, vacant frequency bands or time slots in LTE UL (or DL) are exploited for low power DL (or UL) transmission, depending on the traffic asymmetry. In order to estimate the benefits of flexible duplexing, the radio resource utilisation needs to be monitored in both transmission directions and in time and frequency domains. The possibility of exploiting flexible duplexing depends also on the UE capabilities.

5.3. Discussion on Low-Layer Abstractions for Spectrum Management

Let us now outline the assumptions about the spectrum sharing/management architecture and then propose possible low-layer abstractions in the support for spectrum management. Please let us remind that detailed discussions on the abstraction aspects have been included in WP3 deliverables, i.e., [COHERENT_D31] and [COHERENT_D32].

5.3.1. Basic Assumptions and Main Functions

If the spectrum management tasks are distributed between a Spectrum Manager and C3 as shown in Figure 10, there is a need for identifying the division of duties between the two components.

The Spectrum Manager is assumed responsible for any communications with external entities, like peer operators, regulators, and other third parties relating to spectrum sharing arrangements. These duties include registrations with databases or other servers, verification of the continuity of the connections, and exchange of spectrum availability information. Further, if a spectrum sharing policy poses a need to translate interference protection requirements into constraints pertaining to the network configuration, the Spectrum Manager should be responsible for such translations.

However, it is questionable whether the Spectrum Manager or C3 should determine which particular RTs are to be reconfigured, e.g., by assigning more spectrum resources. One approach is to let the Spectrum Manager have the ultimate authority on the reconfigurations but permit it, at its own discretion, to delegate decisions to a spectrum control function in C3. This can be achieved by allowing flexibility in the definitions of the network configuration constraints such that they may be met by C3 with a variety of alternative RAN configurations. For example, an aggregate constraint may apply to a cluster of Small Cells in a region, in which case C3 can decide on the individual RT configurations. The fine-grain spectrum sub-carrier assignments may be made locally by RRM control functions in RTC or by proprietary RRM functions or OAM agents, for example. Thus, the hierarchy of spectrum management functionality (Spectrum Manager, C3, and RRM) will naturally operate in different granularities of time, space, and chunks of frequencies. Possible high-level control and information flows between the components are outlined in Figure 12.

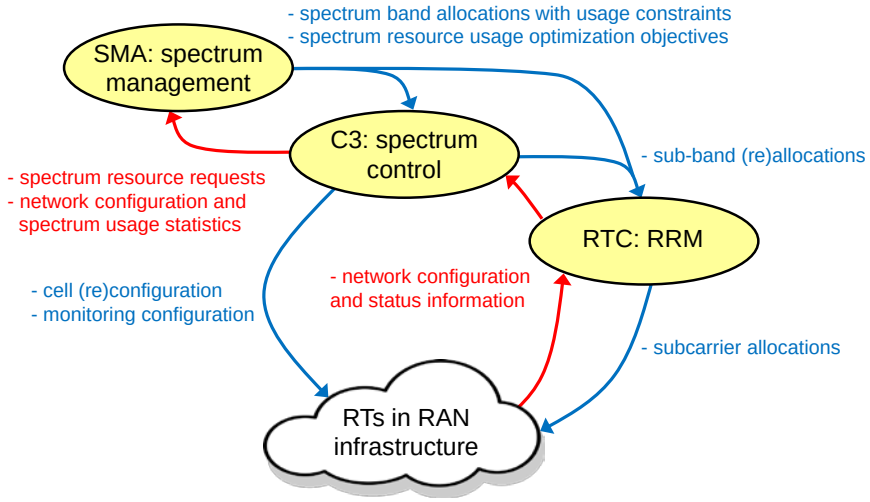

Figure 12. A high-level view to spectrum management operations

The Spectrum Manager and C3 need a view of the network state in order to decide how to make best use of the available spectrum resources. The relevant network state consists of a combination of network configuration information and statistics about measured network performance and user behaviour. This state information should be available in COHERENT network graph or it should be derivable from the graph.

Figure 12 suggests that the Spectrum Manager could also provide high-level resource usage optimization targets towards C3. However, alternatively, policy rules that cover the overall network operation may originate from a generic policy manager application. Thus, this section assumes the role of the Spectrum Manager to be more inclined towards a "spectrum provider/broker" (as opposed to a policy manager).

A further architectural option would be to extend the support for spectrum sharing functionality to C3 such that inter-operator spectrum sharing occurs between C3 entities of the different operators, Then C3 would provide an east/west-bound interface for the spectrum sharing protocols. This option, which is not considered further in the following, could be used in co-primary sharing, for example.

5.3.2. Spectrum Sharing in the Context of RAN Infrastructure Sharing

In infrastructure sharing, with MNO-specific dedicated spectrum, the resources of a radio transceiver point may be shared between operators. In principle, COHERENT's network slicing/virtualization framework takes care of the isolation between the operators such that they can apply distinct spectrum sharing and management policies and strategies. However, a sharing rule may impose network configuration constraints that are impossible to enforce without impacts across operators (e.g., if the antenna would need to be redirected).

The concept of infrastructure sharing may also involve spectrum sharing, with a common spectrum pool between operators. The frequency bands in the pool may be statically split between the MNOs, which comes back to the sharing case of dedicated spectrum in the previous paragraph, or the pool may be fully shared, or the MNOs may have certain quotas of the spectrum, for example.

The case in which the RAN infrastructure is shared among operators needs further study.

5.4. Spectrum Management Operation

This section proposes, based on the use case requirements in section 5.2, possible basic spectrum management operations and related parameters, and network state information that may be used for making spectrum management decisions.

It should be noted that not all of the identified pieces of network configuration and state information are specific to spectrum management but they can be also used for other control and management purposes.

5.4.1. Spectrum Management Events and Actions

This section introduces possible elementary events and actions at the C3-SM interface. The conceptual events relate to the Spectrum Manager becoming aware of the need for spectrum re-assignment in the RAN infrastructure and the activation of the spectrum re-assignment through network re-configuration.

The control and information flows at the C3-SM interface are described in more concrete terms in section 6, which presents an API for the spectrum management SDK.

5.4.2. Notification of Spectrum Resource Shortage

C3 may issue a spectrum resource shortage notification towards the Spectrum Manager in order to inform that there is a need for acquiring more spectrum resources. The notification includes the identities of the set of RTs that are proposed to be the targets for the supplementary spectrum. For example, C3 might notify the Spectrum Manager of a long-term resource deficiency if there are radio access links that remain persistently overloaded, even after any prior efforts to reduce load by means of load balancing, traffic steering/offloading, interference mitigation, etc.

The Spectrum Manager may eventually respond to the notification by initiating a spectrum configuration procedure (see section 5.4.3).

5.4.3. Spectrum Configuration

The Spectrum Manager configures a set of RTs by issuing a new spectrum configuration to C3, RTCs, or OAM agents in RTs, which then enforce the configurations in the RTs.

The spectrum configuration may contain the following types of cell-specific configuration information (for each spectrum block):

- spectrum characteristics (centre frequency, band range, spectrum quality)
- duplexing modes
- transmit power (maximum, recommended)
- antenna direction constraints (maximum and recommended elevation/azimuth range)
- parameters related to the spectrum mask
- time constraints.

Here, spectrum quality is an indication of the level of service (e.g., best-effort or guaranteed) that can be provided on the spectrum. This may depend on the sharing scheme and on the radio technology. The division into “maximum” and “recommended” constraints make a distinction between regulative constraints that must be complied with and MNO’s own policies and constraints (e.g., initial settings coming from deployment planning) that should be followed.

The Spectrum Manager may re-configure the network as a response to C3’s spectrum shortage notification (see section 5.4.2), or the Spectrum Manager may autonomously initiate a configuration based on its awareness of the current or prospective network state that may be exposed in the network graphs, for example. The re-configuration may also be triggered because of changes in the spectrum sharing conditions, e.g., in a sudden need for evacuating an LSA spectrum band.

5.4.4. Spectrum Management Information

This section outlines, at the conceptual level, the information that may be used as input for spectrum control and management decisions.

Network configuration information

- network topology (cell locations, neighbour relations, backhaul links).

Cell properties and capabilities information

The cell characteristics in this section are assumed to be static and not reconfigurable by the Spectrum Manager.

- radio technology (GPRS, WCDMA, LTE, Wi-Fi, …)
- cell type (macro, pico, femto, other)
- radio transceiver capabilities (supported frequency bands, duplexing modes)
- maximum transmit power
- antenna characteristics (antenna type, gains, height, elevation/azimuth range)

Cell configuration information

This includes configuration information that relates to the spectrum usage. The parameters may be given separately for UL and DL (to support configuration for flexible duplexing).

- spectrum characteristics (centre frequency, band ranges, resource granularity, spectrum quality)
- theoretic peak rate
- duplexing modes
- transmit power
- antenna direction (elevation/azimuth)

User device capabilities information

UE capabilities have an impact on which frequency resources and radio transceivers are potentially applicable for the establishment of the access connections.

- supported radio technologies (GPRS, WCDMA, LTE, Wi-Fi, …)
- radio capabilities (supported frequency bands, flexibility in duplexing modes)

Network status information

Network status information covers the “dynamic” aspects (long-term statistics) of the network state that may be used in making spectrum management decisions. The information is based on cell-specific measurements. Some of the PHY/MAC measurements have technology-dependent representations, which are listed in section 6.1 (for LTE and Wi-Fi).

Load information

Load information consists of statistics that relate to resource availability, in DL and UL directions.

- radio access load (e.g. virtual load, latency, packet error rate)
- transport network load (latency, packet loss rate)
- rejects in radio admission control (due to radio resource load or transport network load)

Interference information

Interference information is based on measurements reported by UEs. The information may be available in the form of interference graphs.

- intra-operator/network interference

- inter-operator interference

Energy consumption information

Energy consumption may be a significant factor in spectrum mobility decisions.

- power consumption (digital units, RF units)

User traffic information

Traffic statistics in different time scales and QoS commitments can be used to estimate the bandwidth demand (in DL and UL directions).

- traffic characterization (peak and average rates)
- QoS requirements for bearers (QCI, GBR, AMBR, …)

User mobility information

User mobility information may be used for determining which frequency bands, cell size, and radio technology would best serve the user.

- user mobility state
- handover failures (reasons for the failures)

Radio frequency environment information

The Spectrum Manager may become aware of the radio frequency environment. This may require monitoring that is not required in all spectrum sharing schemes or which is not available in all radio technologies. However, the Spectrum Manager may get the information from external sources (which are not in the scope of this framework).

- radio environment maps (REM)
- spectrum sensing.

6. SDK and APIs for Spectrum Management

This section considers spectrum sharing and management from application programming point of view, highlighting the control and information flows at the interfaces between and among Spectrum Management Applications, Central Controllers and Coordinators, and Radio Transceivers. The complete details of the COHERENT SDK supporting spectrum management and other control applications at different levels of control abstractions (e.g., C3 and/or RTC) are detailed in [COHERENT_D22]. This section summarizes the features in the COHERENT SDK that are relevant to the SMA functionality.

Software applications are seldom self-contained entities and rely on other processes to provide additional functionalities to operate properly. This reliance generally spans across all the functional units of a software program which includes collecting the required information, processing them and providing an output. Application Programming Interfaces (API) specify the interfaces through which one application can request supporting functionalities or services from another application. Typically, APIs are implemented through function calls and the relevant API modules are bundled together with a Software Development Kit (SDK) that can be used to create new applications. The COHERENT architecture provides a software-based control framework over heterogeneous networks to higher level control applications and the developed COHERENT SDK is a realization of that framework.

The Spectrum Management Application (SMA) is a COHERENT network control application that runs on top of the control hierarchy defined in the COHERENT architecture [COHERENT_D22] and optimizes the radio resource utilization including spectrum sharing. The functions of SMA require handling several types of information (short-term and long-term inputs) aggregated through the upstream control flows, processing those inputs, making spectrum sharing and/or management decisions, and implementing them through interaction with the control entities i.e., C3 and RTCs. Because the SMA relies on the provision of these abstraction (northbound) and control (southbound) functionalities within the COHERENT architecture, these features have been developed in the SDK and accessible through programmable APIs. To support this development, and to facilitate future interest in the utilization of the developed SDK for spectrum management in heterogeneous networks, the requirements of the SMA for both real-time measurements and spectrum management specific abstractions had to be detailed. This was also important since not identifying the requirements properly could have led to missing functionality and APIs in the COHERENT SDK for spectrum management tasks. This section summarizes the broad sets of parameters and abstractions provided through APIs in the COHERENT SDK that are relevant to the functionality of the SMA.

6.1. APIs for Northbound Flows

Spectrum management concerns optimization of the RF spectrum utilization and the main source of this information is the radio access network (RAN). Many primitive parameters are inherently sensed/collected by different devices that operate in the RAN segment. Additionally, wireless networks generally maintain network state information based on these observed parameters, e.g. network load, interference, and radio resource utilization. These parameters and measurements can be used to create a diverse set of abstract network views depending upon the actual abstraction process implemented in the network. In COHERENT, the abstraction process is carried out by the controller entities in response to the requests coming from network management applications. The controller not only keeps the current network graph up-to-date, but can also create further application-specific abstractions/subsets. These network abstractions are essentially data structures suited to the requirements of the control applications.

For brevity and to confine the focus to SDK and APIs definitions for spectrum management, we shall address LTE and Wi-Fi networks specifically for the available APIs for both abstractions and re-programmability. The end-user terminals in these networks are connected to the network infrastructure through wireless links from eNodeB and Wi-Fi Access Points to the respective UEs and Wi-Fi Stations. The eNB and APs together with UEs and Wi-Fi Stations gather many parameters related to radio spectrum inherently in the normal network operation. As spectrum access issues relate to the physical and MAC layers, the measurements of interest from the spectrum management perspective also come

from these layers. However, additional measurements taken at higher layers in the end-user terminals as well as in the rest of the network entities are also important for spectrum sharing decisions. Table 1 provides the list of well-known measurements/parameters associated with physical and medium access layers in LTE and Wi-Fi networks. Please note that similar or additional measurements can be associated with other types of networks such as spectrum sensing results in cognitive radio networks which serve to indicate secondary access opportunities. The description of parameters presented in Table 1 is provided in other project documents, specifically in [COHERENT_D31]. While these parameters are available per standard in LTE and Wi-Fi networks, they are not directly available for outside entities for control and management purpose. The COHERENT SDK provides the required APIs to gather these parameters from the network and expose them to the SMA in both unprocessed form or via abstractions derived through these parameters such as spectrum utilization, interference levels etc.

Apart from the APIs for collecting these primitive parameters, the COHERENT SDK also provides generic functions that facilitate developing higher lever abstractions using these parameters. For example, for LTE networks, the eNB can host agent module reports the utilization of the Physical Resource Blocks and the channel state reports. Instead of exposing these in the raw numbers, the agent can aggregate them over time, if required, to expose a time series of load variations in a particular LTE cell.

Table 2 PHY and MAC layer measurements in LTE and Wi-Fi networks

LTE Measurements	RSRP, RSSI, RSRQ, CQI, Received Interference Power, Thermal Noise Power, Sounding Reference Signal, Uplink Receive SINR, Time Difference of Arrival, Angle of Arrival, Timing Advance, Channel State Indicator, PMI, RI, Frame Structure Parameters, Resource Utilization/Availability Statistics, UE capability.
Wi-Fi Measurements	RSSI, Received Channel Power Indicator, Beacon Report, Frame Report, Channel Load, Scheduling Granularity Information, Noise Histogram, Station Statistics, Neighbour Reports.

6.2. APIs for Southbound Flows

The southbound flows are primarily meant to implement any specific spectrum management and sharing decision through the COHERENT software control. These decisions could be very granular, e.g., setting transmit/receive parameters in a particular small-cell or very broad, e.g., enforcing a network-wide spectrum sharing rules. The core module in COHERENT architecture to implement these decisions is the C3 module which shall exercise its software control functions on top of the virtualized network infrastructure.

The specific set of APIs and functionality provided for software control through C3 can be derived from the different spectrum management and sharing use-cases. For example, implementing LSA rules shall require the provision of information about the concerned networks, scope of sharing, and relevant parameters. These could be provided as input to particular functions (e.g. through direct function calls) provided by the C3 to the spectrum manager application. Considering that a large number of decisions related to spectrum can be taken at the application level in heterogeneous networks, the SDK shall provide the following sets of functionality and associated APIs.

APIs for spectrum management: Based on the network graph abstraction, the SMA can take different decisions about the utilization of radio spectrum in the network that can apply to the whole or a particular segment of the network such as a macro cell or a cluster of small cells. The COHERENT SDK will provide control over the parameters that govern spectrum access at these different levels. APIs for configuring the radio resource management functions of the network and spectrum utilization will be considered.

APIs for spectrum sharing: The second major consideration for SMA is sharing the spectrum with other networks based on the sharing agreement. Although the overall scope of spectrum sharing between/among networks may be determined by the applicable policies and regulations, the SDK should provide the necessary controls to acquire and release the shared spectrum on demand of the SMA. Additionally, SMA can utilize the shared spectrum differently than the dedicated spectrum and will therefore need the necessary APIs to do the required configurations.

6.3. System Level Simulation Model for Analysing Multi-Tenant RAN and Spectrum Sharing

Multi-tenancy in the RAN segment and sharing of radio resources among the RAN tenants is an important targeted 5G networks feature. While multi-tenancy concepts are active discussion topics among researchers of the field, spectrum sharing has already received considerable attention in the cognitive radio research domain where dynamic spectrum access models have been investigated extensively [Fette_2009]. However, most of the opportunistic and dynamic spectrum access concepts have not materialized for reasons including rigidity of the legacy network architectures, deficient spectrum sensing and the competitive nature of network operators. RAN sharing has also been considered, albeit mostly passively, in the form of base-station location, mast, power and cooling infrastructure sharing. The 5G network architecture is expected to change this with the realization of multi-tenant networks including shared RAN. A bottleneck in evaluating multi-tenancy and spectrum sharing concepts under the new multi-tenant 5G networks context is the lack of capable, open access simulation models. We aim to address this concern in this section which presents details of a system level, discrete events simulation model developed within the scope of COHERENT project to evaluate spectrum sharing and multi-tenant radio access networks at different levels of abstractions. The model simulates LTE/LTE-Advanced networks as tenants, sharing RAN and radio spectrum resources under the architectural guidelines of the COHERENT network control and coordination framework. This model has been developed for OMNeT++ simulation platform which is well known, open source discrete events simulation system [Andras_2017].

6.3.1. System Model

The system model for simulating multi-tenant RAN and spectrum sharing scenarios is based on the COHERENT architecture for network control, coordination and management [COHERENT_D2.2]. The centralized network is a depiction of an aggregated network state on which the control applications such as spectrum management application operate. The RTCs however take into consideration, the network state that is bound by the control domain of the particular RTC. For the simulation model, these concepts have been supported and controlled entities are modelled at similar abstraction levels as shown in Figure 13.

Each cell (LTE/LTE-A based) in the simulated network architecture is augmented with a module serving as RTC. Furthermore, each has been modelled as being multi-tenant where isolated resource slices can be allocated to the tenants. The cells are tied together by the C3 which, besides providing upstream network state information to the control applications, serves as a router between the RTC and the control applications such as Spectrum Management Application. We shall now look into the details of the RAN elements to describe how multi-tenant RAN is modelled and how this simulation model can be used for evaluating several spectrum sharing scenarios.

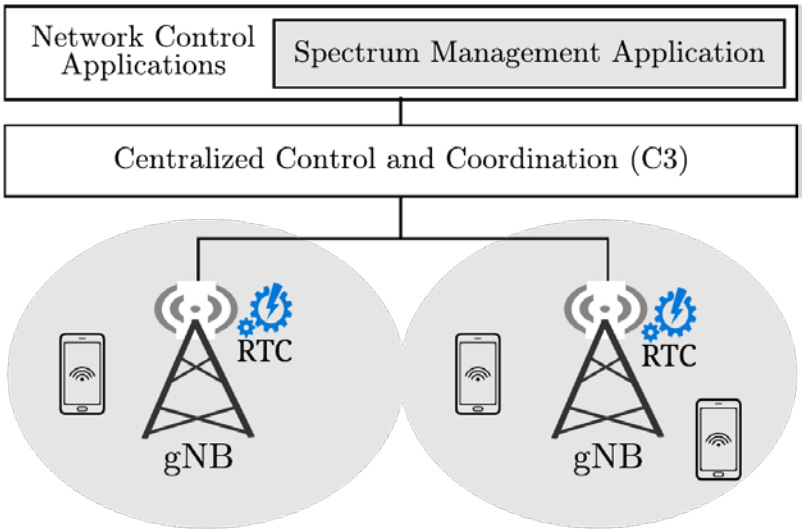

Figure 13. The system level control components in the simulation model.

6.3.2. Modified SimuLTE Model

The starting point for the development of this model has been the SimuLTE model. SimuLTE is an open source, system level LTE/LTE-A user-plane simulation model for OMNeT++ [Andras_2017] and has been used in several research works to demonstrate its correctness and network modeling potential [Mohammad_2015]. In its most recent version (v1.0.1 at the time of this writing), the SimuLTE model can simulate LTE/LTE-A (RAN and ePC) in Frequency Division Duplexing (FDD) mode with heterogeneous nodes using omni-directional antennas including realistic channel models and resource scheduling in both Uplink (UL) and Downlink (DL) directions. The control plane procedures are highly abstracted with utility modules that help in simplifying the basic network control procedures. At its core, the SimuLTE model provides User Equipment (UE) and Base Station (eNodeB) nodes along with some additional modules to form system level simulation scenarios. Figure 14 shows the fundamental functional components and internal architecture of the core SimuLTE nodes i.e., the UE and eNodeB. The common functions are shown in solid boxes while the optional components (either in UE or eNodeB) are shown in dotted boxes. Fundamentally, the LTE/LTE-A functions are enclosed in a Network Interface Card (LTE-NIC) compound module that brings the main LTE stack operations into a single box. The UE node uses additional modules for end-user applications (TCP and UDP Applications) and for sending channel status reports (Feedback Generator) to the associated eNodeB. The eNodeB uses a “Deployer” module for many of the physical layer resource specifications (LTE frame structure, Antenna specification, etc.) and UE association details. The implementation details of all these components are available as open source code for the research community.

The 5G multi-tenant RAN concept is expected to manifest itself in the form of shared base stations with a certain degree of tenant-specific resource isolation guarantees. While this can be realized at several abstraction levels above the physical layer, a well-qualified option is maintaining radio resource segmentation and management using distinct slice-specific medium access control procedures including resource scheduling. To realize this abstraction level in SimuLTE, we have modified the existing structure of the nodes to enable multi-tenant eNB having tenant-specific MAC modules and physical layer resources.

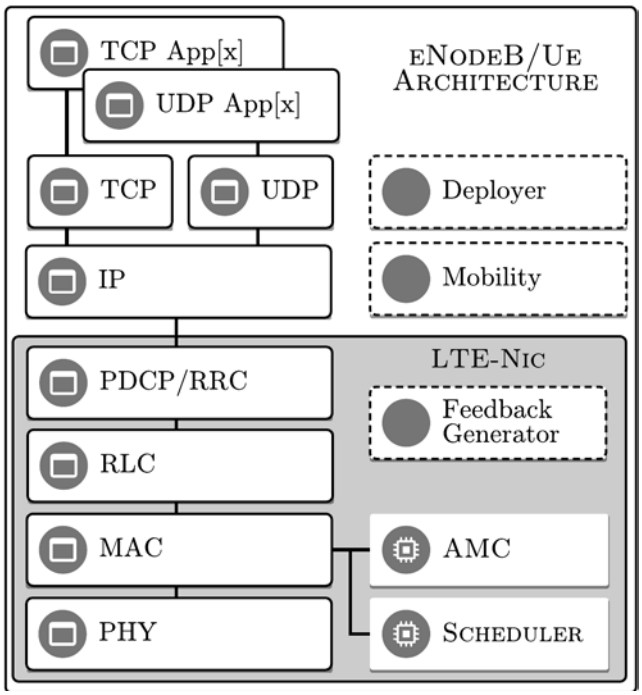

Figure 14. eNodeB and UE internal architecture in SimuLTE model

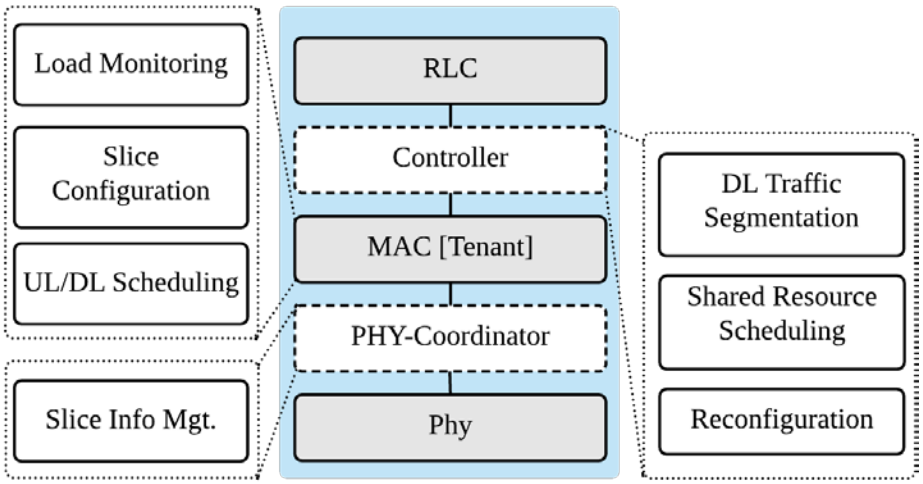

Figure 15. New modules and functions added to SimuLTE eNB architecture

Figure 15 shows the new and modified submodules (in dashed boxes) in the LTE-NIC compound module. Each eNB supports a user-defined array of tenant-specific MAC submodules which are coordinated by two new submodules appropriately named “Coordinator” and “PHY-Coordinator”. The MAC modules have been modified from the SimuLTE model to support new communication (interfaces and messages) and maintain distinct set of physical layer resources for each tenant. Each MAC module maintains its own set of scheduler and Adaptive Modulation and Coding (AMC) sub-modules to manage uplink and downlink traffic scheduling of slice-specific UEs. The layers including and above the RLC have not been modified significantly and the large set of options available to configure these modules have been maintained from the original SimuLTE model. The roles of Controller and PHY-Coordinator modules are somewhat reflected by their names. The Controller is a real-time controller and coordinator of the resources configured for each tenant-specific MAC module. It receives higher level configurations from the spectrum manager application (an application outside the eNodeB architecture) and configures parameters that control spectrum sharing among RAN tenants. The controller monitors the resource utilization in each slice and if enabled, facilitates the sharing of spectrum among the tenants in an active, fine-grained manner. In the downlink (DL) the controller segments the incoming traffic and directs it to the appropriate MAC module and vice-versa in the uplink

(UL) direction. To manage spectrum exchanges among the RAN tenants, it receives offers and requests from the managed MAC modules and coordinates the resulting increment and decrement of slice-specific bandwidth. While the current implementation requires the total number of tenants to be specified before the simulation runs, a future planned modification to the controller is anticipated to bring dynamic addition and deletion of new slices including reconfiguration of operational parameters. The PHY-Coordinator module is more generic and simply coordinates the access to the physical layer module in DL and segmentation of traffic in UL towards the appropriate MAC module.

6.3.3. Simulation Workflow

In the developed system level simulation model, a network is described, using the OMNeT++ network modelling language (NED), in terms of the number of cells and the network topology i.e., the interconnectivity among the network elements. Any number of cells/eNB nodes can be specified with tenant-specific UEs which can be configured dynamically. At the beginning, a configuration file (config.ini) is used to set the main parameters for the functional components (UE, eNodeB) including configurations for their internal sub-modules (MAC, PHY, Mobility model, Controller etc.). The association of UEs with a particular tenant is also configured statically with runtime handover support being developed. At instantiation time, a UE begins cell association procedure to register with the tenant based on the configuration file provided as input. The UEs send frequent channel feedback messages to the eNodeB and once a UE application requires some uplink/downlink data, it starts the normal LTE resource acquisition procedure (random access). The eNodeB receives the feedback reports and channel access requests from the UEs and performs the uplink and downlink scheduling at the MAC sub-module. The three scheduling algorithms available for UE scheduling are Deficit Round Robin, Proportional Fair, and Maximum CQI. Most of the modules above the LTE-NIC are taken from INET-framework [INET_2017] including TCP/IP and Application layer modules such as VoiP and Video streaming applications. The model also supports UE mobility and handovers.

6.3.4. Summary

The simulation model presented in this section was developed with the intention of realizing the COHERENT network management and control architecture for analysing multi-tenancy and spectrum sharing aspects in 5G networks. This model has been used for the research on fine-grained spectrum sharing and co-primary resource scheduling work presented in this document. The capabilities of this model are well beyond these targets however, and further development will be pursued in future.

7. Performance Evaluation of Various Spectrum Management and Spectrum Sharing Use Cases

All investigations within the working package devoted to spectrum management have been conducted in two parallel ways, creating two pillars of the spectrum sharing research. The first one was related to the high-level design of the spectrum management architecture as part of the whole COHERENT system (and was presented in preceding chapters), the second, on the other hand was devoted to the development of new, advanced spectrum sharing schemes in intra-operator and inter-operator sharing scheme, as well as in micro-scale sharing. The selected results are presented in detail below.

7.1. Inter-Tier Resource Allocation Problem for HetNets

Goal of the study and connection to the COHERENT architecture

We address the problem of sharing frequency resources in the context of intra-operator spectrum sharing. We formulate an inter-tier resource allocation problem in a HetNet as an optimization problem, aiming to maximize a network sum utility function. We provide an algorithm to determine the amount of resources with muted transmission in each tier. The algorithm is executed in the COHERENT SMA, taking as input abstracted parameters from the network, aiming to have a low signalling overhead. The algorithm returns the amount of muting for each tier to the base stations or RTCs in the HetNet.

Task covered:

This work covers the activities undertaken within Task 4.1 (intra-operator spectrum sharing).

Managing interference is a crucial topic in HetNets with a frequency reuse factor of 1. We study the problem of allocating orthogonal and non-orthogonal frequency resources, considering different tiers. In inter-tier resource allocation, the principle is to coordinate transmission of nodes using resources non-orthogonally, as well as orthogonally, between different tiers (i.e. cell categories). Non-orthogonal transmissions occur simultaneously between tiers. Inter-tier orthogonal resources are obtained by muting transmission in other tiers. In this context, muting transmission is equivalent to muting the resources assigned to the transmission. Muting allows protecting users in other tiers from harmful interference, and thus benefit from a higher Signal-to-Interference-plus-Noise Ratio (SINR). Examples of users that benefit of muting include users in the Cell Range Extension (CRE) region, femto-cell users in a Closed Subscriber Group (CSG), and Device-to-device (D2D) user pairs.

Allocation of orthogonal and non-orthogonal frequency resources is formulated as an optimization problem. The objective in the optimization is to maximize a system utility function, over the set of scheduling weights of all the users, for different muting conditions. The system utility function is the aggregation of the utilities of the users.

Below we describe a system model for inter-tier resource allocation, with muting in two tiers. Next, we develop a heuristic algorithm to determine an approximate solution, abstracting the user population with a reduced number of parameters. Finally, we test the algorithm in two HetNet scenarios, and compare its performance to a global solution.

7.1.1. System Model for Inter-Tier Resource Allocation Problem with Muting in Two Tiers

Muting in two tiers is motivated by the possibility to extend coordination to HetNets. We address here the case of downlink transmission. In the problem formulated here, the term small cell is used to refer to a cell smaller than the macro cell and operating in the same coverage area, underlying macro cell transmissions. Examples of cells categorized here as small cell are femto-cells, pico-cells, and D2D pairs. The formulation covers e.g. Macro-Femto, Macro-D2D, and Macro-Pico cases. . For D2D communication as made possible by LTE-Advanced, a generalization to uplink is needed. Protection of macro cellular users from D2D interference can be realized by power control, where instead of the power allowed by conventional uplink power control, an additional power reduction is applied. Then,

muting macro transmissions with similar resource allocation methods as discussed below will benefit D2D users that suffer from damaging macro interference. Such an arrangement would be transparent for legacy cellular uplink use.

Figure 16, depicts as example an arrangement of users and resources for a downlink scenario, consisting of one macro cell and two small cells. The fraction of resources for each user is represented by a scheduling weight *w*. In each resource a user experiences a spectral efficiency, which is an abstraction of the physical layer of the network. Macro cells mute resources to benefit small cell users, whereas small cells mute resources to benefit macro cell users. In the figure, we observe that resources at both sides can be muted to provide orthogonal, protected, resources to the users in the other tier. On the other hand, resources in the middle can be shared non-orthogonally between tiers.

In our system model, there are *M* macro users associated to a macro cell, arranged in the set $\mathcal{M}$. There are *C* small cells arranged in set $\mathcal{C}$. There are $S(c)$ users in small cell *c*, which are arranged in the set $\mathcal{S}(c)$. When a small cell represents a D2D communication pair, there is only one user in that cell. The union of all the sets of small cell users is $\mathcal{S}$.

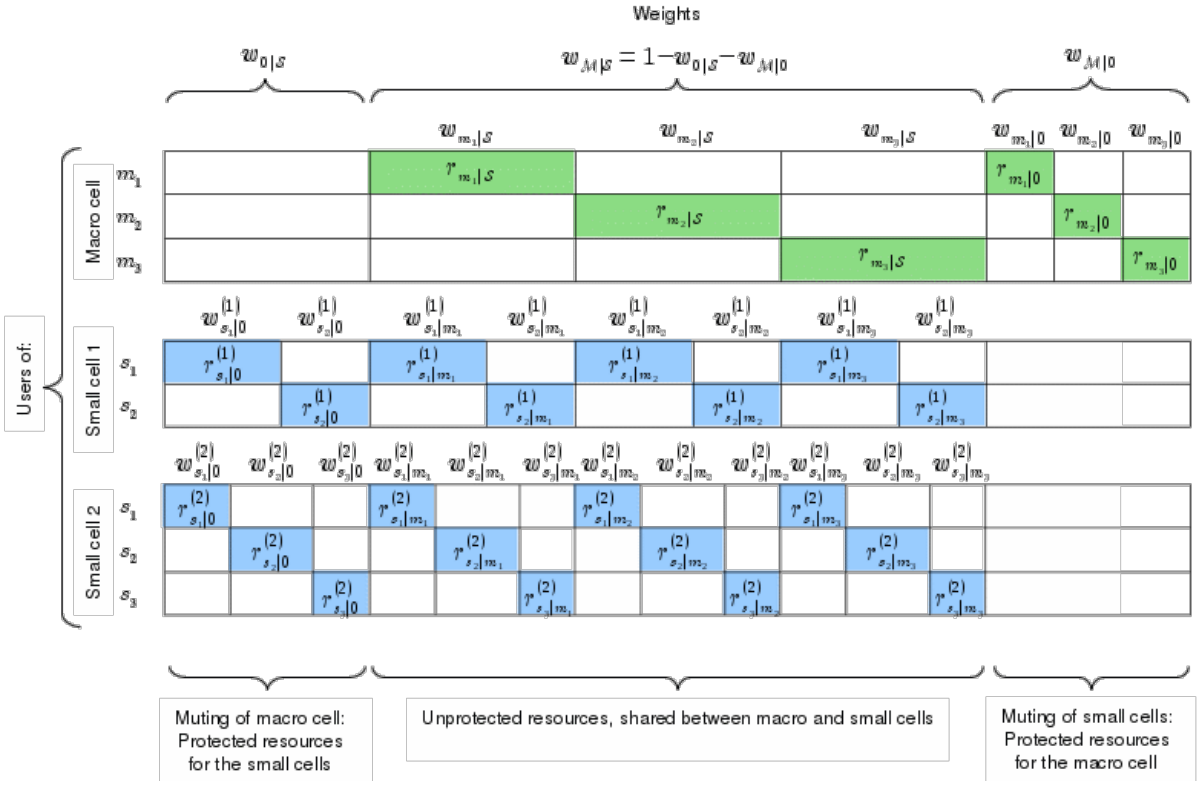

Figure 16. Arrangement of users and resources in a two-tier scenario with two small cells and a macro cell.

In the example of Figure 16, small cells are muted in a fraction $w_{\mathcal{M}|0}$ of the total resources, to protect macro cell users. The macro cell schedules its users *m*, having a spectral efficiency $r_{m|0}$, in fractions $w_{m|0}$, as shown in the figure. Macro cells are muted in a fraction $w_{0|\mathcal{S}}$ of the total resources, to protect small cell users. Each small cell schedules its users *s*, having a spectral efficiency $r^{(c)}_{s|0}$, in fractions $w^{(c)}_{s|0}$, as shown in the figure, where the indexing $s|0$ is from the perspective of the small cell. For non-orthogonal transmission between the tiers, the macro cell schedules its users, having a spectral efficiency $r_{m|\mathcal{S}}$, in fractions of resources $w_{m|\mathcal{S}}$, Each small cell *c* schedules its users, having a spectral efficiency $r^{(c)}_{s|m}$, in fractions of resources $w^{(c)}_{s|m}$. The corresponding spectral efficiencies are a function of the SINR experienced by the user when transmission in the other tier is muted and non-muted. The total amount of resources in the system is normalized to 1. Hereafter, $w_{\mathcal{M}|0}$ and $w_{0|\mathcal{S}}$, are referred to as orthogonalization weights.

The data rate of the users is directly proportional to the allocated amount of resources. The expected rate of a macro user *m* is,

$$x_m = w_{m|S} r_{m|S} + w_{m|0} r_{m|0},$$

and the data rate of a small cell user *s* is,

$$x_s^{(c)} = w_{s|0}^{(c)} r_{s|0}^{(c)} + \sum_{m \in M} w_{s|m}^{(c)} r_{s|m}^{(c)}.$$

We formulate the optimization problem with a network utility function. We assume that macro and small cell users, in general, are of the same type, in the sense that there is no hierarchical level of importance of one kind of user over the other. For this, we assume that user well-being is characterized by an α-proportionally fair utility function,

$$u(x) = \begin{cases} \frac{1}{1-\alpha} x^{1-\alpha} & \text{for} \quad \alpha \neq 1 \\ \log(x) & \text{for} \quad \alpha = 1 \end{cases}.$$

The α-parameter can be used to set the degree of fairness. In the context of cellular networks, α can be used to determine the trade-off between capacity and coverage. The sum utility function of the users in the macro ell, and in small cell c, is

$$U_m = \sum_{m \in M} u\,(x_m),$$

$$U_c = \sum_{s \in S^{(c)}} u\left(x_s^{(c)}\right),$$

respectively. The network utility is

$$U = U_m + \sum_c U_c.$$

Our objective is to maximize the sum utility in the network, over the set of all scheduling weights. We assume that the resources are infinitely divisible, so that the scheduling weights are continuous variables.

For a required level of fairness, an optimal solution will balance the amount of protected and unprotected resources assigned to the cells. The optimization objective is

$$W^* = \text{argmax}_W U.$$

Here, the convex set of scheduling weights is

$$W = \{w_{m|0}, w_{m|S}, w_{s|0}^{(c)}, w_{s|m}^{(c)}\}_{(m,c,s) \in M \times C \times S^{(c)}},$$

subject to having non-negative scheduling weights, and

$$w_{0|S} + w_{M|S} + w_{M|0} = 1,$$

where $w_{M|S}$, is the scheduling weight for non-orthogonal resources.

The problem is convex, it can be solved by centralizing all the spectral efficiencies, and executing a gradient search algorithm looking for the global maximum. However, the cost in signalling overhead and computing becomes a problem when the number of nodes in the network increases. We proceed next to propose a method to calculate an approximate solution, requiring a smaller overhead in the information to be centralized.

7.1.2. Heuristic Algorithm for Determining Orthogonalization Weights

An alternative to a gradient search algorithm, with complete centralized information, is to develop an algorithm that returns an approximation of the orthogonalization weights $w_{M|0}$ and $w_{0|S}$. These weights are determined in the COHERENT SMA, and communicated to base stations in the HetNet. Each base station then adjusts the local scheduler to mute resources according to the orthogonalization weights.

In the algorithm proposed next, the goal is to get a solution for the orthogonalization weights, $w_{M|0}$ and $w_{0|S}$, from a classification of the type of users, based on instantaneous and/or historic results. To describe the characteristics of the user population, each small cell c first classifies its users, and the macro users, to victim/non-victim users. Where, victim users, can be determined for example, by a threshold in their SINR. The numbers of victim/non-victim macro cell users are denoted $N^{(c)}_{mv}$, and $N^{(c)}_{mn}$, and the numbers of victim/non-victim small cell users are denoted $N^{(c)}_{sv}$, and $N^{(c)}_{sn}$. Victim users are allocated only protected resources, and non-victim users only non-protected resources. The resulting average spectral efficiencies $r^{(c)}_{mv}$, $r^{(c)}_{mn}$, $r^{(c)}_{sv}$, and $r^{(c)}_{sn}$, of the user classes are then calculated. The numbers of users, and their average spectral efficiencies are communicated to the COHERENT SMA. The SMA aggregates the opinions of the small cells into system level averages of spectral efficiencies, r_{mv}, r_{mn}, r_{sv}, and r_{sn}, and numbers of users N_{mv}, N_{mn}, N_{sv}, and N_{sn}.

The user population is then abstracted by a set of representative users. A scheduling problem is then formulated to maximize the sum utility of this representative user population. The scheduling weights involved are $w_{M|0}$, $w_{M|S}$, and $w_{0|S}$. The representative victim/non-victim, macro/small cell user then has the expected data rate

$$x_{\mathrm{mv}} = \frac{w_{M|0}}{N_{\mathrm{mv}}} r_{\mathrm{mv}},\ x_{\mathrm{mn}} = \frac{w_{M|S}}{N_{\mathrm{mn}}} r_{\mathrm{mn}},\ x_{\mathrm{sv}} = \frac{w_{0|S}}{N_{\mathrm{sv}}} r_{\mathrm{sv}},\ x_{\mathrm{sn}} = \frac{w_{M|S}}{N_{\mathrm{sn}}} r_{\mathrm{sn}}.$$

The sum utility function is

$$U_{\mathrm{UC}} = N_{\mathrm{mv}} u(x_{\mathrm{mv}}) + N_{\mathrm{mn}} u(x_{\mathrm{mn}}) + C\left(N_{\mathrm{sv}} u(x_{\mathrm{sv}}) + N_{\mathrm{sn}} u(x_{\mathrm{sn}})\right),$$

where C is the number of small cells. The weights constraint is

$$w_{0|S} + w_{M|S} + w_{M|0} = 1.$$

In this case, all weights are non-zero, so we have the Lagrangian,

$$L_{\mathrm{UC}} = U_{\mathrm{UC}} + \lambda\left(1 - \left(w_{0|S} + w_{M|S} + w_{M|0}\right)\right),$$

which yields

$$w_{0|S} = \lambda^{-\frac{1}{\alpha}} C^{\frac{1}{\alpha}} N_{\mathrm{sv}} r_{\mathrm{sv}}^{-1+\frac{1}{\alpha}},$$

$$w_{M|S} = \lambda^{-\frac{1}{\alpha}} \left(r_{\mathrm{mn}} \left(\frac{r_{\mathrm{mn}}}{N_{\mathrm{mn}}}\right)^{-\alpha} + C r_{\mathrm{sn}} \left(\frac{r_{\mathrm{sn}}}{N_{\mathrm{sn}}}\right)^{-\alpha} \right)^{\frac{1}{\alpha}},$$

$$w_{M|0} = \lambda^{-\frac{1}{\alpha}} N_{\mathrm{mv}} r_{\mathrm{mv}}^{-1+\frac{1}{\alpha}}.$$

To solve for the Lagrange multiplier λ, we require the sum of these to be one, leading to

$$\lambda = \left(N_{\mathrm{mv}} r_{\mathrm{mv}}^{-1+\frac{1}{\alpha}} + C^{\frac{1}{\alpha}} N_{\mathrm{sv}} r_{\mathrm{sv}}^{-1+\frac{1}{\alpha}} + \left(r_{\mathrm{mn}} \left(\frac{r_{\mathrm{mn}}}{N_{\mathrm{mn}}}\right)^{-\alpha} + C r_{\mathrm{sn}} \left(\frac{r_{\mathrm{sn}}}{N_{\mathrm{sn}}}\right)^{-\alpha} \right)^{\frac{1}{\alpha}} \right)^{\alpha}.$$

The estimates of the orthogonalization weights $w_{M|0}$ and $w_{0|S}$ are then used as an approximation to the global solution.

An algorithm can be implemented operating at different time scales. Here, two variants are considered. In both of them, the average spectral efficiencies, r_{mv}, r_{mn}, r_{sv}, and r_{sn}, are collected from historical information, and used without considering the instantaneous network state.

1) Static orthogonalization: in this variant, also the numbers of users N_{mv}, N_{mn}, N_{sv}, and N_{sn}, are collected from historical information. The orthogonalization weights are static.

2) Instantaneous classification: in this variant, the classification of the users is performed in a shorter timescale, e.g., in each frame. The instantaneous numbers N_{mv}, N_{mn}, N_{sv}, and N_{sn}, are reported regularly to the SMA.

Next, we study the performance of the heuristic algorithm with the two variants. It will be shown that the heuristic algorithm considered shows a feasible way to approximate the global solution with limited and abstracted signalling.

7.1.3. Numerical Results

In the following examples we model two HetNet scenarios with a customized system simulator. We assume a saturated system transmitting in DL with infinite buffer model. The system is static during each network instance. Frequency selective fast fading is not modelled. Perfect, non-quantized, SINR information is assumed. A spectral efficiency cut-off is applied to represent the maximum allowable Modulation and Coding Scheme (MCS). The system is assumed to be perfectly synchronized, and muted resources are totally muted. Infinitely subdivided resources are assumed.

The layout common to the two HetNet scenarios consists of seven circular macro cells, based on [ITU-R M.2135]. Each macro cell has a base station in the centre, transmitting in downlink. The algorithm with the two variants is evaluated for users in one of the three sectors of the central cell. The six cells surrounding the main central cell act as interferers toward the users in the central cell. These are located following a hexagonal pattern with an inter-site-distance (ISD) of 1000 meters [ITU-R M.2135]. Tables Table 3, Table 4 and Table 5, summarizes the parameters for the scenarios.

Simulations are executed in 1000 network instances for a given value of fairness α. In each instance, users are dropped in the scenario with a uniform probability distribution, and the resulting path losses, SINR and spectral efficiencies are calculated for modes of transmission using protected and unprotected resources. A numeric solution of the scheduling weights is calculated using a gradient search algorithm, assuming centralized knowledge of all the spectral efficiencies in the system. Results are evaluated in terms of the trade-offs between network coverage and capacity for different values of fairness α. Coverage is measured by an outage point, which is taken to be the 5% point of all the users' data rate. Capacity is measured by the mean of all the users' data rate in the system.

Table 3 Parameters common to both scenarios

Parameter	Setting
Macro cell radius (sectors)	500 meters (120 degrees)
Number of macro users M	4
Number of small cells C	2
Other interferences	Surrounding tier of macro cell base stations
MBS Tx Power	46 dBm
User receiver noise figure	9 dB
Shadow (Fast) fading Std. Dev.	4 dB (None)
Thermal noise level	-174 dBm / Hz
Path loss model	L = 128.1 + 37.6 log10 d (d: distance in km.)
SINR to rate mapping	Shannon rate formula
Spectral efficiency cut-off	6 b/s/Hz

Table 4 Macro-femto scenario - specific parameters

Parameter	Setting
Indoor ratio θ	50 %
Number of users per femto cell F	3
Building wall attenuation	8 dB

Femto-BS Tx Power	8 dBm
Building size	30 x 30 m

Table 5 Macro-pico scenario specific parameters

Parameter	Setting
Number of users P_{NoCRE} (P_{CRE})	2 (1)
Cell Range Extension bias	6 dB
Minimum distance between pico cells	120 meters
Pico-BS Tx Power	30 dBm

Macro-Femto Scenario in downlink

1) Simulation scenario: The HetNet consists of the macro cell network, and C non-overlapping buildings uniformly distributed in the sector of the central macro cell. The centre of the building is at least 30 meters from the macro cell base station. Each building consists of one room of 30 x 30 meters, with one floor. One femto cell base station is located in the centre of the room forming a network operating in CSG mode.

In each simulation instance users are placed in random locations with a ratio $\theta = 50\%$ of indoor users; there are θM macro-indoor users uniformly distributed inside the buildings, and $(1-\theta)M$ macro-outdoor users, uniformly distributed in the cell sector, outside the buildings and at least 10 meters from the macro base station. F femto users are located uniformly in the ring cantered at the centre of the room, with an inner radius of 3 meters and outer radius of 13 meters. The scenario is represented in Figure 17. Additional parameters are listed in Table 3, and Table 4.

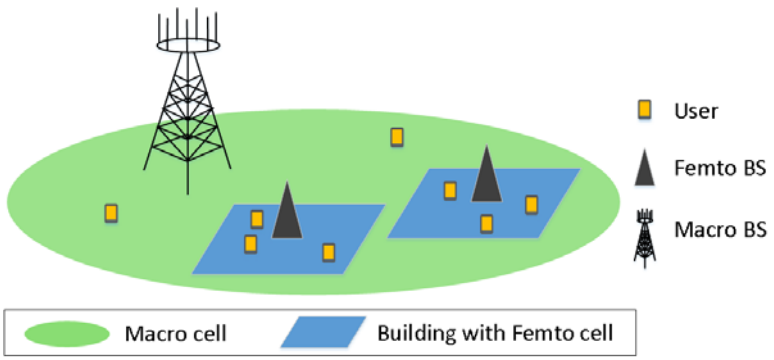

Figure 17. Representation of Macro-Femto scenario. The example shows four macro users deployed in the cell sector of the macro cell base station. Two are outdoor-macro users, and two are indoor-macro users, one in each building. Buildings contain one femto BS operating with a CSG.

2) Simulation results: Figure 18 shows the performance obtained for different α. The two variants of the algorithm perform close to the centralized solution for $\alpha < 1$, and deviate slightly as α grows larger than 1. As expected, the instantaneous classification variant performs better than the static orthogonalization one. The difference grows for large α, which is understandable, as the higher fairness is strived for, the more important instantaneous information becomes. With increasing α, many resources are allocated to the few users which have a low rate.

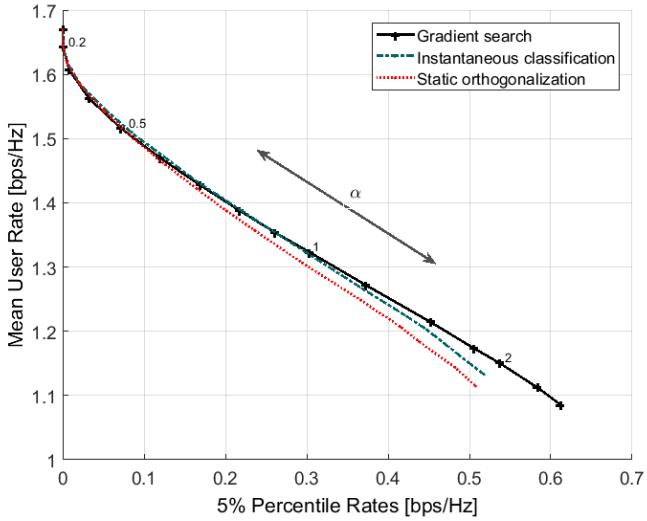

Figure 18. Coverage-capacity trade-off curves in Macro-Femto scenario. Setting for 4 macro users, of which 2 are indoor users, and 2 femto cells with 3 femto users each one in CSG. Numbers along the curves denote values of α.

Macro-Pico Scenario in downlink

1) Simulation scenario: The HetNet consists of the macro cell network, with non-overlapping pico cells separated at least by 200 meters, distributed uniformly in the sector under consideration in the central macro cell, the centres of the pico cells are between 105 and 450 meters from the central macro cell base station.

In each simulation instance users are uniformly distributed in the macro cell sector. Users are associated to the cell which has the higher received power considering a CRE bias applied to the pico cells. Situation with M macro cell users, P_{NoCRE} conventional pico cell users, and P_{CRE} pico cell users inside the CRE region are chosen. The scenario is represented in Figure 19. Additional parameters are listed in Table 3, and Table 5.

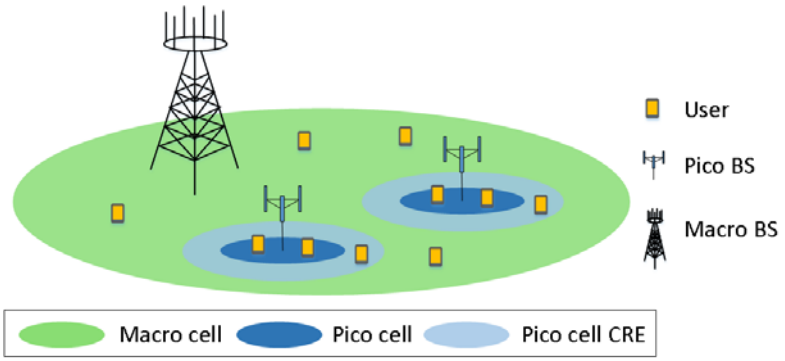

Figure 19. Representation of Macro-Pico scenario. The example shows four macro users deployed in the cell sector of the macro cell base station, and two pico-cells, with 3 users each one, of which one user is in the CRE region.

2) Simulation results: Figure 20shows the performance obtained for different α. The two variants of the algorithm perform close to the centralized solution. The instantaneous classification variant performs only slightly better than the static orthogonalization one.

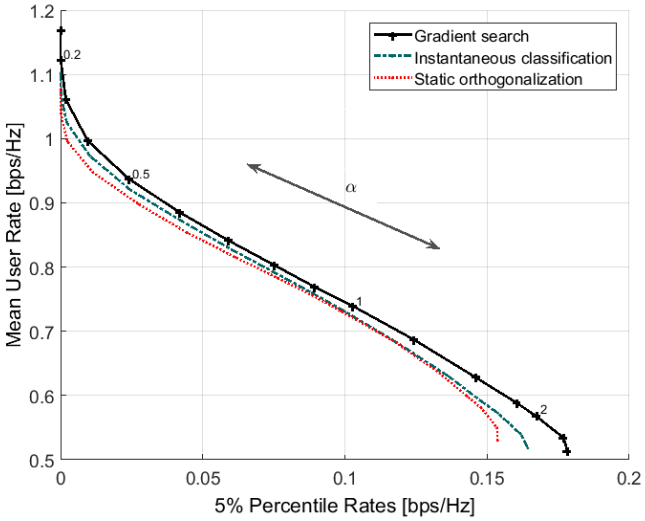

Figure 20. Coverage-capacity trade-off curves in Macro-Pico scenario. Setting for 4 macro users, and 2 pico-cells with 3 pico-users each one, of which one is in the CRE region. Numbers along the curves denote values of α.

7.1.4. Summary

In this section, performance evaluation of intra-operator spectrum sharing was considered. Methods to divide the bandwidth between a macro cell, and small cells under its umbrella coverage were considered. The problem was formulated in downlink direction, and performance was evaluated by Monte Carlo simulations in a macro-femto and macro-pico scenario. The results show the efficacy of the considered inter-operator spectrum management method. With a centralized solution based on limited measurement information conveyed to the SMA, the performance is nearly as good as for a centralized solution with full information of the user channel qualities. More details on the spectrum network management algorithms and the performance evaluation can be found in [Lembo_2017b, Chapter 3], and [Lembo_2017_c].

7.2. Fine-Grained Spectrum Sharing in Multi-Tenant RAN

Goal of the study and connection to the COHERENT architecture

This section presents a study on using the COHERENT spectrum management architecture to enable very fine-grained time and frequency domain spectrum sharing. A multi-tenant RAN scenario is considered where the SMA defines the parameters for the spectrum sharing among RAN tenants and the COHERENT control entities, particularly the RTC implements them in the RAN cells. Per RAN tenant load, derived at the cell level is considered as the main input to exchanging spectrum favours among the RAN tenant. At the SMA level, the number of tenants, their dedicated resources and the policy that controls the spectrum sharing granularity are defined based on SMA knowledge base.

Task covered:

- Task 4.1
- Task 4.2

7.2.1. Motivation & Goals

The global network traffic is increasing at an unprecedented rate along with demands for more innovative and immersive applications [CISCO_2016]. In addition, new technologies such as Software-Defined Networking (SDN) and Network Function Virtualization (NFV) have created scope for a new network architecture and resource management & control practices. The 5G networks development roadmap targets a convergence of new technologies, including SDN and NFV, to address the capacity and QoS challenges but also create an elastic network infrastructure for efficient service addition and delivery. SDN and NFV in particular, make it easier to bring new services to the end-users in a time and resource efficient manner. They also enable new players (service providers, virtual network operators etc.) to use a shared (multi-tenant) network infrastructure. Important resources that can be shared in the context of multi-tenant 5G networks include the RAN and RF spectrum, for which, several models of sharing can be realized including mutual renting, co-primary sharing and spectrum leasing [Yang_2016]. RAN and spectrum sharing are expected to be an integral part of a multi-tenant 5G network architecture. Figure 21 shows an abstract representation of the three main network segments where tenant-specific resource slices can be allocated i.e., the Core, Backhaul and RAN, based on the classic SDN architecture where control application located at a higher abstraction manage control elements located near the physical elements.

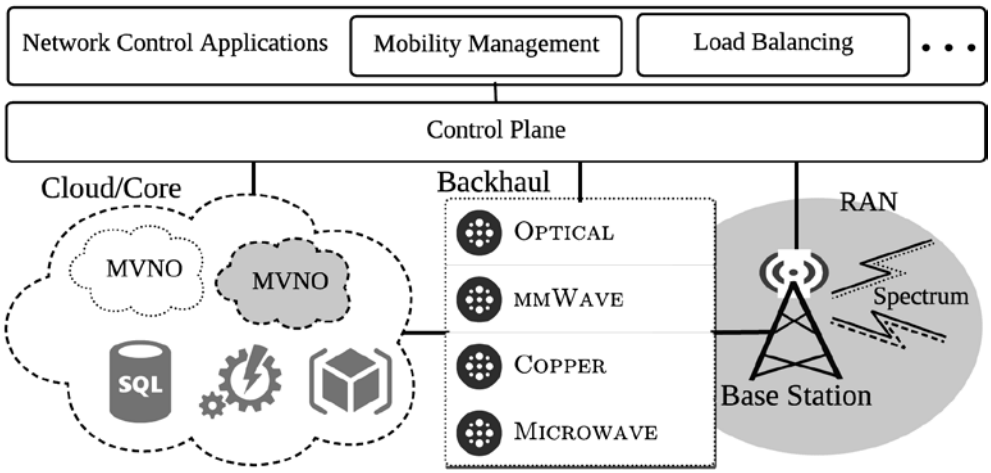

Figure 21. Centralized network management and control architecture

In such a software-defined, multi-tenant network architecture, where distributed control elements deployed at different locations communicate with a centralized network controller, the resource sharing models can be realized actively and with a very fine-grained time frequency granularity. Therefore, the main motivation for this study was to investigate a centralized, active RAN and spectrum sharing approach in a multi-tenant 5G RAN based on the COHERENT network management and control architecture.

7.2.2. Network Architecture & System Model

As it has been already stated, most of the opportunistic and dynamic spectrum access concepts have not materialized for many reasons. These include, i.e., the rigidity of the legacy network architectures, as well as deficient spectrum sensing and the competitive nature of network operators. RAN sharing has also been considered, albeit mostly passively, in the form of base-station location, mast, power and cooling infrastructure sharing. The 5G network architecture is expected to change this with the realization of multi-tenant networks including shared RAN. This architecture has the potential to facilitate achieving significantly more benefits than the passive RAN sharing options considered thus far.

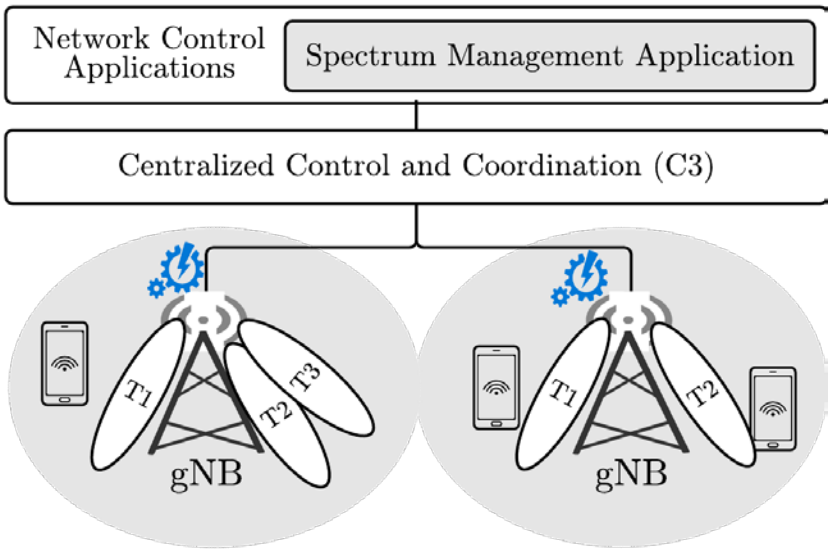

Figure 22. Multi-tenant RAN architecture with hierarchical control elements

Figure 22 shows the considered multi-tenant RAN architecture within the scope of COHERENT spectrum management and control framework. The spectrum management application (see D4.1 for detailed specifications) is responsible for overall control and management of radio resource in the network. However, at that abstraction level, fine-grained resource allocation such as slice/tenant specific scheduling, issues that are severely time constrained, cannot be addressed. The architecture therefore provides real-time control elements (called Real Time Controllers, RTCs) that are located close to the real radio transmission elements (indicated by blue gears in Figure 22). In essence, the spectrum management application sitting on top of the centralized control layer makes high level configuration decisions such as bandwidth allocation to RAN tenants, allowing/disallowing spectrum sharing in network segments and etc.. At the same time, control entities located in base station/eNB/gNB translate those higher-level directives into low-level control decisions related to spectrum sharing. In our system model, a RAN tenant takes a dedicated slice of radio resources that do not overlap the resources of other RAN tenants. With this system architecture in perspective, a very fine-grained, active spectrum sharing approach can be realized where micro-transactions of spectrum favours are carried out among RAN tenants while the whole RAN being controlled, at a higher abstraction, by a centralized spectrum management application.

7.2.3. Control elements & Abstractions

The 5G multi-tenant RAN concept is expected to manifest itself in the form of shared base stations with a certain degree of tenant-specific resource isolation guarantees. While this can be realized at several abstraction levels above the physical layer, a well-qualified option is maintaining radio resource segmentation and management using distinct slice-specific medium access control procedures including resource scheduling. To make the subsequent description specific for such a scenario, we shall consider the tenants to be virtual LTE networks sharing an eNodeB. Figure 23 shows the fundamental functional control components interfaced with the internal architecture of the eNB protocol stack and their associated functions. There are two added control elements namely, the controller and PHY-Coordinator. The controller is responsible for not only allocating dedicated resources to specific tenants but also, within the fine-grained spectrum sharing scope, facilitating spectrum favour exchange among the allocated tenants. The controller is transparent to the slice-specific data streams but integrates into the resource management and sharing functions. With this architecture, each eNodeB supports an array of tenant-specific medium access control (MAC) submodules which are coordinated by the controller and PHY coordinator. The amount of dedicated resources allocated to a particular tenant is decided at the spectrum management application level. In addition, other parameters (described later) that are used to specify an acceptable spectrum offers are also associated with the spectrum management application.

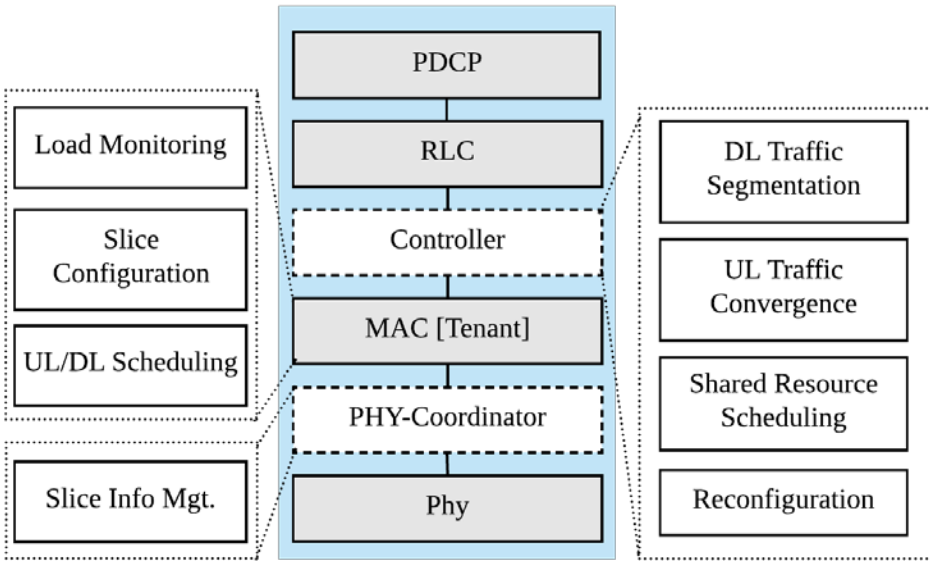

Figure 23. eNodeB protocol stack with added control elements for spectrum sharing

To support spectrum favour exchange, the individual tenant specific slices derive load specific abstractions that are exposed to the controller. Each MAC submodule observes the load in its dedicated resources (number of used/available resource blocks), derives, if possible, spectrum sharing offers, and exposes them to the controller with a specified time-out. The spectrum offer abstraction is based also on the configurations specified by the controller. The controller subsequently facilitates the exchange of these favours, in very fine-grained time-frequency granularity, among the RAN tenants. Each MAC module is independent with its own set of scheduling policy and modulation and coding scheme to manage uplink and downlink traffic of slice-specific User Equipments (UEs). The PHY-Coordinator module is more generic and only coordinates the access to the physical layer.

7.2.4. Spectrum Sharing Granularity

Spectrum sharing among RAN tenants guarantees quantifiable benefits in the overall cell performance metrics. However, identifying and using the most suitable time-frequency granularity is not trivial and depends largely on real-time network load and interference situation. In time-domain, as LTE networks use a well-defined frame structure for radio resource allocation, the most fine-grained option of spectrum sharing is one Transmit Time Interval (TTI), which is equal to $1ms$. This is the most granular level of time-domain resource sharing model achievable in LTE/LTE-A networks. However, sharing radio resources at this time granularity does require real-time computation of tenant-specific network load and almost no latency to communicate/expose any offers or requests to the controller. Specifically, a tenant must compute its uplink/downlink spectrum requirement per TTI, determine if excess is available for sharing, expose it to other tenants, and the cell has to make the necessary re-configurations to scale up or down the resource pool of the involved tenants. While physical or technological constraints will be a challenge, on one hand, this granularity level guarantees the most effective use of overall spectrum resources in the considered multi-tenant RAN context. On the other hand, for consideration such as latency, load computation and tenant isolation, this fine-grained resource sharing among tenants may not be practical in real systems without making a compromise on some of these parameters. For a comparative evaluation however, we do consider spectrum sharing at this level of time-domain granularity to serve as an upper-bound for the achievable benefit of spectrum sharing. For our evaluation, we focus on downlink where each tenant computes its resource block requirements from the data buffers, the number of attached UEs and the channel feedback reports. From these parameters, a tenant offers excess resources, if available, to the other tenants in real-time via the controller. The controller module can coordinate the resource exchanges among tenants by doing runtime reconfiguration of the bandwidth allocated to each tenant. The higher end of the time-domain granularity for spectrum sharing is subject to many considerations including its benefits (e.g., achievable throughput) and interference concerns. Furthermore, in multi-cell dense deployments, identifying the most suitable cells and tenants for shared resource allocation becomes a non-trivial problem to solve.

In the frequency-domain, the most fine-grained spectrum sharing option in LTE/LTE-A is a single physical resource block (equal to 180 kHz). Beyond this minimum, the frequency domain sharing is constrained by the overall dedicated bandwidth available to the slice and the rules for spectrum exchanges. In addition, practical limitations such as the possibilities of aggregating additional spectrum will determine the actual specification of frequency-domain granularity for spectrum sharing.

For this study we have developed a system level simulation model based on the architecture described below (see Section 8.1.3). Figure 24 shows the basic configurations options available at the eNodeB considered for active spectrum favour exchanges. While most of the configuration options are self-explanatory, the options that control the time-frequency granularities are the *componentCarrierSharing*, *keepReserve*, *reserveValue*, *sharingInterval* and *calculationMethod*. The c*omponentCarrierSharing* parameter controls the conformance of the shared bandwidth to the LTE/LTE-A standard i.e., when set to true, six Physical Resource Blocks must be shared at the very minimum among RAN tenants. The *keepReserve* parameters allow tenants to enable spectrum sharing in a subset of its dedicated resource blocks with its reserved bandwidth controlled by *reserveValue* parameter. Setting *keepReserve* to false in essence means that a tenant could potentially go into a sleep/no-service state when there is no DL traffic. The *sharingInterval* (given in TTI) is the main time-domain granularity parameter and controls the duration of spectrum sharing offers. Finally, the *calculationMethod* controls the estimation function used by a tenant's MAC module to estimate its offer and request granularity in frequency domain rather than relying on real-time load.

```
numberOfTenants          = default(2);
enableResourceSharing    = default(false);
componentCarrierSharing  = default(false);
keepReserve              = default(false);
reserveValue             = default(6);
sharingInterval          = default(10);
calculationMethod        = default(Avg);
```

Figure 24. Parameters defining fine-grained spectrum sharing

7.2.5. Evaluation

For this study, we carried out simulation analysis using a modified SimuLTE model to analyse the benefits of active spectrum sharing (see Section 6.3). Figure 25 presents the main configuration parameters used for the simulation analysis. A single cell having two tenants has been considered to analyse the potential benefits and trade-offs of different time-frequency granularities. The following set of configurations for the eNodeB has been used. **1T**: Single cell with one tenant taking all the available bandwidth and simulated UEs. This is similar to a traditional eNodeB having no multi-tenancy feature.

2T-NS: Single eNodeB having two tenants taking equal cell bandwidth but not allowing any exchange of spectrum favours. **2T-FS:** Single eNodeB having two tenants allowing spectrum sharing per alternate radio frame. In this configuration, each tenant evaluates its average DL resource block utilization in a single frame i.e., 10ms and offers the excess, if available, to the other tenant in the subsequent frame. The other tenant may or may not accept the offer depending on its own real-time traffic in the slice. **2T-TS:** One cell and two tenants allowing resource sharing at each TTI i.e., 1ms time-interval. In this configuration, no latency is assumed in the overall sharing process.

	Parameter	Value	Parameter	Value
General	No. of Cells	1	No. of UEs	5-20
	No. of Tenants	1-2	UE Mobility	RandomWP
	Sim Area	1 Sq Km	Geography	Urban Macro
PHY Layer	eNB Tx Power	10W	Frequency	2100MHz
	eNB Bandwidth	10-20 MHz	Slice Bandwidth	5MHz
	Antenna config	Omni-directional	eNB Height	25M
MAC Layer	eNB Scheduler	Max CQI	Queue Size	1MB
Application	Apps per UE	1	UE Application	Video
	App Packet Size	1500B	Pkt Send	2ms

Figure 25. Evaluation parameters for the simulated scenarios

Figure 26 (A) shows the joint average cell throughput (sum of both slices) of the four different configurations described above. The results are provided in general box plots showing the lower and upper bounds, average across runs, median and outliers. The figure clearly shows the benefits of resource sharing including the effects of realizing this at different time-intervals. In the 1T configuration, all resources and UEs belong to a single scheduler, which makes scheduling decisions using maximum CQI based scheduler. All things being equal, the 1T scenario serves as an optimum reference for the spectrum sharing scenarios. This result confirms that the more granular the spectrum sharing, the closer we get to the optimum and therefore, architecture pursuing and supporting fine-grained spectrum sharing should be prioritized in a multi-tenant RAN. The same can argument is supported by Figure 26 (B), where the average DL resource block utilization is shown. It is evident that the downlink resource utilization for the cell increases with the granularity of spectrum sharing. Figure 27 which depicts the impact of spectrum sharing granularity on the UE application layer throughput further strengthens the argument that in a multi-tenant RAN, the most granular levels of spectrum sharing should be pursued.

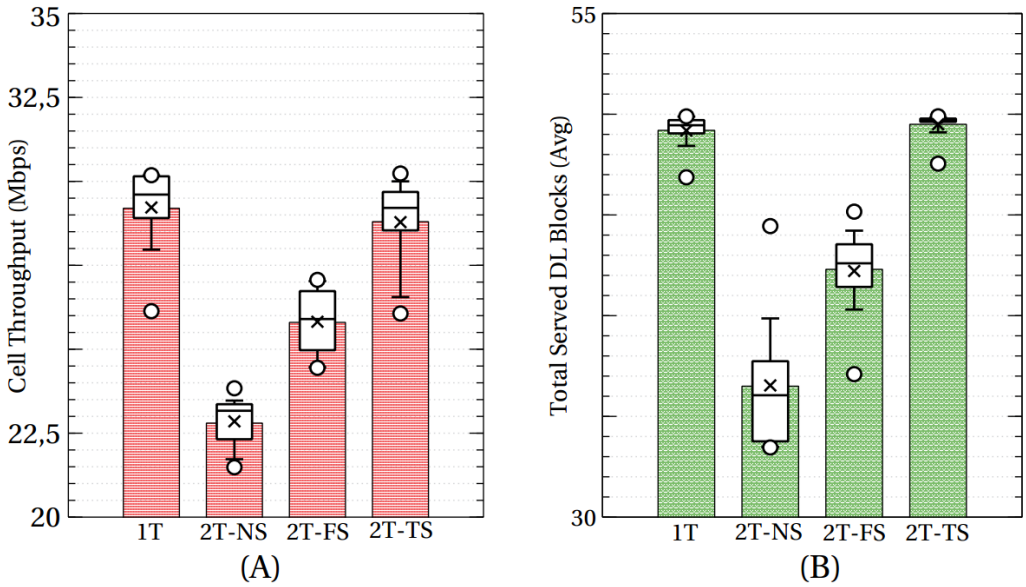

Figure 26. Average cell throughput and DL resource block allocation

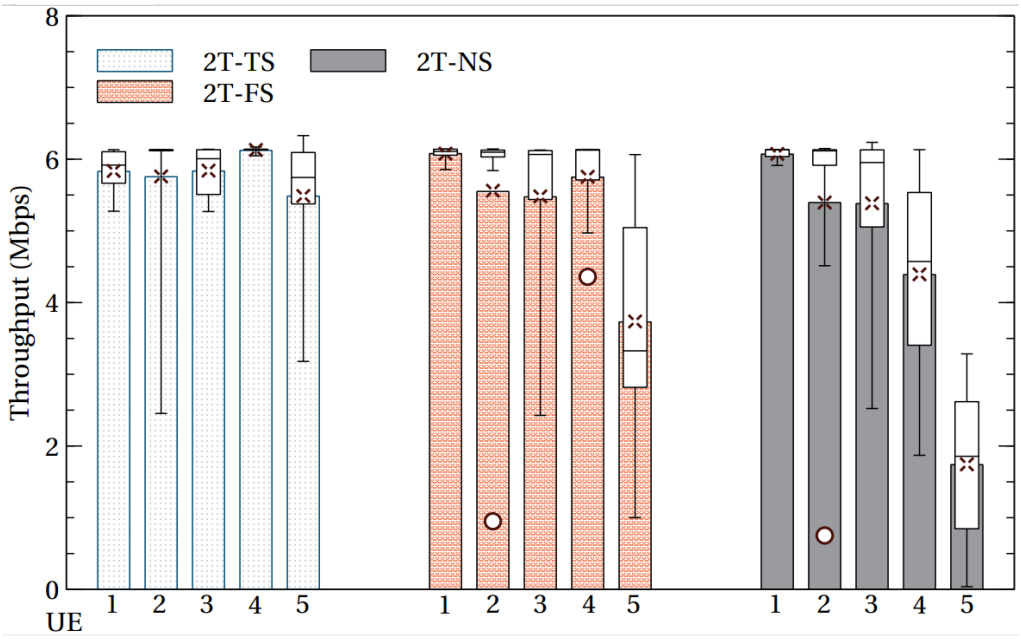

Figure 27. Average UE application layer throughput

Figure 28 shows the impact of slice-specific load variance (given in number of UEs per slice) on the achievable cell throughput. As the load in a particular slice goes down, simple RAN multi-tenancy without spectrum sharing results in wastage of significant radio resources. In contrast, allowing fine-grained spectrum sharing among RAN tenants avoids this micro-level wastage of radio resources. This gives further arguments for RAN tenants or infrastructure-providers to aim at achieving the most fine-grained active, RAN and spectrum sharing implementation practically possible. However, competition, isolation concerns and complex RF environments will make the selection of optimum time-frequency granularity a complex problem and an important research topic to investigate.

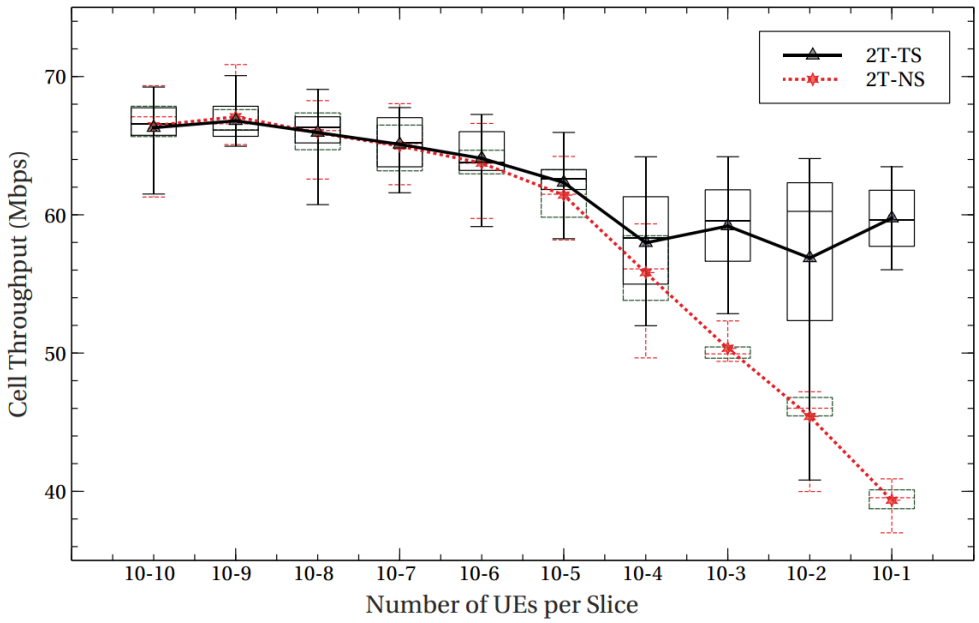

Figure 28. Cell throughput as function of slice specific load variance

7.2.6. Summary

In this study, a fine-grained spectrum sharing approach was presented in the context of multi-tenant 5G RAN and the COHERENT spectrum management architecture. A candidate control and management

architecture was presented to support a very fine-grained spectrum sharing approach together with evaluation results. With this architecture and control framework, micro-level radio resource wastage can be avoided to the benefits of all the RAN tenants.

7.3. Fine-Grained Scheduling of Co-Primary Shared Spectrum

Goal of the study and connection to the COHERENT architecture

Continuing from the previous section, this study further investigates a well-known co-primary spectrum sharing paradigm with emphasis on scheduling policies for the common/shared radio resources. Several RAN tenants get their dedicated radio resources and are entitled to accessing additional common/shared resources, both of which are defined by the SMA. The SMA additionally chooses a scheduling policy for the distribution of the shared resource which is implemented by the COHERENT control entity i.e., the RTC. This study highlights the trade-offs involved in adopting a particular sharing policy relating to fairness and overall cell-throughput.

Task covered:

- Task 4.1
- Task 4.2

7.3.1. Motivation & Goals

The performance targets for 5G wireless networks in terms of data throughput are very ambitious and cannot be achieved with mere optimization of existing network architecture, management functions and radio resource utilization. Additional radio resources will be needed in different frequency bands to address both macro and micro area coverage and capacity concerns. Traditionally, network operators have met these concerns with acquiring exclusive use licenses for different spectrum bands. However, the abundant literature available on Cognitive Radio technology and dynamic/opportunistic spectrum access give a contrasting message of non-availability of exclusive access spectrum. Going forward, network operators will find it more difficult and expensive to acquire exclusive use licenses for additional radio frequencies to provide macro and micro area coverage. Therefore, operators will have to adopt spectrum sharing models in new bands rather than rely on dedicated resources. Resource sharing has traditionally been a sore topic for network operators and realized only passively (e.g., eNodeB mast sharing) due to competition fears. However, in the 5G networks context, particularly with the advances in technologies such as cloud-infrastructures, Software Defined Networks (SDN) and Network Function Virtualization (NFV), resource sharing and multi-tenancy across all segments of the network has become more feasible. Significant work has already been done on defining the possible models of cooperation and spectrum sharing among multiple networks which are also valid for 5G networks [Mustonen_2014]. The existing works on this topic however, are either based on a primary-secondary networks concept where the roles and priorities of associated operators are different or based on using models where sharing of spectrum implies non-overlapping coverage. Moreover, the existing models offer a very coarse-grained distribution of shared radio spectrum among network operators. The main motivation for this study is to evaluate spectrum sharing models that fit the 5G multi-tenant RAN scope and take a more fine-grained approach to spectrum sharing. We therefore, evaluate different fine-grained scheduling approaches for allocation of shared spectrum to different RAN tenants in co-primary spectrum sharing model.

7.3.2. Co-Primary Spectrum Sharing

Co-Primary spectrum sharing, where a number of network operators agree on sharing a common pool of radio resources is an important model that fits the scope of multi-tenancy and resource sharing in 5G networks. The common or shared pool of resources can be a dedicated band authorized for common use or consist of aggregated spectrum vacated voluntarily by the involved network operators for mutual benefit. This model not only creates scope for research on how operators can contribute to the shared pool but also for how access to the shared resources can be coordinated. Most of the existing work on co-primary spectrum sharing addresses issues such as interference mitigation, access coordination to the common resource and policies to acquire the common radio resources. Moreover, multi-tenancy is

not considered in individual cells rather, interference reduction is targeted in multiple small cells where the coverage of the cells overlap but individual identity of the cells are associated to a particular operator. In the context of 5G however, RAN sharing scenarios are also anticipated to manifest in the forms of cells that are used by multiple operators at the same time with individual slices of radio resources. Similar to how multiple processes on a microprocessor share the compute and memory resources while maintaining isolation and performance guarantees, several RAN tenants with dedicated and shared radio resources can be co-located in distinct macro/small cells. We aim to address the issue of allocating shared co-primary radio resources in this context and present an active approach where several tenants can dynamically appear in a RAN segment with both dedicated resources and entitlement for access to the shared radio resources. We take the spectrum management and control architecture presented in the previous section, where control plane functions are separated from the user-plane data processing for facilitating spectrum sharing at different levels of abstractions. The main goal of this study was to evaluate different fine-grained scheduling policies for the co-primary shared spectrum among several RAN tenants.

7.3.3. System Model & Control Flow

The overall system architecture and the control entities involved are assumed to be exactly the same as presented in the previous section on fine-grained RAN and spectrum sharing (See Section 7.2). At the top of the hierarchy, the spectrum management application interacts with the Centralized Control and Coordination layer (C3) to configure operational parameters related to network management, in this case, RF spectrum use in the RAN. The C3 layer, via northbound interface, provides abstract network state information and exposes control parameters that the spectrum management application can use to configure RAN elements and define parameters of spectrum access and sharing. The spectrum management application takes its domain knowledge (assumed static information such as policies, regulations, agreements between MVNOs and infrastructure providers, and geolocation data) and the network state information exposed by the C3 layer to define the high level rules of spectrum sharing to which the individual network cells must adhere. The control applications placed above the C3 layer determine the network level configurations and policies that are not time-critical and mainly define the operational behaviour of the network. For example, the allocation of resources to new network tenants (bandwidth, compute, storage), defining the applicable policies to new and existing tenants (defining, allowing/disabling spectrum access rules) etc., can be decided at the control application level. To enforce the policies and configurations at the granular and time-critical level of individual cells or a set of few cells, Real-Time Controllers (RTC) are used. At the RTC level, the real-time network state is exposed through primitive parameters observed by the RAN elements such as eNB and UEs. The control applications above C3 and the real-time control entities located at the granular levels in the network cater for both real-time and non-real time management and control requirements related to spectrum access.

In the co-primary spectrum sharing context, the spectrum management application specifies, via the C3 layer, the amount of bandwidth available for co-primary spectrum sharing and the policy to be used for scheduling the tenants' access to these resources. While trivial to the actual scheduling of shared radio resources, the control application may also define the cells in which tenants are given resource slices. However, the capability of dynamic provision of tenant specific resource slices is very important for scenarios where a tenant may require occasional coverage in a particular area, for example, for event coverage. The other important configuration defined at the control application level is the granularity of resource scheduling which is non-trivial and depends on many factors including sharing agreements, access technologies, and actual value of the shared resource such as achievable throughput using the shared resource.

To make the subsequent description more specific and facilitate practical evaluation, we take LTE based networks as RAN tenants and Physical Resource Blocks (PRB) as the most granular level of resource sharing in both time and frequency domains. The spectrum management application defines maximum sharing window in the time domain that can be allocated to a tenant from the shared co-primary resources. The duration of this window, expressed in number of Transmit Timer Intervals (TTI) for fine-grained allocation, is a parameter that the spectrum management application can define and change over time based on the network state information exposed by the C3 layer and the parameters described

above for tenant-specific resource allocation. The real-time controller at cell level subsequently uses this window as the maximum threshold for the tenant's shared resource utilization.

7.3.4. Co-Primary Spectrum Scheduling Policies

Generally, resource scheduling among multiple entities is always related to finding an acceptable compromise between fairness and extracting the maximum benefit from the common/shared resource. In our spectrum sharing context, once the spectrum management application feeds the configuration for the sharing window, the controller module in the RAN takes an active approach to allocating the common co-primary shared resources to the tenant operators. The fine-grained scheduling policies detailed in this section are based on how much information is exposed by the tenant networks to the controller and on the sharing windows defined by the spectrum management application. We have considered four different policies depicted in Figure 29, which are used by the controller at cell level to allocate the common resource based on the defined window size by the spectrum management application. The figure shows the time axis segmented into chunks of window size defined by the spectrum management application (*w1, w2, … wn)* and three tenants who are scheduled within these segments according to the four policies detailed below.

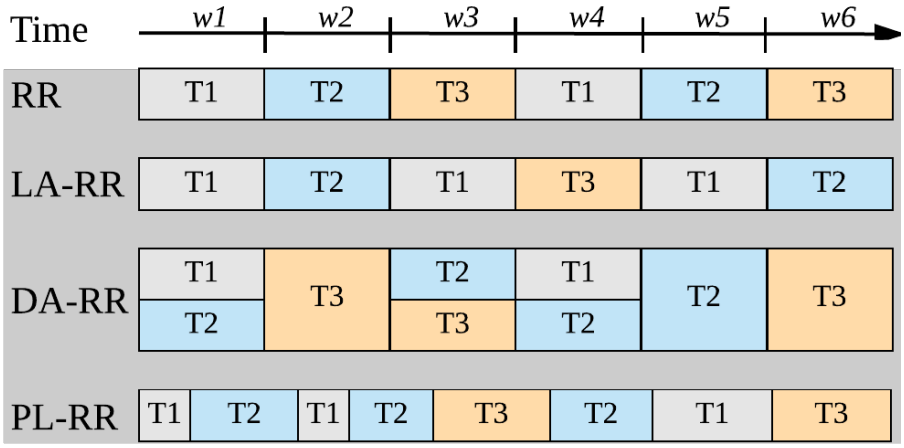

Figure 29. Fine-grained co-primary spectrum allocation policies

The most basic and well known approach is the Round Robin (**RR**) scheduling in which the controller iterates over all the RAN tenants and allocates the shared spectrum sequentially. The duration of resource allocation is always equal to the sharing window size and a constant waiting time is guaranteed for all the RAN tenants. This approach prioritizes fairness among tenants over the best possible use of the co-primary shared radio resources and tenants get a predictable level of benefit from the shared resource. An additional benefit of the round robin scheduling is that this approach does not require the tenants to expose any information about the load in their slices and the state of their dedicated resource consumption. From the controller's perspective, basic RR is also the simplest policy to implement as the only necessary information required is the number of tenants and the duration of sharing window. The second scheduling approach, called Load-Aware Round Robin (**LA-RR**) requires the tenants to explicitly communicate their needs for additional spectrum, if any, to the controller in order to be considered for allocation in the shared resources. This approach filters down to RR if all tenants require additional resources all the time. However, if a tenant does not communicate a request for additional spectrum, the controller does not consider it as candidate for allocation. This scheduling approach also does not require information about the state of the dedicated resources of the tenants. The tenants can be fair in their communication and only request resources when they are actually needed in their slice but may also be selfish and request even when there is no load in their slice. There may be valid reasons for such a behaviour, for example, in cases where the tenants can accurately predict an upcoming overload situation. The controller has no way to validate the requests and has to consider all tenants as being fair in their requests for additional resources. It should be noted, that if the tenants are always fair in their requests, this policy does not guarantee fairness at the controller level as the overload situations in all tenants are not considered to be synchronized. In the two policies described thus far (RR and LA-RR), the controller is not aware of the actual demands of the tenants and therefore has to allocate the

whole co-primary shared bandwidth to each tenant in its scheduling window. These approaches however, are not fully optimized for the best use of the co-primary shared spectrum. The third scheduling policy called Demand Aware Round Robin (**DA-RR**) requires the tenants to expose their actual slice-specific load so that the controller can assign only a subset of the shared resource rather than allocating the entire co-primary shared bandwidth. This policy can therefore, schedule more than one tenant in a single sharing window if their demands for additional resources can be accommodated in the co-primary shared resources. This added efficiency of the shared resource use comes at a cost of even lesser fairness among the tenants. In essence, a tenant that needs additional resource sporadically is scheduled sporadically and only for the resources it needs rather than its fair share. The fourth scheduling policy called Pre-emptive Load Aware Round Robin (**PL-RR**) gives full authority to the controller regarding the shared radio resources. This policy requires that the controller is fully aware of the instantaneous load characteristics of the dedicated resources of all tenants (at TTI granularity) particularly the tenant that is scheduled for the shared resources. Once the co-primary shared bandwidth is allocated to a tenant, the controller monitors its resource consumption continuously. If the load drops to a level that can be accommodated by the tenant's dedicated resources, the controller pre-empts the scheduled tenant even if it's sharing window has not been consumed. This scheduling policy specifically targets achieving the best possible use of the shared spectrum without taking fairness as a primary consideration. While, theoretically, it never seems acceptable to compromise on fairness in a shared resource context, in a multi-tenant RAN, a tenant's performance targets can be ensured if the spectrum scarcity is avoided by the controller. It can be anticipated that the controller maintains a log of the shared resource consumption and expose it over a time frame to the spectrum management application. The spectrum management application can in-turn compensate the tenants in other parts of the RAN or by changing its dedicated share of resources if required.

7.3.5. Evaluation

For evaluation of the scheduling policies described above, we have used the system level simulation model for multi-tenant RAN developed within the scope of COHERENT project (see Section 6.3). Figure 30 shows some of the simulation parameters considered for this evaluation.

	Parameter	Value	Parameter	Value
General	No. of Tenants	4	UE Mobility	RandomWP
	Sim Area	1 Sq Km	Geography	Urban Macro
PHY Layer	eNB Tx Power	10W	Frequency	2100MHz
	Shared Bandwidth	10 MHz	Slice Bandwidth	5MHz
	Antenna config	Omni-directional	eNB Height	25M
MAC Layer	Slice Scheduler	MaxCQI, PF	Queue Size	1MB
Application	Apps per UE	1	UE Application	Video Stream
	App Packet Size	1500-2500B	Pkt Send Interval	1-3ms

Figure 30. Configuration and parameters for evaluation

We consider 4 LTE network based tenants, each having 5MHz dedicated bandwidth and the controller configured for additional 10MHz bandwidth available as common pool for co-primary spectrum sharing. The controller module uses four different policies detailed previously to schedule the 10MHz shared bandwidth among these four tenants. The dedicated resources of the tenants are scheduled independently from scheduling policy of the controller and uses Maximum CQI or Proportional Fair scheduling algorithms provided by the SimuLTE model. Figure 31 shows tenant specific load variation for the four simulated tenants in their dedicated bandwidth (5MHz). To smooth out the repeated fluctuations and improve readability of the figure of resource block allocation, we have applied a sliding window average function to all four curves. As evident in Figure 31, Tenant-1 (T1) is the least loaded slice with average resource consumption always below its dedicated bandwidth. However, it should be noted that even though the T1 specific red curve never seems to touch the maximum dedicated bandwidth (25 PRBs), this does not imply that T1 never needs any additional resource in any TTI during

the simulation. There are numerous instances where the load in T1 touches the maximum 25 PRB but those instances have been removed by the average function for the sake of visual clarity. The other three tenants are more loaded and their average consumption mostly exceeds their maximum dedicated bandwidth thereby indicating frequent need for additional resources.

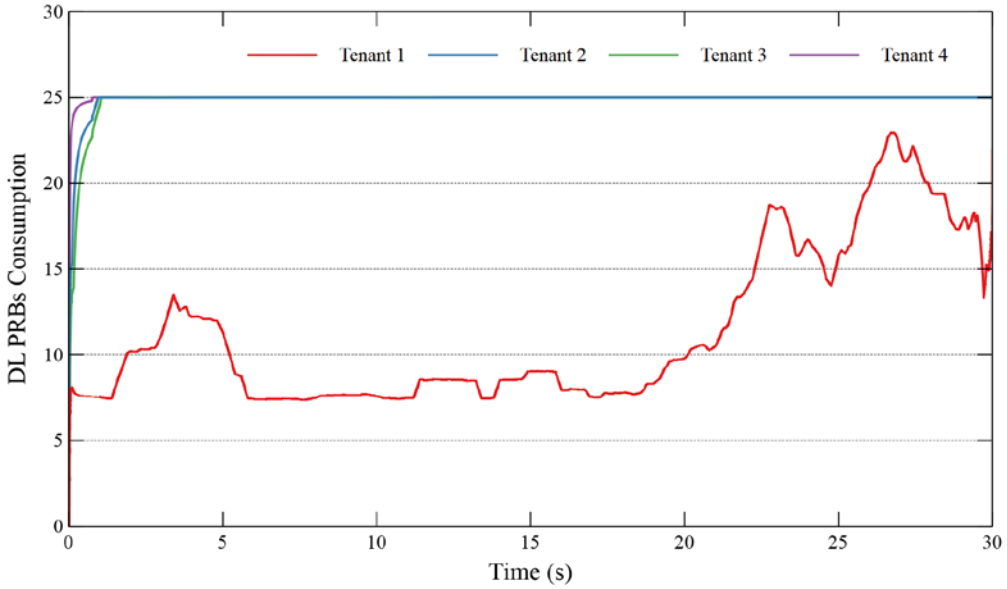

Figure 31. Average downlink dedicated PRB consumption by 4 tenants

Figure 32 shows the downlink resource block consumption when the co-primary spectrum is available to the tenants and the controller uses the four different scheduling policies. The figure indicates that all tenants benefit from the granular scheduling of the shared bandwidth in all four scheduling policies. We also see the effect of the policy on the effective benefit for the involved tenants. In Figure 32 (A), the RR approach ensures parity between the two most loaded tenants T3 and T4. The figure also shows that the pre-emptive resource allocation achieves the maximum benefit for all tenants with the basic RR being the least optimum. Based on this result, it can be argued that at the cell-specific controller level, the maximum benefit achievable from the shared resource should be targeted and that the unfairness can be compensated at a higher abstraction such as spectrum management application level.

The impact on cell throughput (joint application level throughput of all four tenants) is shown in Figure 33 together with the impact on downlink resource block allocation of all tenants. As indicated, the PL-RR scheduling policy achieves the best performance for these targets. This figure also supports the argument that at a granular level the overall cell throughput should be targeted and the unfairness can be compensated either at higher abstraction or at a later timeframe with the same granularity level. Figure 34 shows a segmented view of the overall cell throughput according to the specific throughput of each tenant. It can be seen that the more cell throughput we target, the higher the benefit of the overloaded tenants, thereby taking bigger chunks of the shared resources. As the pre-emptive scheduling policy optimizes the utilization of the shared resources, that benefit largely goes to the tenants that are more loaded. If adequate supplementary measures are in place to compensate for the micro-level unfairness among the RAN tenants, then the controller can allocate the shared resource for the best utilization possible provided that the tenants expose all required information and allow fine-grained reconfiguration of resources.

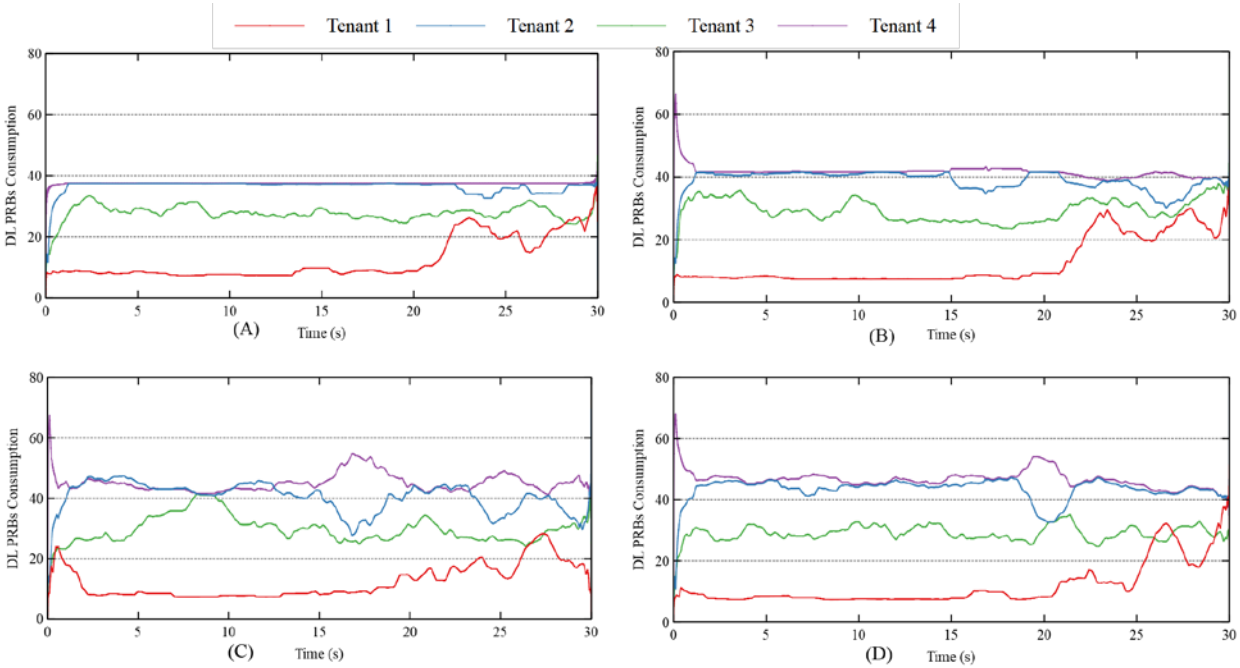

Figure 32. Average downlink PRB allocation with share resources

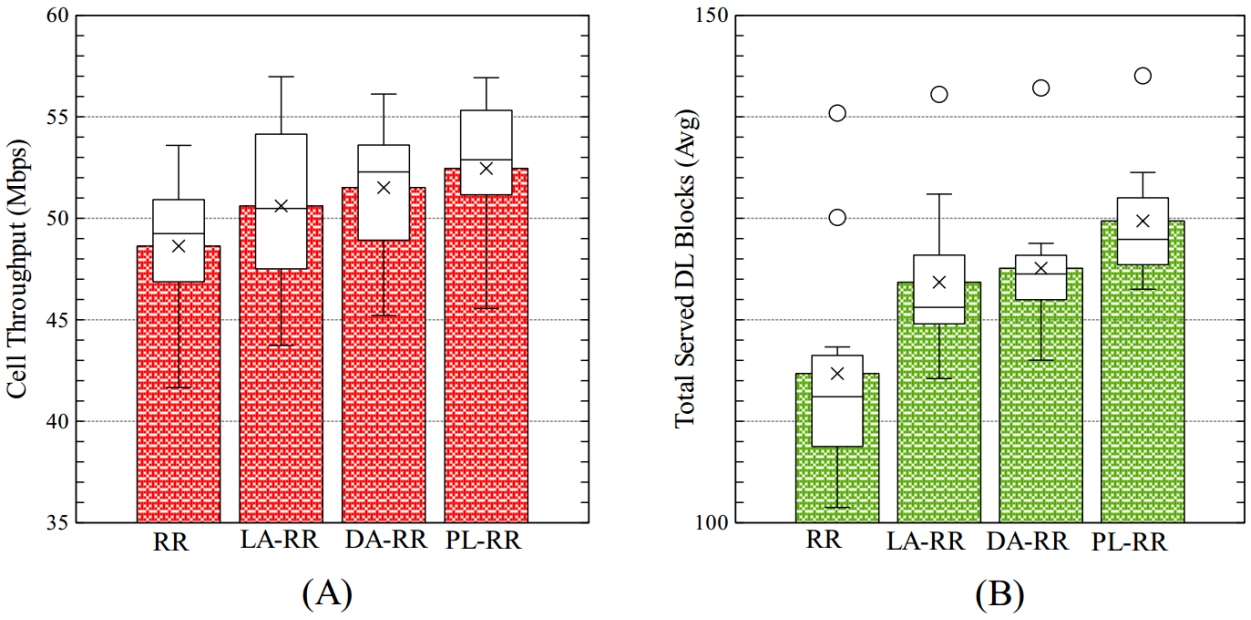

Figure 33. Joint average cell throughput and downlink allocated PRB

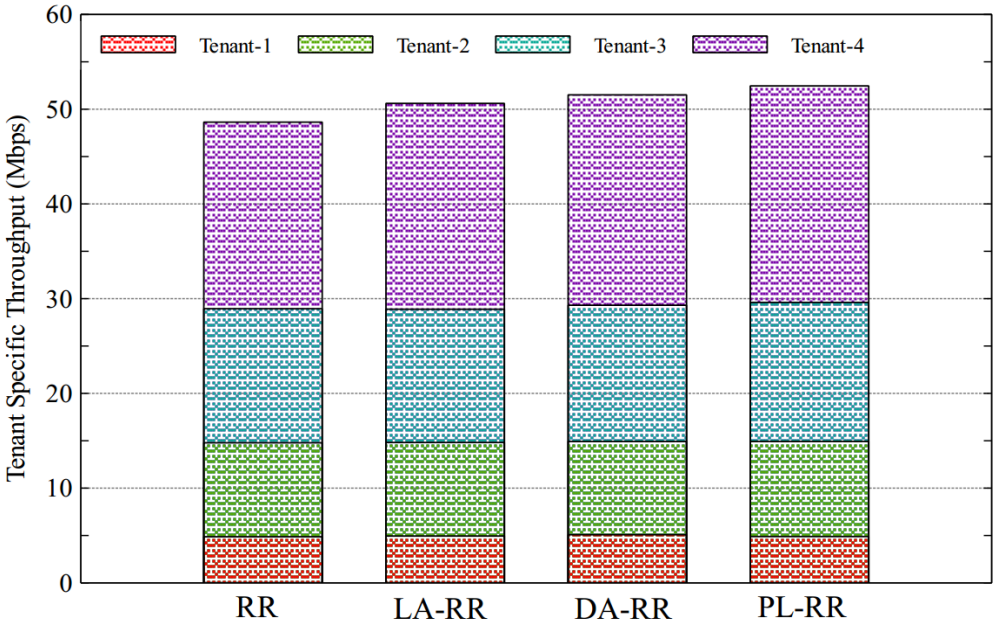

Figure 34. Average cell and tenant throughput at application layer

7.3.6. Summary

This section presented scheduling policies for fine-grained (at TTI level) allocation of co-primary shared spectrum using the real-time controller module located at eNB. Four different scheduling policies were analysed at this granularity level to emphasize not only the benefit of sharing at the granular level but also the compromises that can be made in terms of fairness and achievable throughput. Realizing these scheduling policies requires a different amount of integration of the controller function into the actual tenant-specific resource allocation process in order to expose the required load information. Subsequent work in this area can be focused on dynamically scaling the allocation window based on real-time network load and resource availability.

7.4. Management of Coexistence Between LTE and Wi-Fi in Unlicensed Bands

Goal of the study and connection to the COHERENT architecture

The goal of this study is to enable improved coexistence between LTE and Wi-Fi networks when operating over the 5 GHz unlicensed band by means of the COHERENT SMA and C3. The idea is to identify the new threshold that Wi-Fi should use in the energy detection operation prior to doing a transmission as part of the CSMA/CA algorithm, as well as determine the impact of the LTE transmitted power. The assumption is that both LTE and Wi-Fi networks are under the control of C3. Before transmitting over the 5 GHz band, an exchange between the LTE small cell and the C3 should take place to request access permission. The C3 shall rely on the Spectrum Reasoning and Optimization functionalities inside the SMA for this purpose. Through the SBI, the C3 should enforce the new values to both LTE and Wi-Fi.

Task covered: Task 4.2 and Task 4.3

7.4.1. Introduction

Significant advances and new features have been introduced recently to the mobile network technology by 3GPP in Release 12 and 13. One of the most notable is the possibility to do carrier aggregation between a licensed carrier and an unlicensed one. This new feature, has given LTE the possibility to step into unlicensed spectrum, which traditionally has been used by other systems. Such frequency bands are regarded to as Industrial Scientific & Medical, or ISM. Particularly, 2.4 GHz and 5 GHz bands have been used successfully by mass market devices through Wi-Fi, Bluetooth and Zigbee, just

to name a few technologies, with the main rule to fulfil specific technical constraints (power spectral density mask, indoor/outdoor use, etc.).

Since LTE over unlicensed bands is a form of carrier aggregation, at least one licensed carrier must always be used. Hence, this feature does not stem as a complete switch over of the licensed carrier towards the unlicensed one. Two main types of LTE in unlicensed spectrum were developed by 3GPP: LTE-U (or LTE-Unlicensed) that was developed in 3GPP Release 12, and it uses an adaptive duty cycle (i.e. on/off periods) to harness coexistence with other systems operating within the same unlicensed band, and LAA (or Licensed Assisted Access), which is based on a Listen-Before-Talk (LBT) channel access scheme to improve channel access fairness and coexistence with other systems already operating in ISM bands. Until 3GPP Release 13, carrier aggregation with an unlicensed carrier was limited to downlink communications only, but in 3GPP Release 14 this feature has been extended to include also some uplink communication channels [Kwon_2016].

Depending upon the channel access scheme adopted, the behaviour of an unlicensed LTE system could be more or less aggressive towards pre-existing technologies. Therefore, the motivation in this study to refer to LTE as the 'aggressor' system, and other ones that traditionally operates over unlicensed bands as the 'victim' systems. Among the possible victim systems, this study revolves around the effect of letting LTE operate into the 5 GHz band, considering Wi-Fi as the victim system. The choice is motivated by the fact that Wi-Fi is probably the most popular and used unlicensed technology and, in addition to that, 3GPP has started investigating how to improve coexistence with LTE specifically targeting Wi-Fi.

All features that were developed for Wi-Fi in past years made the endeavour to improve the physical layer (Layer-1) technology, as well as the Medium Access Control (MAC/Layer-2) algorithm. Anyway, it is worth noticing that all features of Wi-Fi have targeted performance enhancements within the Wi-Fi network, where different Wi-Fi technologies (legacy standards) may operate. Since the presence of LTE transmission over unlicensed bands has raised concerns about performance degradation of Wi-Fi, it is worth stressing the fact that all mechanisms developed so far are not adequate to relieve the problem arising from uncoordinated LTE transmissions.

Target of the study: quantify and relieve the Wi-Fi performance degradation caused by LTE transmissions over the same unlicensed band (aggressor-victim system). Wi-Fi performance degradation is evaluated looking at the Clear Channel Assessment (CCA) operation that any Wi-Fi station has to carry out prior to transmitting a data packet over the radio channel. Particularly, a way of quantifying the degradation is through the probability of false alarm (P_{fa}) and detection (P_d) of the segment of the whole Wi-Fi preamble sequence that is used for assessing the channel status.

As 3GPP developed different approaches to LTE in unlicensed bands, interference caused by LTE is still possible under certain circumstances. Even in case of LAA that relies on the LBT channel access mechanism, which is very similar to CSMA/CA, hidden terminal problems are still possible as shown in Figure 35. Two scenarios are depicted by the figure. On the left hand-side, the scenario shows the case of a Wi-Fi station (STA2) that upon doing CCA will detect the channel busy, though idle from any other Wi-Fi transmission (scenario for studying false alarm). In this case the Wi-Fi station will refrain from transmitting due to CSMA/CA, thus reducing the Wi-Fi channel access efficiency. On the other hand, the figure on the right hand-side shows the case in which the Wi-Fi STA2 is the target of a communication from the access point (AP) but at the same time victim of the interference created by an LTE eNB that is unable to detect the channel busy, and hence may begin transmitting (scenario suitable for studying detection). Wi-Fi station throughput degradation is expected in this case.

Observation 1: the preamble sequence exhibits similarity through different 802.11 standards. Typically, the whole Wi-Fi preamble (e.g. in the IEEE 802.11g) includes short and long training sequences, guard intervals and synchronization symbols for determining the start of frame delimiter (the point after which a Wi-Fi node can begin decoding a packet). Starting with the IEEE 802.11n, the preamble was enriched with other fields such as the high-throughput field options.

Observation 2: the CCA operation is carried out through the non-coherent energy detection (ED) process. The ED operation has shown to be simple to implement, it is fast to provide a response and reliable in overall. Anyway, the additional presence of LTE transmissions over the same unlicensed band might affect the ED reliability.

Observation 3: the increased false alarm would cause the Wi-Fi network to access less frequently the channel, leaving in practice even more room for LTE to transmit. On the other hand, a lower detection probability would lead to a higher number of collisions over the Wi-Fi channel. Both cases stand for different types of Wi-Fi performance degradation (see Table 6 for Layer-1 parameters).

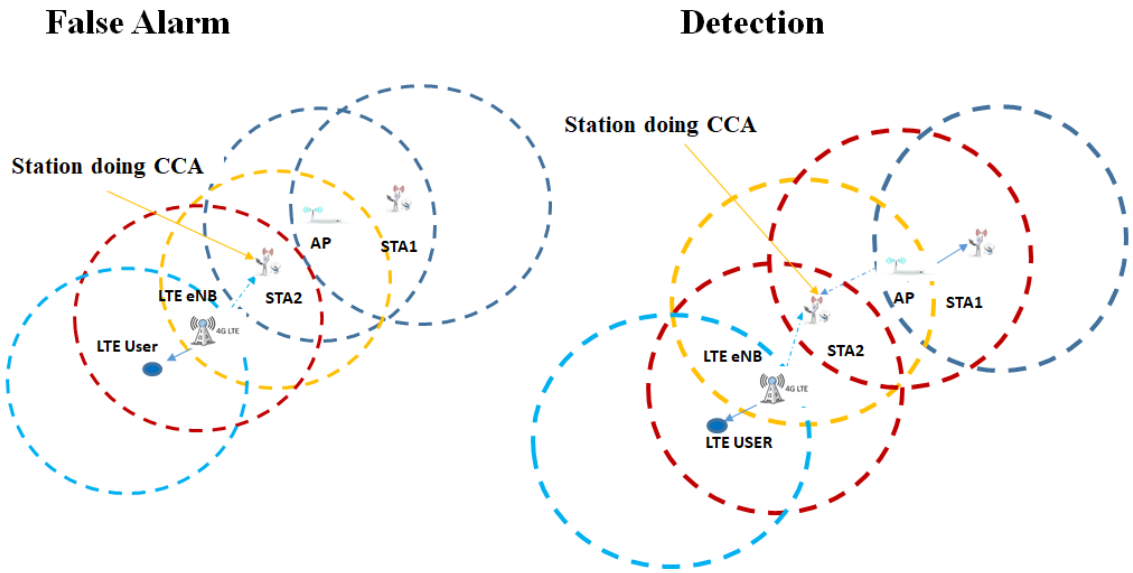

Figure 35: Hidden LTE node scenarios that lead to interference onto the proximate Wi-Fi network

Table 6. Comparison between LTE and Wi-Fi parameters [Sesia_2011], [802.11n_2009]

Parameter	Wi-Fi	LTE Small Cell
Transmit power	20 dBm	24 dBm
Number of data sub-carriers	52	12 per resource block
Number of resource blocks	-	110 for 20 MHz bandwidth
Bandwidth	20 MHz / 40 MHz	{3, 5, 10, 15, 20} MHz
Sub-carrier spacing	312.5 kHz	15 kHz
FFT size	64	2048
Preamble length for CCA	5 symbols of the short training sequence	-
Preamble symbol duration	0.8 μs	-
CCA training sequence	4 μs	-
Cyclic prefix	0.8 μs (standard prefix: no high-throughput)	4 μs
Data symbol duration	3.2 μs	CP + 1/15 kHz = 71 μs

7.4.2. False Alarm and Detection Probability Analysis

Relying on the general theory of OFDM modulation, the bandpass representation of the A_n transmitted OFDM symbol without cyclic prefix can be written as shown below [Giorgetti_2005].

$$S_{BP}(t) \triangleq \frac{1}{\sqrt{N}} \sum_{n=0}^{N-1} A_n(t) e^{j2\pi f_n t} e^{j2\pi f_c t} = S_{LP}(t) e^{j2\pi f_c t} \ , \tag{1}$$

where N stands for the number of sub-carriers, $f_n = \Delta f (n - \frac{N-1}{2})$, with $\Delta f = 1/t_s$ the sub-carrier spacing and t_s the symbol duration, f_c the carrier frequency and $A_n(t)$ the symbol information. To avoid Inter-Symbol-Interference (ISI), the last G tail bits are replicated on top of the OFDM signal to form the cyclic prefix (CP): $[A_{N-G},\ldots,A_{N-1}]$. While data symbols are obtained through a specific modulation format (M-PSK, M-QAM, etc.), the whole OFDM signal is obtained through the extremely computationally efficient IFFT operation done at the transmitter side. On the other hand, Wi-Fi preamble symbols are unmodulated.

The communication through the radio channel is assumed corrupted by the Additive White Gaussian Noise (AWGN) with zero mean and variance σ^2, which is assumed a Circularly Symmetric (CS) Complex Gaussian random variable $CS\aleph(0, \sigma^2)$. The transmitted signal is affected by the slow-fading channel $h(t) = \xi(t) e^{j\vartheta(t)}$, where ξ and ϑ are respectively the channel random amplitude and phase. The channel impulse response is such that the square-law operation implies: $h^2 = \left(\xi e^{j\vartheta}\right)^2 = \xi^2 = g$, and $E(h^2) = 1$, where $E(\cdot)$ stands for the expectation operation[1].

The first step prior to introducing the effect of the interference consists of showing how to obtain the probabilities of false alarm and detection in the standard ED receiver. After doing the down-conversion from the carrier frequency, the received signal (r(t)) can be expressed through the lowpass representation of the transmitted signal [Digham_2007]

$$r(t) \triangleq \mathrm{Re}\{(S_{LP}(t) h(t) + n_{LP}(t)) e^{j2\pi f_c t}\}, \tag{2}$$

where n_{LP} is the lowpass representation of the AWGN noise. It is also worth pointing out that the received signal in eq. (2) represents the signal received after the bandpass filter just before the ED operation.

In order to express the preamble sequence that is used in the energy detection process during the CCA operation eq. (1) is manipulated to obtain the following representation

$$S_{LP}(t) = \sum_{k=1}^{N_s} \sum_{n=0}^{N-1} a_n p(t - k t_s) e^{j2\pi f_n t} = \sum_{k=1}^{N_s} X(t - k t_s), \tag{3}$$

where $a_n = \sqrt{\frac{\varepsilon / t_p}{N}}$ is the equally distributed energy in each sub-carrier, and $p(t)$ is the unit-energy pulse used to transmit the N_s symbols that are part of the preamble sequence. For clarity, the energy ε_p of the pulse $p(t)$ is such that

$$\varepsilon_p = \frac{1}{t_p} \int_0^t p(v)^2 dv = 1, \tag{4}$$

with t_p the pulse duration.

[1] In the derivation it is was used the fact that $\cos(\vartheta)^2 + \sin(\vartheta)^2 = 1$.

Relying upon the definition of the transmitted signal $s(t)$ shown in eq. (3), and dropping the subscript LP, the received signal can be rewritten in the following manner

$$r(t) = \sum_{k=1}^{N_s} X(t - kt_s) + n_k(t), \tag{5}$$

The ED receiving operation applied to the received preamble signal does the following operation

$$Z \triangleq \frac{1}{2\sigma^2} \int_0^T r^2(t)dt, \tag{6}$$

in which Z is the analogue (in the continuous time-domain) decision variable (d.v.) of the energy detection operation, and T is the integration time.

It is worth noticing at this point that the d.v. Z depends on the distribution of the squared additive noise term, which is known to follow a Chi-squared (χ^2) distribution. After applying the sampling theorem, the analogue decision variable Z is converted into a digital d.v. Y and compared to the energy threshold λ. The expression of the digital decision variable can be hence expressed as follows

$$Y \triangleq \frac{1}{2\sigma^2} \sum_{k=1}^{N_s} \sum_{q=1}^{2Q} \frac{r_{k,q}^2}{2W} = \frac{1}{2\sigma^2} \sum_{k=1}^{N_s} \sum_{q=1}^{2Q} \frac{\left(X_{k,q} + n_{k,q}\right)^2}{2W}, \tag{7}$$

where W is the signal bandwidth, and $r_{k,q}$ is the sampled received OFDM signal corrupted by noise at the output of the ED, respectively. The upper value $Q=WT$ in the first summation in eq. (7) stands for the time-bandwidth product, assuming a Nyquist sampling rate $2W$ and integration time T.

Definition 1 (False Alarm): The event of false alarm corresponds to the case in which the CCA operation erroneously assesses the channel busy whereas instead it is idle (no Wi-Fi signal is being transmitted during the time T).

Definition 2 (Detection): The event of signal detection corresponds to the case in which the CCA operation correctly detects the presence of a signal over the wireless channel. In other words, the Wi-Fi signal is being transmitted during the time T and it is correctly detected.

Two statistical test hypotheses are usually defined for these two events. The first hypothesis, denoted as H_0, corresponds to the event of false alarm; the second hypothesis, denoted as H_1, corresponds to the case of correct signal detection.

Definition 3 (H_0): The test hypothesis H_0 is applied in correspondence of the event of false alarm.
Definition 4 (H_1): The test hypothesis H_1 is applied in correspondence of the event of detection.

Based on the definitions of false alarm and detection, it is possible to define formally the probability of false alarm using the discrete d.v. Y and the detection threshold λ as follows

$$P_{fa} \triangleq P_r\{Y > \lambda | H_0\}, \tag{8}$$

Similarly, for the probability of detection

$$P_d \triangleq P_r\{Y > \lambda | H_1\}, \tag{9}$$

In the next section, the probabilities are derived starting first with the simple case of additive noise only. As a subsequent step, interference is added, as well as channel fading and path-loss.

7.4.3. False Alarm and Detection Probability Analysis in AWGN Channel

To work out the standard derivation of the probability of false alarm P_{fa} and detection P_d in the presence of AWGN noise (without fading) for a Wi-Fi link, it is sufficient to assume $\xi^2=2$ in the expression of $h(t)$ [Dighma_2007]. The expressions for P_{fa} and P_d are well-known in the literature, and are shown in this section for the sake of completeness. In case of the test hypothesis H_0, the distribution of Y follows a central Chi-squared distribution with $2Q$ degrees of freedom. Vice versa, under the test hypothesis H_1, Y follows a non-central Chi-squared distribution with $2Q$ degrees of freedom and a non-centrality parameter μ. Referring to [Digham_2007] the probability of false alarm can be written as

$$P_{fa} = \frac{\Gamma(Q,\beta)}{\Gamma(Q)}, \tag{10}$$

with $\beta = \lambda/\sigma^2$ that stands for the normalised detection threshold. Furthermore, $\Gamma(x) = \int_0^\infty v^{z-1}e^{-v}dv$ is the Gamma function and $\Gamma(z,x)$ the upper incomplete Gamma function.

Similarly, the probability of detection can be obtained as

$$P_d = Q_Q\left(\sqrt{\xi^2\mu}, \sqrt{\beta}\right), \tag{11}$$

where $\mu = \frac{1}{2\sigma^2}\sum_{k=1}^{N_s}\sum_{q=1}^{2Q}\sum_{n=1}^{N} a_{k,q,n}^2$ and $Q_Q(\cdot,\cdot)$ stands for generalised Marcum-Q function.

7.4.4. False Alarm and Detection Probabilities Analysis with Interference

As discussed earlier, the CCA operation is typically reliable for assessing the wireless medium idle or busy prior to a packet transmission. In the study it is assumed that interference arises from downlink LTE transmissions in the same unlicensed band of Wi-Fi. Particularly, downlink LTE transmissions are due to small cell base stations.

Since also the LTE signal is also based on the OFDM modulation, relying on the general expression provided already in eq. (1), it is possible to write the lowpass expression of the signal. Since LTE is the aggressor, i.e. the one causing interference, it will be denoted as $I(t)$. Therefore, the lowpass representation of the interfering signal can be written as follows

$$I(t) \triangleq \frac{1}{\sqrt{M}}\sum_{m=0}^{M-1} A_m(t)e^{j2\pi f_m(t-\tau)}, \tag{12}$$

where τ denotes the asynchronous behaviour of the interferer with respect to the Wi-Fi transmission since those are not time synchronised, M stands for the number of sub-carriers in the LTE signal and $f_m = \Delta F(m - \frac{M-1}{2})$ the sub-carrier frequencies in LTE, with ΔF the sub-carrier spacing. Numerical values for both Wi-Fi and LTE transmissions have been provided in Table 6. Furthermore, it is worth noticing that $N \neq M$ and $f_n \neq f_m$ for the two systems. As for the Wi-Fi signal, it can be assumed a unit-energy pulse $b(t)$ to transmit the preamble symbol. The interfering signal $I(t)$ can be rewritten as

$$I(t) = \sum_{m=0}^{M-1} a_m b(t)e^{j2\pi f_m(t-\tau)} = \sum_{m=0}^{M-1} a_m x_m(t)\ , \tag{13}$$

where $a_m = \sqrt{\frac{\varepsilon_I/t_b}{M}}$ stems for the equally distributed sub-carrier energy of the LTE signal.

Observation 4: the analysis shown hereinafter targets to obtain expressions for the probabilities of false alarm and detection in the Wi-Fi network affected by LTE interference taking into account the effects of Rayleigh distributed fading and distance-dependent path-loss.

Observation 5: Two main assumptions are done for studying the effect of interference. The first is to consider a single LTE interferer, while the second consists of studying the effect of aggregate LTE interference.

Relying on eq. (2) and dropping the subscript LP, the received signal expression in the presence of a single LTE interferer can be written in a general manner as follows

$$r(t) \triangleq \mathrm{Re}\{(S(t)h_0(t) + I(t)h_I(t) + n(t))e^{j2\pi f_c t}\}, \tag{14}$$

where h_0 and h_I are the statistically independent fading channels affecting respectively the useful Wi-Fi signal and the interfering signal.

In case of multiple LTE interferers, as it could be the case of multiple LTE transmissions within the same unlicensed band (e.g. proliferation of unlicensed LTE systems), the Wi-Fi transmission is affected by aggregate interference degradation. In this case, the aggregate interfering signal can be written as

$$I(t) \triangleq \sum_i I_i(t). \tag{15}$$

Therefore, the received signal can be generally rewritten as

$$r(t) \triangleq \mathrm{Re}\{(S(t)h_0(t) + \sum_i I_i(t)\, h_{Ii}(t) + n(t))e^{j2\pi f_c t}\}. \tag{16}$$

Considering the signal expression provided in eq. (16) applied to eq. (6), the analysis in the presence of interference becomes non-trivial since the non-linearity operation introduced by the energy detector. As shown in [Dighma_2007] and [Atapattu_2011], even without interference, the analysis with fading turns immediately complex, with closed-form expressions that can be derived for specific cases but anyway are difficult to extend. For such reason, a different approach will be pursued relying on the work done in [Rabbachin_2007].

Before providing the main results for both false alarm and detection, it is worth doing few more manipulations of the received signal. At first, the expression of the energy per sub-carrier of both Wi-Fi and LTE signals can be modified to include the effect of the path-loss as follows

$$a_{r0n} \triangleq \sqrt{\frac{1}{N}\frac{1}{t_p}}\sqrt{\varepsilon_{0r}} = \sqrt{\frac{\varepsilon_0/t_p}{N}}\sqrt{r_0{}^{-\alpha}}, \qquad \forall n \in [0, N) \tag{17}$$

$$a_{rIm} \triangleq \sqrt{\frac{1}{M}\frac{1}{t_b}}\sqrt{\varepsilon_{Ir}} = \sqrt{c\frac{\varepsilon_I/t_b}{M}}\sqrt{r^{-\alpha}}, \forall m \in [0, M)$$

where ε_{0r} denotes the received energy of the Wi-Fi signal, ε_{Ir} denotes the received energy of the LTE signal, α denotes the path-loss exponent, r_0 the random distance separating a Wi-Fi transmitter from the intended Wi-Fi receiver and r the random distance separating the LTE interfering transmitter from the victim Wi-Fi receiver. Furthermore, c denotes an oversampling factor that takes into account the different sampling frequencies of LTE and Wi-Fi. The motivation for calculating the factor c, as well as the expression will be provided in the section devoted to the results.

Observation 6: The interfering signal affected by channel fading and propagation loss that depends on the random distance from the victim Wi-Fi receiver is modelled as a random process.

In order to simplify subsequent derivations, it is convenient to manipulate the lowpass representation of eq. (16) in the presence of a single LTE interferer as follows

$$r(t) \triangleq \sum_{k=1}^{N_s}\sum_{n=0}^{N-1} \xi_0 a_{r0n} p(t-kt_s) e^{j(2\pi f_n t+\vartheta_0)} + \sum_{m=0}^{M-1} \xi_I a_{rIm} b(t) e^{j(2\pi f_m (t-\tau)+\vartheta_I)} + n(t)\ . \quad (18)$$

The following step consists in computing the analogue d.v. Z

$$Z \triangleq \frac{1}{2\sigma^2}\int_0^T \big(r(t)\big)^2 dt = \frac{1}{2\sigma^2}\int_0^T \big(h_0 S(t) + h_I I(t) + n(t)\big)^2 dt = \quad (19)$$

$$\frac{1}{2\sigma^2}\int_0^T \Big(\big(h_0 S(t)\big)^2 + \big(h_I I(t)\big)^2 + n^2(t) + 2h_0 S(t) h_I I(t) + 2h_0 S(t) n(t) + 2h_I I(t) n(t)\Big)\, dt.$$

All terms that include $n(t)$ have null contribution on overage. On the other hand, the cross-talk product $2h_0 S(t) h_I I(t)$ is assumed negligible with respect to the other terms. Therefore, the d.v. Z can be approximated as

$$Z \simeq \frac{1}{2\sigma^2}\int_0^T \Big(\big(h_0 S(t)\big)^2 + \big(h_I I(t)\big)^2 + n^2(t)\Big)\, dt = \quad (20)$$

$$\frac{1}{2\sigma^2}\int_0^T \Big(X_0^2(t) + X_I^2(t) + n^2(t)\Big)\, dt.$$

The first two terms in eq. (20) under the integration operation denote the energy of the useful signal and of the interfering signal, respectively. Similar to the analysis with noise only, the following step consists of obtaining the digital d.v.

$$Y \simeq \frac{1}{2\sigma^2}\sum_{q=1}^{2Q} \frac{r_q^2}{2W} = \frac{1}{2\sigma^2}\sum_{q=1}^{2Q} \left(\frac{X_{0q}^2 + X_{Iq}^2 + n_q^2}{2W}\right). \quad (21)$$

The d.v. Y can be hence distinguished between the test hypotheses H_0 and H_1 as shown below.

$$Y_0 = \frac{1}{2\sigma^2}\sum_{q=1}^{2Q}\left(\frac{X_{Iq}^2 + n_q^2}{2W}\right) \quad (22)$$

$$Y_1 = \frac{1}{2\sigma^2}\sum_{q=1}^{2Q} \left(\frac{X_{0q}^2 + X_{Iq}^2 + n_q^2}{2W}\right).$$

Using Observation 6, and conditioning upon the interference distribution, the decision variable Y_0 is a non-central Chi-Squared distributed r.v. with non-centrality parameter μ_0. Similarly, the decision variable Y_1 is a non-central Chi-Squared distributed r.v. with non-centrality parameter μ_1 and $\mu_0 \neq \mu_1$.

To compute the first non-centrality parameter μ_0 it suffices to set the noise term to zero in Y_0.

$$\mu_0 = \frac{1}{2\sigma^2}\sum_{q=1}^{2Q} X_{Iq}^2 = \frac{1}{2\sigma^2}\sum_{m=0}^{M-1}\sum_{q=1}^{2Q}\big(h_{Iq} a_{rIm,q} x_{m,q}\big)^2 = \quad (23)$$

$$\frac{1}{2\sigma^2}\sum_{m=0}^{M-1}\sum_{q=1}^{2Q} \xi_{Iq}^2 a_{rIm,q}^2 = g_I \frac{c\times\varepsilon_I}{2\sigma^2} r^{-\alpha}\ ,$$

where g_I is the channel power fading coefficient that affects the interfering signal.

The following computations are for the non-centrality parameter μ_1. To obtain subsequent derivations, the useful signal before sampling is rewritten as

$$S(t) = \sum_{k=1}^{N_s}\sum_{n=0}^{N-1} \xi_0 a_{r0n} p(t-kt_s) e^{j(2\pi f_n t+\vartheta_0)} = \sum_{k=0}^{N_s-1}\sum_{n=0}^{N-1} \xi_0 a_{r0n} w_{k,n}(t-kt_s+\vartheta_0)\ .$$

The steps to compute μ_1 are similar to what shown above for μ_0 setting first the noise term to zero.

$$\mu_1 = \frac{1}{2\sigma^2}\sum_{q=1}^{2Q}\left(X_{0q}^2 + X_{Iq}^2\right) = \frac{1}{2\sigma^2}\left[\left(\sum_{k=1}^{N_s}\sum_{n=0}^{N-1}\sum_{q=1}^{2Q}\xi_{0q}a_{r0n,q}w_{k,n,q}\right)^2 + \left(\sum_{m=0}^{M-1}\sum_{q=1}^{2Q}\xi_{Iq}a_{rIm,q}x_{m,q}\right)^2\right]. \quad (24)$$

After few further manipulations it can be shown that

$$\mu_1 = \frac{1}{2\sigma^2}g_0 N_s \varepsilon_0 r_0^{-\alpha} + \frac{1}{2\sigma^2}g_I c\varepsilon_I r^{-\alpha}\,. \quad (25)$$

Observation 7: As shown in [Dai_2012], it is worth noticing an interesting and general result that states that the probability of detection without interference is not less than the probability of detection affected by interference.

Proposed method: It was already mentioned the complexity of deriving the probability of false alarm and detection when fading and in addition interference are included in the analysis. This is the limit of a solution worked out through the standard probability density function (PDF) approach. Several research papers have shown that the aggregate interference is a shot noise process [Haenggi_2009] [Rabbachin_2011] [Andrews_2011] [Elsawy_2016] [Win_2009]. It was demonstrated also that the aggregate interference follows a Stable distribution, which is part of the heavy tail family. Aiming to model the probability of false alarm and detection, the proposed method passes through the characteristic function approach, aided by a numerical evaluation of the integral that provides inversion of the characteristic function. Such a result is due to Gil-Pelaez [Davies_1973].

Theorem 1 (Gil-Pelaez Inversion Theorem): Given the characteristic function (CF) $\Psi_x(\upsilon)$ of a real r.v. X, the Pr{X<x} can be numerically computed in the following way

$$P_r\{X < x\} = \frac{1}{2} - \frac{1}{2\pi}\int_{-\infty}^{\infty} Im\left(\frac{\Psi(v)e^{-jvx}}{v}\right)dv = \frac{1}{2} - \frac{1}{\pi}\int_{0}^{\infty} Im\left(\frac{\Psi(v)e^{-jvx}}{v}\right)dv \quad (26)$$

where $Im(\cdot)$ stands for the imaginary part operator, and the last equality that holds due to symmetry. Therefore, the complementary probability can be computed as $1 - P_r\{X < x\}$ that yields

$$P_r\{X > x\} = \frac{1}{2} + \frac{1}{\pi}\int_{0}^{\infty} Im\left(\frac{\Psi(v)e^{-jvx}}{v}\right)dv\ . \quad (27)$$

The result shown above for the Gil-Pelaez inversion theorem will be used in the computation of the probabilities of false alarm and detection.

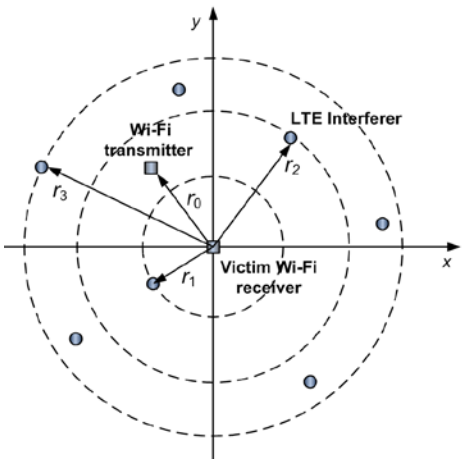

Figure 36: Scenario for studying aggregate interference

To obtain the expressions of the probabilities of false alarm and detection, the proposed technique relies on the powerful tool of stochastic geometry [Stoyan_2008]. Stochastic geometry is a branch statistic the deals with random spatial point processes. Stochastic geometry provides a very effective tool to model and solve problems in which the random distribution of points (i.e. interferers in this case) in the *d*-dimensional space follows a specific pattern. Although it is easy to end up with complex expressions a special case of spatial random process, or point process (PP), is that of Poisson (PPP). PPPs allow to obtain appealing closed form solutions and offer mathematical tractability. At the same time, several research papers [Win_2009] [Elsawy_2016] [Haengii_2009] argued the suitability of PPPs to model aggregate interference in wireless networks. Therefore, a PPP of intensity, or spatial density λ_s, will be used to model the aggregate LTE interference.

Following the well-known Poisson distribution, the probability to find exactly

$$P_r\{\kappa = K|A\} = \frac{(\lambda_s|A|)^K}{K!}\exp(-\lambda_s|A|), \tag{28}$$

with $|A|$ the Lebesgue measure of the region A in the d-dimensional space. Since the study focuses on a 2-dimensional Euclidean space, and the shape of the region A is assumed a circle it holds that $|A|=\pi r^2$.

Observation 8: The analysis of Wi-Fi CCA performance is carried out considering the victim Wi-Fi receiver at the center of a reference system as shown in Figure 36. Upon this assumption, the PDF of the random distance between a LTE interferer and the victim Wi-Fi receiver follows the 2-dimensional uniform distribution within [0, R), where R is the radius assumed for the Area A. In addition, when modelling the aggregate interference with a PPP, the aggregate effect arises from an infinite spatial displacement of interfering transmitters. Looking at eq. (28), the aggregate effect is assumed arising from the interferers located within the radius [0, R), and assuming negligible the interference beyond distances greater than R.

Observation 9: Derivation of the probabilities of false alarm and detection is obtained under the hypothesis of a Rayleigh distributed amplitude fading, which implies an exponentially distributed channel power fading. Probabilities are obtained for both a single interferer case, and in the presence of aggregate interference. It is finally worth to remind that conditioning upon the distribution of the interference, the digital d.v. is still Chi-squared distributed.

In the remainder of this section, to deal with the aggregate interfering process, it will be used the following theorem that comes from stochastic geometry and PPPs.

Proposition 1 [Stoyan_2008]: Let Φ be the PPP that characterizes the distribution of point pattern, and f be a non-negative measurable function on a bounded set. The probability generating functional (PGF) of the PPP with intensity measure λ_s can be expressed as follows

$$E\{\prod_{x\in\Phi} f(x)\} = \exp\left(-\lambda_s \int_{\boldsymbol{R}^2}(1-f(x))dx\right). \tag{29}$$

Useful facts:

Before showing the complete derivation of the probabilities of false alarm and detection, it is worth providing some results that will be used in the subsequent proofs.

- $P_r\{r \le u \le r+dr\} = \frac{2r}{R^2}dr$, 2-dimensional uniform distribution.
- $\Psi(v) = \frac{1}{(1-2jv)^Q}\exp\left(\frac{jv}{1-2jv}\mu\right)$, characteristic function of the non-central χ^2 distribution.
- $\Phi(s) = \frac{\rho}{\rho-s}$, moment generating function of an exponential distribution with mean ρ.
- $E\{g^\delta\} = 2^\delta\Gamma(1+\delta)$, moments of the Rayleigh distributed r.v. g.

Lemma 1: For any complex constant $G \in \boldsymbol{C}$, path-loss exponent α>2 and real $R \in \boldsymbol{R}$ with R that denotes the radius of an area of interest, the following integral holds

$$\int_0^R \frac{1}{1+Gr^{-\alpha}} \frac{2r}{R^2} dr = \frac{2R^{\alpha} 2F_1\left(1, \frac{2+\alpha}{\alpha}, 2+\frac{2}{\alpha}, -GR^{\alpha}\right)}{G(2+\alpha)}. \quad (30)$$

Lemma 2: For any $s \in \boldsymbol{C}$, path-loss exponent α>2 and $R \in \boldsymbol{R}$, the following integral holds

$$\int_0^{\infty} \frac{1}{1+s^{-1}r^{\alpha}} \frac{2r}{R^2} dr = \frac{2\pi s^{2/\alpha} csc\left(\frac{2\pi}{\alpha}\right)}{\alpha R^2}. \quad (31)$$

The results shown in Lemma 1 and Lemma 2 were obtained through the tool of Mathematica.

Theorem 1 (Probability of false alarm in a single interferer network): Let us assume the victim receiver located at the centre of the reference system, and a single LTE interfering device located at random within the two-dimensional plane in an area of radii R. Both interferer and useful transmissions are affected by independent and identically distributed (i.i.d.) Rayleigh distributed amplitude fading coefficients, and the path-loss exponent is α>2. Hence, the *probability of false alarm* is computed through eq. (27) by replacing the CF with the following

$$\Psi(v) = \frac{1}{(1-j2v)^Q} \frac{2R^{\alpha}}{c\frac{\varepsilon_I}{N_0}\left(\frac{jv}{j2v-1}\right)(2+\alpha)} 2F_1\left(1, \frac{2+\alpha}{\alpha}, 2+\frac{2}{\alpha}, \frac{R^{\alpha}}{\frac{\varepsilon_I}{N_0}\left(\frac{jv}{1-j2v}\right)}\right),$$

where N_0 is the one-sided power spectral density of the flat additive noise, and ${}_2F_1()$ stands for the hypergeometric function.

Proof:

At first, it is worth reminding that the false alarm probability is computed under hypothesis H_0. Hence, the characteristic function of the Chi-squared distributed d.v. is computed in correspondence of the non-centrality μ_0.

$$\Psi_{\chi^2}(v) = \frac{1}{(1-j2v)^Q} e^{\frac{jv}{1-j2v}\mu_0} = \frac{1}{(1-j2v)^Q} e^{\frac{jv}{1-j2v} gc\frac{\varepsilon_I}{N_0} r^{-\alpha}} = \Psi_{\chi^2|g,r},$$

which is conditioned upon the power fading coefficient g and the random distance r.

It is worth reminding that $g=\xi^2$ and Eg=1, which can be replaced in the expression of $\Phi(s)$ in the place of the mean ρ of the exponential distribution. Considering the expression above, the idea is to remove the conditioning upon the fading g and the distance r.

$$E_g E_r \Psi_{\chi^2|g,r} = \Psi_{\chi^2}.$$

To remove the condition on g, it is sufficient to notice that with respect to fading all other terms are constants. Moreover, it is worth to remind that the moment generating function of a r.v. is defined as

$$\Phi(s) \triangleq Ee^{sg}.$$

Therefore, the Laplace transformation of the exponential fading can be computed in correspondence of $s=c\varepsilon_I/N_0 r^{-\alpha}$, which yields

$$\Psi_{\chi^2}(v) = \frac{1}{(1-j2v)^Q}\frac{1}{1-\frac{jv}{1-j2v}c\frac{\varepsilon_I}{N_0}r^{-\alpha}} = \frac{1}{(1-j2v)^Q}\frac{1}{1+\frac{jv}{-1+j2v}c\frac{\varepsilon_I}{N_0}r^{-\alpha}}.$$

After doing the sign change above, the theorem is finally proved by removing the conditioning upon *r*, and using the result shown in Lemma 1.

Theorem 2 (Probability of detection in a single interferer network): Let us assume the victim receiver located at the centre of the reference system, a single LTE interfering device is located at random within the two-dimensional plane in an area of radii *R*. Both interferer and useful transmissions are affected by i.i.d. Rayleigh distributed amplitude fading coefficients. Denoting by r_0 the useful link distance and α>2 the path-loss exponent, the *probability of detection* is computed through eq. 27) by replacing the CF with the following

$$\Psi(v) = \frac{1}{(1-j2v)^Q} \times \frac{1}{1-\frac{jv}{1-j2v}\frac{\varepsilon_0}{N_0}r_0^{-\alpha}} \times \frac{2R^\alpha}{c\frac{\varepsilon_I}{N_0}\left(\frac{jv}{j2v-1}\right)} \frac{2F_1\left(1,\frac{2+\alpha}{\alpha},2+\frac{2}{\alpha},\frac{R^\alpha}{\frac{\varepsilon_I}{N_0}\left(\frac{jv}{1-j2v}\right)}\right)}{(2+\alpha)}$$

Proof:

The proof is similar to what already shown in Theorem 1 for the probability of false alarm. The main difference is to substitute the non-centrality parameter μ_1 in the characteristic function of the non-Central Chi-Squared distributed r.v.

$$\Psi_{\chi^2} = \frac{1}{(1-j2v)^Q}e^{\frac{jv}{1-j2v}\mu_1} = \Psi_{\chi^2|g,g_0,r}$$

The following step consists of removing the conditioning upon the fading channels of both useful signal and interferer, as well as remove the conditioning upon the random distance separating the interferer from the victim receiver.

$E_{g0}E_gE_r\Psi_{\chi^2|g,g_0,r} = \Psi_{\chi^2}$

Since the two fading coefficients g_0 and g_I are i.i.d, relying on the moment generating function of an exponentially distributed r.v. with ρ=1, computed in s=jv/(1-j2v)$\varepsilon_0/N_0r^{-\alpha}$ for the useful signal, and s=jv/(1-j2v)$c\varepsilon_I/N_0r^{-\alpha}$ for the interferer, this can be inserted in the characteristic function $E_r\Psi_{\chi^2|r}$.

To complete the proof it is sufficient use the result in Lemma 1.

Theorem 3 (Probability of false alarm with aggregate interference): In a network where the victim receiver is located at the centre of the reference system, multiple interferers are displaced within the two-dimensional plane according to a PPP n an area of radii *R*. The channel amplitude fading coefficients are Rayleigh distributed, and all power fading coefficients are i.i.d. r.vs. For any path-loss exponent α>2, the *probability of false alarm* is computed through eq. (27) by replacing the CF with

$$\Psi(v) = \frac{1}{(1-j2v)^Q}\exp\left(-\lambda_s\left(\frac{jv}{-1+j2v}\frac{c\varepsilon_I}{N_0}\right)^{2/\alpha} \times \frac{2\pi^2}{\alpha}csc\left(\frac{2\pi}{\alpha}\right)\right)$$

Proof:

The proof begins conditioning upon that exactly *K* interferers transmit during the reception time of the victim receiver.

$$I = \sum_{k=0}^{K} I_k .$$

Similar to the single interferer case, the received interference power I_k can be written as follows

$$I_k = g_k c_k \times \varepsilon_I r_k^{-\alpha} \ ,$$

where $\{g_k\}$ are the i.i.d. channel power fading coefficients, and $\{r_k\}$ are the i.i.d random distances, particularly from the k interferers to the victim receiver in the 2-dimensional plane.

Conditioning upon the aggregate interference distribution, the d.v. Y is non-central Chi-squared distributed with a non-centrality parameter

$$\mu = \frac{1}{2\sigma^2}\sum_{k=0}^{K} g_k I_k = \frac{1}{2\sigma^2}\sum_{k=0}^{K} g_k c_k \varepsilon_I r_k^{-\alpha} \ .$$

It is interesting to notice that the non-centrality parameter shown above has the same form of the non-centrality parameter μ_0 computed in eq. (23) for the single interferer case. Therefore, the non-centrality parameter μ can be inserted in the characteristic function of the non-Central Chi-squared distributed r.v.

$$\Psi_{\chi^2}(v) = \frac{1}{(1-j2v)^Q}\exp\left(\frac{jv}{1-j2v}\mu\right) = \frac{1}{(1-j2v)^Q}\exp\left(\frac{jv}{1-j2v}\frac{1}{2\sigma^2}\sum_{k=0}^{K} I_k\right) = \frac{1}{(1-j2v)^Q}\exp\left(\frac{jv}{1-j2v}\frac{1}{2\sigma^2}\sum_{k=0}^{K} g_k c_k \varepsilon_I r_k^{-\alpha}\right) \ .$$

Since the energy of each signal and the scaling factor c are the same for each interferer, the index k can be dropped

$$a = \frac{jv}{-1+j2v}\frac{1}{2\sigma^2} c\varepsilon_I \ \forall \ k \ ,$$

and the expression above can be rewritten as

$$\Psi_{\chi^2|g_k,r_k} = \frac{1}{(1-j2v)^Q}\exp\left(-a\sum_{k=0}^{K} g_k r_k^{-\alpha}\right) = \frac{1}{(1-j2v)^Q}\prod_{k=1}^{K}\exp(-a g_k r_k^{-\alpha}) \ .$$

The characteristic function is conditioned upon the specific realisation of the fading and distances g_k and r_k, respectively.

$$E_{g_k} E_{r_k} \Psi_{\chi^2|g_k,r_k} = \Psi_{\chi^2} .$$

The following step consists of removing the dependence upon fading, which is equivalent of computing the moment generating function of the r.v. g_k. Since all r.vs. are i.i.d. and the expectation is a linear operator, the expectation operations can be swapped. Recalling the expression of the moment generating function of the exponential fading with ρ=1, it is possible to obtain that

$$\Psi_{\chi^2|r}(v) = E_{r_k}\frac{1}{(1-j2v)^Q}\prod_{k=1}^{K}\frac{1}{1+sr_k^{-\alpha}} ,$$

where the last expression will be then computed in s=a. Dropping the index k also in the random distance, it can be written

$$\Psi_{\chi^2|r}(v) = E_{r_k}\frac{1}{(1-j2v)^Q}\left(\frac{1}{1+sr^{-\alpha}}\right)^K .$$

Applying now the result provided in Proposition 1, it is obtained that

$$\Psi_{\chi^2}(v) = \frac{1}{(1-j2v)^Q} e^{-\lambda_s \int_{\boldsymbol{R}^2}\left(1-\frac{1}{1+sr^{-\alpha}}\right)dr} = \frac{1}{(1-j2v)^Q} e^{-\lambda_s \int_{\boldsymbol{R}^2}\left(\frac{1}{1+s^{-1}r^{\alpha}}\right)dr} .$$

The last part of the proof consists of using the result shown in Lemma 2 in s=a.

Theorem 4 (Probability of detection with aggregate interference): Let us assume the victim receiver located at the centre of the reference system and multiple interferers are displaced within the two-dimensional plane according to a PPP in an area of radii R. The channel amplitude fading coefficients are Rayleigh distributed, and all power fading coefficients are i.i.d. r.vs. For any path-loss exponent α>2, the *probability of detection* is computed through eq. (27) by replacing the CF with the following

$$\Psi(v) = \frac{1}{(1-j2v)^Q}\frac{1}{1-\frac{jv}{1-j2vN_0}\varepsilon_0}\exp\left(-\lambda_s\left(\frac{jv}{-1+j2v}\frac{c\varepsilon_I}{N_0}\right)^{2/\alpha}\times\frac{2\pi^2}{\alpha}csc\left(\frac{2\pi}{\alpha}\right)\right).$$

Proof:

The proof of this theorem is essentially the same to what shown already for the probability of false alarm in Theorem 3. The d.v. is indeed non- central Chi-squared distributed but in this case the non-centrality parameter is written as

$$\mu = \frac{1}{2\sigma^2} g_0 \varepsilon_0 + \frac{1}{2\sigma^2} \sum_{k=0}^{K} g_k c_k \varepsilon_I r_k^{-\alpha}.$$

The complete proof relies again on Lemma 2.

7.4.5. Numerical Results

Results of the probabilities of false alarm and detection are shown relying on the numerical values provided in Table 6, assuming a path-loss exponent α=4 (e.g. indoor propagation environment) when the propagation is affected by Rayleigh-distributed fading. In addition, different values of the LTE transmit power were assumed: 20 dBm, 22 dBm and 24 dBm. It is also worth reminding that the Wi-Fi signal bandwidth is assumed to 20 MHz (although 40 MHz bandwidth could also be possible as shown in [802_11n_2009]). Furthermore, also the LTE signal was assumed to have the maximum system bandwidth of 20 MHz.

A link budget was computed to obtain the energy of both useful (i.e. Wi-Fi) and interfering (i.e. LTE) signals. At first it is computed the interfering signal energy at the transmitter side.

$$\varepsilon_I[dBm] = P_{tI}[dBm] - L_0[dB] - 10\log_{10}(R_I), \tag{32}$$

where $L_0 = 20\log_{10}\left(\frac{4\pi}{c} f_c\right)$ stands for the one-meter free space path-loss and R_I is the transmission rate of the interferer.

On a similar basis, the received useful signal energy is computed as follows

$$\varepsilon_0[dBm] = P_{t0}[dBm] - L_0[dB] - 10 \times \alpha \times \log_{10}(r_0) - 10\log_{10}(R_0), \tag{33}$$

where R_0 is the transmission rate of the useful signal.

The reason for computing the energy at the transmitter side for the interfering signal can be found in Theorem 1 and 2, in which it was shown that the effect of interference at the victim Wi-Fi receiver was already averaged with respect to all possible locations of the interference within the maximum distance R. In addition, the distance separating the Wi-Fi transmitter from the intended receiver, r_0, is left as a free parameter. Second, the free space path-loss exponent (α=2) has been considered up to 1 meter. Since the focus of the study is on indoor environments, for any other distance it was considered α=4.

At this point, it is possible to compute the Interference-to-Noise-Ratio (INR) at the transmitter side. Being more specific, the INR is computed one meter away from the transmitter.

$$INR[dB] = P_{tI}[dBm] - L_0[dB] - 10\log_{10}(R_I) - N_0[dBm]. \tag{34}$$

A similar computation is carried out for the useful signal, when the receiver is located r_0 meters away from the transmitter. Thus, the Signal-to-Noise-Ratio (SNR) is computed in the following manner.

$$SNR[dB] = P_{tI}[dBm] - L_0[dB] - 10 \times \alpha \times \log_{10}(r_0) - 10\log_{10}(R_I) - N_0[dBm]. \tag{35}$$

In eq. (19), a factor c was introduced in the definition of the amplitude of the signal received at the victim Wi-Fi receiver. Such a parameter can be defined formally at this point, before showing results.

$$c = INR \times N_{bits/symbol} \times 1/N_{\frac{samples}{symbol}} \times f_s^{(LTE)}/f_s^{(Wi-Fi)}, \quad (36)$$

where $f_s^{(LTE)}$ and $f_s^{(Wi-Fi)}$ are the typical sampling frequency of LTE and Wi-Fi, respectively. In general, it holds that $f_s^{(LTE)} \neq f_s^{(Wi-Fi)}$.

Table 7 Additional Numerical parameters for results [Sesia_2011] and [802.11n_2009]

Parameter	Description	Value
P_{tI}	Interfering LTE transmit power	20 dBm, 22 dBm, 24 dBm
P_{t0}	Wi-Fi transmit power	20 dBm
R	Maximum distance for evaluating interference effect	40 m
r_0	Victim link distance	$0 \leq r_0 \leq R$
α	Path-loss exponent	4
f_c	Centre frequency	5 GHz
λ_s	Spatial density for aggregate interference. The value is computed assuming that in the area of radius R, on average 4 LTE interferers are active: $\lambda_s = N_s/\pi R^2$, following the expression for the PPP in eq. (28)	0.0014
N_0	Noise power spectral density	-174 dBm/Hz
R_I	Transmission rate of the LTE interfering signal	57 Mbit/s
R_0	Transmission rate of the Wi-Fi preamble.	6 Mbit/s
$f_s^{(LTE)}$	LTE sampling frequency	30.72 MHz [Sesia_2011]
$f_s^{(Wi-Fi)}$	Wi-Fi sampling frequency	20 MHz
$N_{bits/symbol}$	Value that depends on the particular Modulation used by LTE; a 64-QAM was assumed	6
$N_{samples/symbol}$	Number of samples per symbol in the LTE transmission	2208 [Sesia_2011]

The results that were obtained through the analytical work shown in previous sections are shown in Figure 37 and Figure 38 for the probability of false alarm and detection respectively.

Figure 37 shows that, without interference (yellow solid line), the threshold for a P_{fa} equal to 10^{-3} is around -63 dBm. On the other hand, the threshold would raise to – 55 dBm when a single interferer is active (red curve) but 10-3 cannot be achieved any more. For an interference power of 24 dBm, the threshold increases even to approximately -51 dBm and also in this case only 10^{-2} is achievable. Therefore, in all cases there is a significant degradation of the CCA performance since P_{fa} raises from 10^{-3} to 10^{-2}. With aggregate interference (blue curves) false alarm performance degrade even more, and

the threshold lays within the interval between -57 dBm and -53.5 dBm for different values of the interfering power but in any case, P_{fa} raises to 10^{-1}, which makes the CCA operation even less reliable in idle channel conditions.

A similar degrading effect of the interference can be observed in Figure 38 for the probability of detection when the probability of false alarm was fixed to 0.1. As expected, the case with aggregate interference provides the poorest performance in terms of detection. On the other hand, to maintain the probability of detection not less than 0.9, the coverage of the Wi-Fi network would shrink to almost 5 m in the worst case of aggregate interference and LTE transmit power of 24 dBm. With a single interferer it is possible to reach nearly 13 m with the same transmit power value. Anyway, even in the presence of a single interferer, the case without interference would assure a probability of detection not less than 0.9 up to 26 m. Hence, even with a single interferer, the loss in coverage of the Wi-Fi network is around 50% in the worst case of 24 dBm. In this case, coverage must be understood as the coverage area that ensures a CCA operation the can achieve the target performance in terms of false alarm and detection probabilities.

Looking at the probability of false alarm, for a target of 0.1 (which is far from a desirable target value), the new ED threshold with a single interferer is similar to that without interference, whereas with aggregate interference it would increase to -53.5 in the worst case of using 24 dBm for the interference power. Even keeping P_{fa} to 0.1, the Wi-Fi network coverage has to be sacrificed to enable reliable CCA operation.

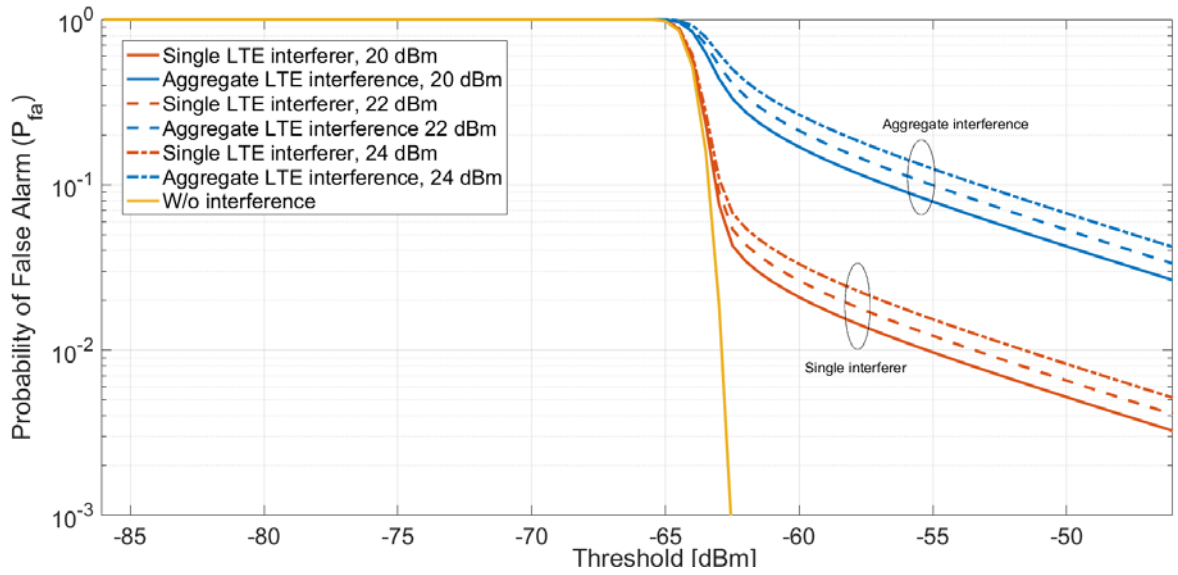

Figure 37: Probability of false alarm (P_{fa}); comparison between the case without interference and the cases with single interferer and aggregate interference, when the LTE transmit power was assumed 20 dBm, 22 dBm and 24 dBm, respectively.

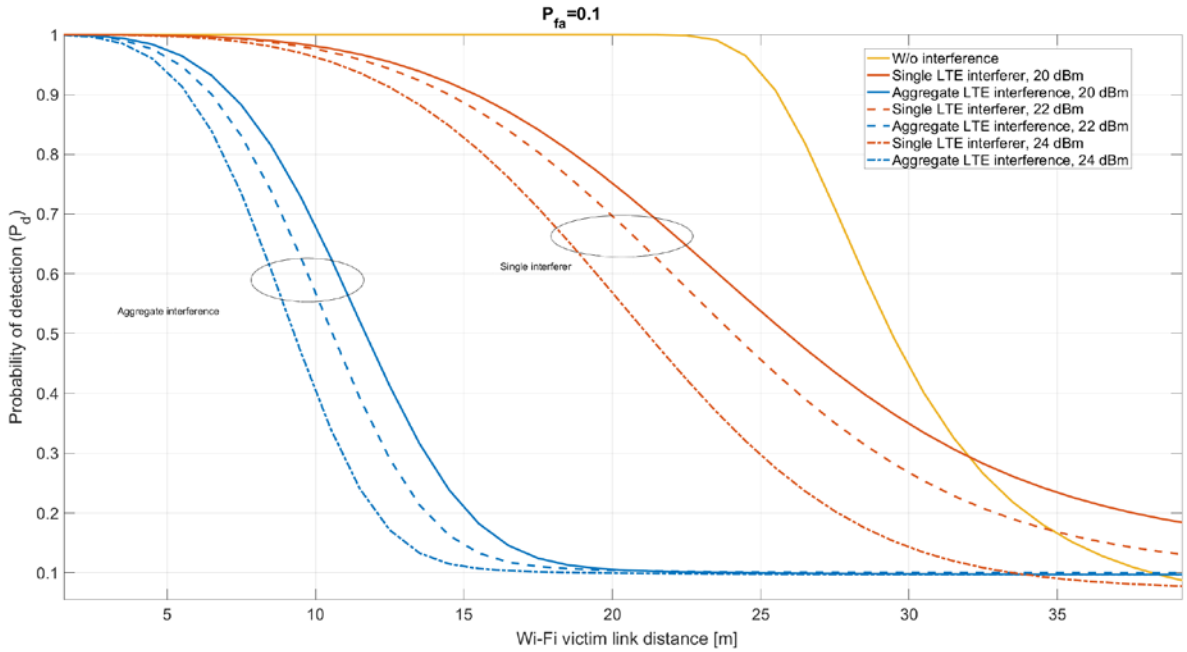

Figure 38: Probability of detection (P_d); comparison between the case without interference and the cases with single interferer and aggregate interference, when the LTE transmit power was assumed 20 dBm, 22 dBm and 24 dBm, respectively.

7.4.6. Concluding Remarks

The analytical work shown in previous sections has allowed us to model both probability of false alarm and detection without and with interference affecting the Wi-Fi CCA operation. Specifically, the cases with single interferer and with aggregate interference were modelled. The added value of the proposed method lays in the characteristic function approach that provides a very powerful tool that leads to closed form expressions of the characteristic functions, and that requires only one numerical integration in the Gil-Pelaez inversion theorem. Numerical results have shown significant degradation of both false alarm and detection performance in the presence of interference. Furthermore, the results have shown sensitivity with respect to interference parameters such as the number of interfering transmitters, and the transmit power used. From the point of view of the Wi-Fi network, the presence of interference implies significant reduction of the coverage area in order to target CCA performance less affected by interference.

7.5. Location-Based Spectrum Sharing

Goal of the study and connection to the COHERENT architecture

In this section, a coordination protocol for co-primary spectrum sharing between coexisting mobile network operators is investigated. The idea is that based on inter-operator interference level and operators' load, the operators use shared spectrum in a flexible and dynamic way. The decisions of the spectrum sharing schemes are made by the SMA and these decisions are implemented and controlled by C3. The goal of this study is to provide a flexible spectrum access mechanism, which maximizes joint spectral efficiency.

Task covered: Task 4.2

7.5.1. Introduction

For decades spectrum has been allocated to users in a command control mode, which gives the users the right to use certain range of frequency exclusively in a given time. The exclusive assignment of a spectrum has an advantage to avoid interference between transmitters. This approach has been working effectively for a long time and brings an immense success to the world of mobile communication. However, from spectral point of view dedicated allocation of a spectrum leads to underutilization of the available spectrum [FCC_2002], [Yang_2004].

Since spectrum is an expensive and scarce resource, an efficient utilization mechanism is a necessity to have. For efficient utilization of resources, a transition from static allocation to flexible and dynamic spectrum allocation has drawn attention of the research community. To cope with the exponential growth of mobile data traffic and demand for high data rates, flexible spectrum usage is an essential solution. Combine the flexible spectrum usage with the deployment of small cells, it will provide a capability to provide a better throughput and improve utilization of frequency.

In our approach, we studied a coordination mechanism for a co-primary spectrum sharing between heterogeneous (HetNet) mobile network operators (MNO). The RANs of the MNOs coexisted in the same geographical area. We modeled the competitive interaction between the operators as a non-cooperative repeated game, where the MNOs are considered as players. The operators are assumed as selfish and try to maximize their own utility, hence cooperation in between is self-motivated.

The aim of this study is to show how operators coordinate to minimize inter-operator interference and benefit from the joint usage of a spectrum. We have shown that for operators getting an option of small or big favor enables them to improve user rate and minimize the excess utility loss.

7.5.2. State of the Art

We considered a downlink co-primary spectrum sharing between HetNet MNOs. The MNOs comprises a microcell and femtocells. Each operator has a licensed frequency band composed of *P* component carriers (CCs). The microcells can transmit over all *P* CCs. Microcells of each operators share their spectrum orthogonally. The operators mutually agree to use their spectrum jointly for efficient utilization of the available resource. For the construction of the common spectrum pool, each operator contributes equal number of CCs. Femto access points of each operator are then allowed to transmit over the common pool, whereas the micro base stations share their frequency orthogonally. Figure 39, shows the spectrum allocation for the microcells and femtocells as well as the common spectrum pool in case of two operators. For simplicity, we consider two operators participating in our spectrum-sharing model, but it can be expanded to a number of operators.

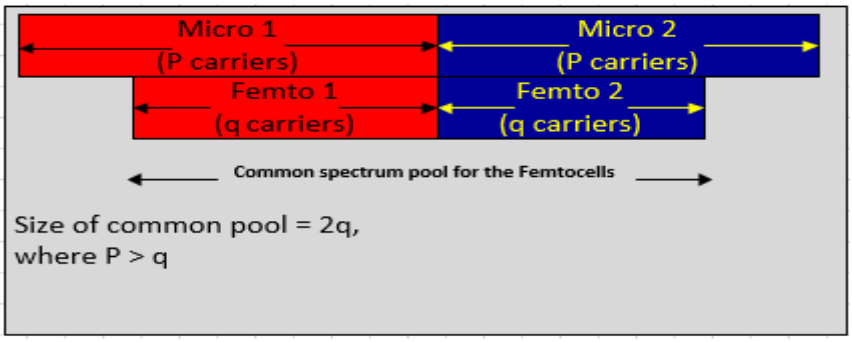

Figure 39. Spectrum allocation between femtocell and microcell and construction of a common spectrum pool for femtocell of operator 1 and operator 2.

Due to common utilization of the spectrum pool, inter-operator interference between femtocells and microcells is expected. To minimize this interference, the operators agree on prior rules for the regulation of the spectrum pool usage. Our model follows the spectrum usage favor introduced in [Singh_2015] for the interaction between the operators. Based on interference profile and traffic load, operators ask each other a spectrum usage favor for exclusive use of some CCs of the common pool. The spectrum usage favor refers to, when an operator asks the other operator to stop using some of the CCs from the common spectral pool for some time [Singh_2015]. In our approach, to avoid the co-tier

and cross-tier inter-operator interference the microcell and femtocell of an operator can ask a spectrum usage favor from femtocell of the other operator. It is possible for both operators to ask and grant a spectrum usage favor at the same time and the utilization of the common pool may even become orthogonal. An operator can ask favor for a maximum of the number of CCs it provided to the common pool.

The location-based spectrum sharing mechanism introduces an option of 'small' and 'big' favor for the fair regulation of the common spectral pool constructed by the operators. For this purpose, the common total coverage area divided into smaller subareas. Each subarea contains a number of base stations of both operators. The subareas known commonly by the operators as A1, A2..., An. The dimension of each subarea is agreed at priori between the operators. A small favor represents a favor from Femtocell Access Points (FAPs) in one of the subareas, whereas big favor constituents all FAPs in all subareas. In this location-based spectrum sharing mechanism, the exchange of favors between the operators follow the same coordination mechanism as [Singh_2015]. The mutually agreed spectrum sharing rules between the operators includes the decision-making mechanism rules, favor validity time, dimension of subareas, and the default state. The default state represents the state at which both operators' femtocells are utilizing the common pool. When an operator granted a favor, the exchanged favor is valid for the certain interval of time called, favor validity time. Favor validity time is fixed and in the range of seconds. As the granted favor necessitates a departure from the default state, the expiration of the favor validity time returns the usage of the common pool to the default state.

In the considered repeated game, the interaction between the operators is based on book keeping of the exchange of favors. At a given stage of the game, an operator is willing to give a spectrum usage favor if and only if the other operator is going to pay it back with equal amount of favor in the future. Since the repeated game encounters a large set of equilibrium points, it is hard to find and analyze its unique NE point. Therefore, we follow heuristic threshold based strategies [Singh_2015_2] to obtain long-term reciprocity. The threshold value keeps monitoring the exchange of favors between the operators.

7.5.3. Location Based Spectrum Sharing Mechanism

Initially the utilization of the spectrum pool is at the default state. At the given state, to determine whether to ask or grant a favor, an operator needs to estimate the utility gain or loss of its own for asking or granting a favor respectively. The utility represents the satisfaction of users for the services offered by the serving operators. To calculate the utility gain or loss an operator needs to estimate the level of the inter-operator interference. For the estimation of the interference level from opponent operator network, an operator can ask its UEs to measure the interference from other opponent operator and report to the serving base station. Normally a UE is able measures the signal strength and quality of the neighbor cells of own operator network through reference signals for cell selection, reselection and handover purposes [Teng_2014]. With the same procedure, it is feasible for a UE to measure the total interference from other operators' network. The UE then reports the total inter-operator interference to the serving base station. Upon receiving the total inter-operator interference from all UEs it serves, a small cell can estimate the impact of the inter-operator interference. Aggregating the reports, a base station or a FAP will send it to the spectrum controller. Once this information is retrieved, the Spectrum Manager Application running on the CCC sums up the aggregated small cells report in each sub areas and sorts the sub areas based on the impact from the inter-operator interference. The spectrum controller selects a sub area with highest interference from other operator networks. If the level of inter-operator interference in all subareas is almost the same, then the spectrum controller selects the total area to ask a favor. Once the area is selected, the spectrum controller evaluates its network utility gain or loss for asking or granting of a presumed favor comparing with the utility in the default state. The system architecture for the co-primary spectrum sharing is shown in Figure 40.

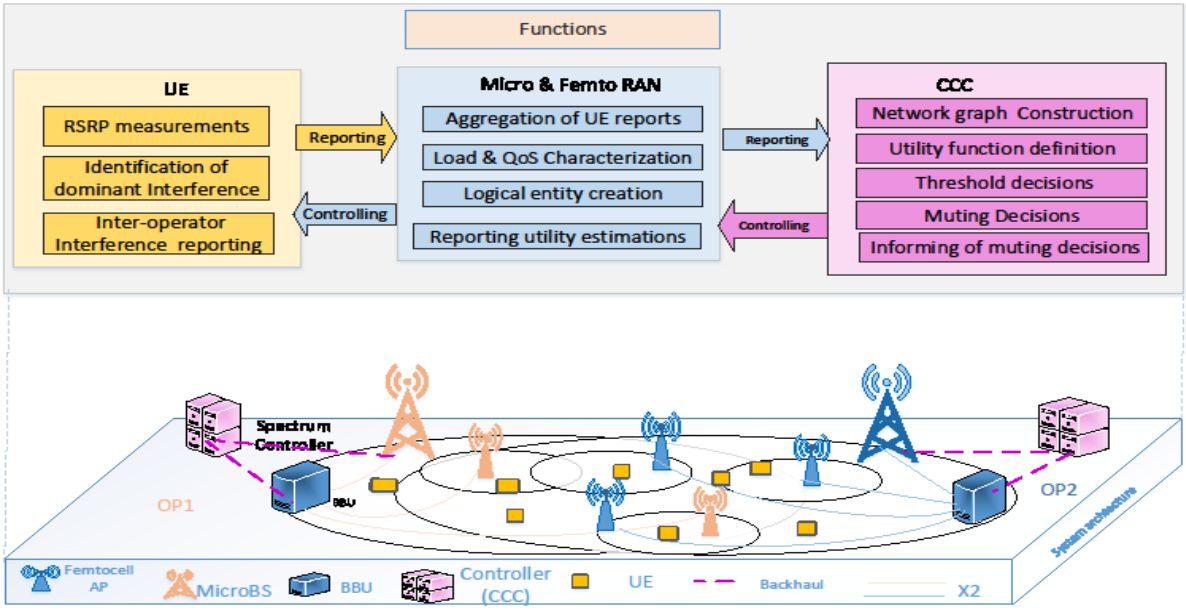

Figure 40. System Architecture for Location-based spectrum Sharing

To decide whether to ask or grant a favor the operator OP1 then compares its immediate utility gain with the threshold values. If the utility gain is greater than the threshold value (expected utility loss) for the given component carrier, then OP1 will ask a favor from OP2. An Operator always attempts to ask the maximum number of CCs, so that its utility gain is greater than the corresponding threshold value. OP2 then accepts the spectrum usage favor request if its immediate utility loss for giving the required spectrum usage favor on the given CC is less than the expected utility gain (threshold value). Then OP1 and OP2 will update their corresponding threshold values. The discussed mechanism in pseudocode format can be found in [Sewda_2017].

Model of Wireless Network

Suppose the common area, A, shared by the operator two operators OP1 and OP2 is divided into *n* subareas $A = \{A_1, A_2 \ldots A_n\}$. The FAPs of operator O € {OP1, OP2} located in subarea A_x gives a service for n_{Ax} number of users. The micro base station of operator O gives coverage for n_M users. The downlink signal to interference plus noise ratio (SINR) of the *n*-th users of operator O on the *i*-th CC can be defined as:

$$SINR_{n,i} = \frac{\beta_{O,i} S_{O,n,i}}{I_N + \beta_{O,i} I_{O,n,i} + \beta_{-O,i} I_{-O,n,i}}. \quad (37)$$

During orthogonal sharing of spectrum between the operators, the SINR is:

$$SINR_{n,i} = \frac{\beta_{O,i} S_{O,n,i}}{I_N + \beta_{O,i} I_{O,n,i}}, \quad (38)$$

where $S_{O,n,i}$ is the downlink received signal power, I_N is the noise power, and $I_{O,n,i}$ and $I_{-O,n,i}$, respectively represents the intra- and inter-operator interference on the *i*-th cc. In the above expressions, the allocation indicator beta (β) indicates whether operator O is using the *i*-th CC. At the default state, both operators are utilizing the spectral pool, β_O=1 and β_{-O} =1, whereas in case of favor exchange if the femtocells of operator O stops using the *i*-th CC the assignment indicator β_O=0.

For the *n*-th UE of operator O the transmission rate on the *i*-th CC can be calculated as:

$$R_{n,i} = \omega_{n,i} BW_i \log_2(1 + SINR_{n,i}), \quad (39)$$

where *BW* is the bandwidth a CC and $\omega_{n,i}$ is the time scheduling weight of the *n*-th user on the *i*-th CC.

Utility function

Initially the operators are at the default state in which both operators' femtocells utilize the common spectral pool. Therefore, at each stage game operators first calculate the network utility at the default

state. We assumed both operators use a proportionally fair utility function. The logarithmic proportional utility function maximizes the overall utility of user rates by providing a compromise between user fairness and maximum throughput [Liu_2008]. The network utility of operator O, U_O defined as:

$$U_O = \sum_{n=1}^{n_{A1}} \log\left(\sum_{i=1}^{2q} R_{n,i}\right) + \cdots + \sum_{n=1}^{n_{An}} \log\left(\sum_{i=1}^{2q} R_{n,i}\right) + \sum_{n=1}^{n_m} \log\left(\sum_{i=1}^{P} R_{n,i}\right), \quad (40)$$

$$U_O = U_{o.A1} + U_{O,A2} + \cdots + U_{O,An} + U_{O,M}. \quad (41)$$

The utility function of operator O in equation (41) is a function of β_O and β_{-O} through equation (37) and equation (38):

$$U_O = U_O(\beta_O, \beta_{-O}). \quad (42)$$

Thus, the utility function of operator O at the subarea A_x:

$$U_{O,Ax} = U_{O,Ax}(\beta_{O,Ax}, \beta_{-O,Ax}). \quad (43)$$

At the default state both operators are transmitting over the $2q$ CCs, thus $\beta_O^{2q} = 1$ and $\beta_{-O}^{2q} = 1$ where $\beta_O^{2q} = \beta_1, \beta_1, \ldots, \beta_{2q}$.

Area Selection

This option of area selection is made for a more localized spectrum sharing mechanism, where operators agree and select subareas to avoid the interference from nearest base stations and the interference from other sub area base stations assumed to be negligible.

As we have discussed in the above section, the operator selects a subarea or the total common area to make a favor request. Thus, the interference level at each area is compared with the total area interference level. The interference level over the total common area I_A can be calculated as:

$$I_A = I_{A1} + I_{A2} + \cdots + I_{An}. \quad (44)$$

where I_{Ax} is the interference at each sub area A_x. The interference over subarea A_x summed up as:

$$I_{Ax} = \sum_{i=1}^{m} I_i. \quad (45)$$

where I_i the interference report from users served by base station i, and m is the number of base stations housed in subarea A_x.

Then to select the subarea with the highest interference level the sum interference at each subarea will be compared to the total area sum interference. If $I_{Ax} > \mu I_A$, where μ is set as a selection coefficient. For example, if μ = 0.6, then a sub area which contains 60 % of the total interference from the other operator is selected. After the selection if the utility gain for the assumed favor is much less than the case where the total area is selected, then other sub area will be considered to make a favor request.

Small Favor

Based on the measurement report from its UEs, let us assume that operator OP1 selects subarea A_x to ask a favor from operator OP2 to stop using q CCs from the common pool. Then operator OP1 estimates its utility gain taking an assumption that Operator OP2's FAPs in the selected subarea A_x stops transmitting over these CCs and the interference coming from the neighboring subarea FAPs are considered negligible. Thus, the assignment indicator of OP2 for subarea A_x will be zero over the given CCs. The immediate utility gain of OP1 for the assumed small favor over q CCs can be calculated as:

$$U_O^{gain} = U_O^{hyp} - U_O^{default} \quad (46)$$

$$U_O^{gain} = U_O^{hyp}(\beta_O, \beta_{-O}) - U_O^{default}(\beta_O, \beta_{-O}). \quad (47)$$

At the hypothetical state the assignment indicator for Operator OP2 (-O):

$$\beta_{-O}^{2q} = \beta_{-O,Ai}^{2q} = 1, \quad (48)$$

where i = (1, 2... n) and $i \neq x$.

For $i = x$ the assignment indicator can be re-written as $\beta_{-O}^{2q} = (\beta_{-O}^{q}, \beta_{-O}^{2q-q})$, where $\beta_{-O}^{q} = (\beta_{-O,1}, \dots, \beta_{-O,q})$ and $\beta_{-O}^{2q-q} = (\beta_{-O,q+1}, \dots, \beta_{-O,2q})$. Thus, the assignment indicator of Operator -O for the subarea A_x is $\beta_{-O,Ax} = (0^q, 1^{2q-q})$.

From (46), the utility gain of operator O at the given stage of game for getting a small favor from OP2 in the q-th CC on the subarea A_x can be estimated as:

$$U_O^{gain} = U_{O,Ax}(1^{2q}, (0^{2q}, 1^{2q-q})) - U_{O,Ax}(1^{2q}, 1^{2q}) \quad (49)$$

Each operator selects a strategy to maximize its utility, but at a single stage of a game, an operator may experience a loss for granting a favor. However, an operator will get the favor back in return in the near future. Upon being asked, Operator OP2 estimates its utility loss for the required favor over the subarea A_x before granting a favor:

$$U_O^{loss} = U_{-O,Ax}(1^{2q}, 1^{2q}) - U_{-O,Ax}((0^{2q}, 1^{2q-q}), 1^{2q}) \quad (50)$$

Big Favor

An operator considers a big favor when the interference from opponent operator affects its utility over all the area shared by both operators. In such a case, an operator selects the whole area to request for a favor. Let us assume operator O selects the given common shared area A, to ask a favor from operator -O over q CCs. The utility gain of operator O estimated, taking in assumption that the FAPs of Operator -O installed over the common area stops using q CCs of the common pool. Thus, the utility gain can be estimated from equation (46) and the assignment indicator of for operator -O at the hypothetical state assumed to be:

$$\beta_{-O}^{2q} = \beta_{-O,Ai}^{2q} = 1, \quad (51)$$

for all i=(1, 2,…,n).

Therefore, the utility gain of Operator O for getting a big favor from Operator -O over q CCs estimated as:

$$U_O^{gain} = U_O(1^{2q}, (0^{2q}, 1^{2q-q})) - U_O(1^{2q}, 1^{2q}). \quad (52)$$

Similarly, operator -O estimates its utility loss for the required big favor:

$$U_O^{loss} = U_{-O}(1^{2q}, 1^{2q}) - U_{-O}((0^{2q}, 1^{2q-q}), 1^{2q}). \quad (53)$$

One can observe from the above equations the difference between a small favor gain/ loss and a big favor gain/loss is that, the change in the utility for small favor is only over the area selected for a given favor. Whereas for a big favor the gain/loss of the operator's utility are calculated over all the common area.

Non-Localized Spectrum sharing

The location-based spectrum sharing presented above discusses a localized spectrum sharing between two operators in common coverage area. By classifying the shared area into subareas, we introduce a more-localized spectrum sharing between the operators. Let us consider a common geographic area which encompasses N multiple independent set of coverage areas such as buildings. The term independent is used to mean that, the transmissions in one building do not interfere with the transmissions in the other building. Thus, in a given common geographic area the operators play N-stage repeated location-based spectrum sharing game, where a single stage game refers to a game in one building.

The non-localized spectrum sharing involves operators in a single stage game over the total geographic area instead of localized game into buildings or more-localized game to smaller areas. Now consider a single stage game where the operators OP1 and OP2 exchange spectrum sharing favors based on the network load or interference profile over the total coverage area. Each operator asks or grants a favor of up to q CCs. Unlike location-based spectrum sharing, in Non-localized spectrum sharing the exchange of favor affects the user's throughput over all the geographic area. When operator O grants a favor of q CCs for operator -O, all base stations of operator O stops transmitting over the q-th CCs.

For an operator O, to ask/ grant a favor it estimates its utility gain/ favor in each building and takes the summation. For N buildings in a given common geographic area, the total utility gain for operator O for getting a spectrum favor over q CCs estimated as:

$$U_O^{gain} = \sum_{j=1}^{N}\left(U_{O,q,j}^{gain}\right), \quad (54)$$

where j = 1, 2,..., N and $U_{O,q,j}^{gain}$ is the utility gain of operator O in the localized area j, and it can be estimated using Eq. (52). Similarly, the utility loss of operator O for granting a favor of q CCs estimated as:

$$U_O^{loss} = \sum_{j=1}^{N}\left(U_{O,q,j}^{loss}\right), \quad (55)$$

where j = 1,2,..., N and $U_{O,q,j}^{loss}$ is the utility loss of operator O for granting q CCs favor over localized area j from Eq. (53).

In Non-localized single stage spectrum sharing game, both operators utilize the common spectral pool at the default stage. In a single stage game, the operator's utility loss/gain depends on the strategic decision made by each operator at this stage of the game. The available set of strategies for each operator is: ask a favor, grant a favor or do nothing. To maximize their utility, it is clear that both operators will ask a favor and never grant a favor. Therefore, the equilibrium solution for this single stage game is for both operators to ask a favor. However, since both operators do not want to grant a favor, the logical decision is that both operators utilize the common spectral pool.

Simulation Results

The simulation environment considers the example deployment in Figure 41 assumed to have 400 buildings laid out in Manhattan-like grid model. The dimension of each building covers 100 m x 100 m and inter building distance of 30 m. Each building allocates to both operators. In each building we consider the deployment of Figure 42, comprising five indoor Femto access points (FAP) per operator. The micro base stations of both operators deployed outside of the building to give coverage to the outdoor users as well as some indoor users. The indoor installed FAPs give coverage to indoor UEs and assist microcells of the operator. The given UE selects the serving base station of home network based on the strongest reference signal received power. During the localized per building spectrum sharing, each building is considered for each single stage game. For the localized per half building, the area of a building is divided into two sub areas A = (A1, A2). Both operators know the sub areas at priori as area1 (A1) and area2 (A2), in which the exchange of favors in these subareas referred to us a small favor. Subarea A1 covers for 50 m x 50 m left half of the building whereas; subarea A2 covers right half of the area. Layout of the simulation scenario is shown in Figure 41 and Figure 42.

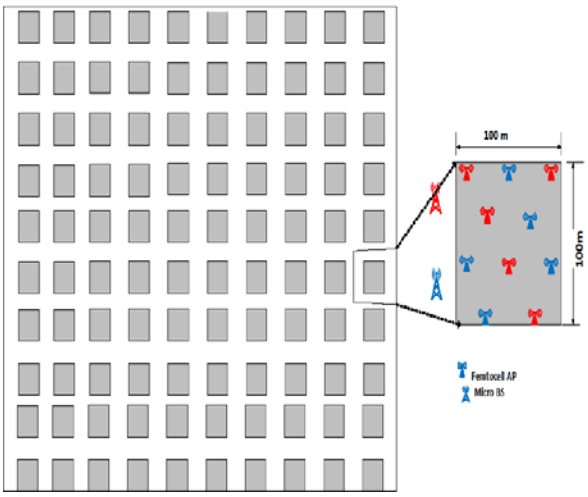

Figure 41. Simulation Environment - Multi-building simulation environment

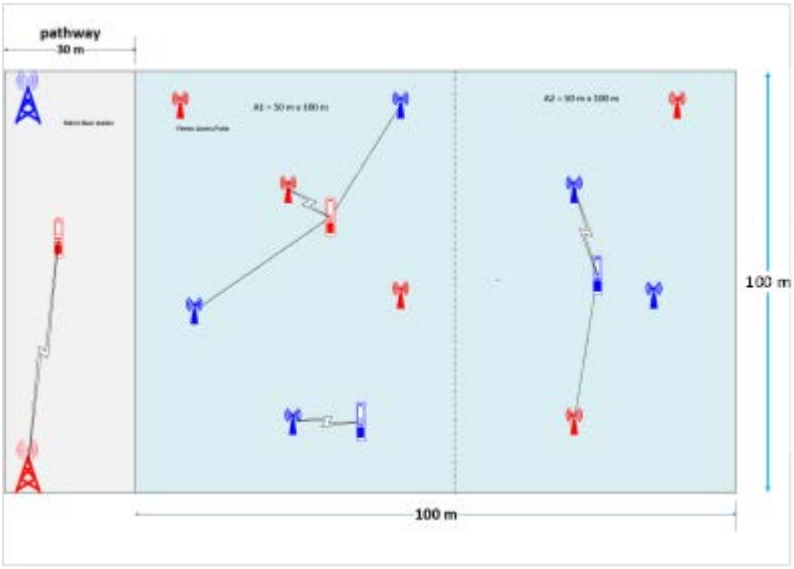

Figure 42. Simulation Environment - Micro base station and FAPs deployment scenario

For the indoor and outdoor signal propagation, we consider a simple power-law distance based propagation path loss model at a carrier frequency of 2.6 GHz. We assumed modern buildings with external thick wall, hence due high wall attenuation the interference from indoor FAPs to outdoor users assumed to be negligible. However, the micro cell transmission interferes the indoor Femto-connected users received signal. For outdoor-to-indoor propagation, we use 17 dB wall attenuation.

Each operators' licensed frequency bandwidth of 30 MHz is divided into 3 equal CCs of 10 MHz each BWc = 10MHz. The outdoor deployed Micro base station of each operator can transmit their signal over 3 CCs of own operator's license with the available power budget of 30 dBm per CC. During orthogonal spectrum sharing, FAPs of the operators can use only two CCs of own operator license to serve Femto-connected UEs. For the construction of the common spectral pool, both operator contributes 2CCs of the femtocells, providing a total size of a pool 4CCs. Thus, as discussed in previous chapter the FAPs can access the common pool simultaneously with the available power budget of 20 dBm per 10 MHZ at default state. However, due to the coexistence of the operators, micro-connected UEs experience an interference from FAPs of the opponent operator from half of the spectral pool. In addition, Femto-connected UEs experiences Femto to Femto interference. Details of simulation parameters are given in Table 8.

The assumed repeated spectrum sharing game between the operators (OP1 and OP2) is a 400 stage, where a single stage game represents an exchange of favor in one building. Simulation results are presented in terms of the cumulative distribution function (CDF) of the throughputs obtained in all the spectrum-sharing scenarios, generated according to the aforementioned parameters. The user rate CDFs are plotted for operators OP1 and OP2 with respective symmetric and asymmetric Poisson distributed mean number of users.
In case of asymmetric mean number of users per operator, a load reversal considered to balance the exchanged number of favors between the operators. Thus, for the first 200 rounds of the simulation the mean load for operator OP1 is 1200 and 800 for operator OP2. Then for the latter 200 rounds, the mean load for operator OP1 is 800 and 1200 for operator OP2. For symmetric case, the mean number of users for both operators equals 800.

Table 8. Simulation setup

Parameter	Value
Number of Operators	2
Number of FAPs/operator	5 per building
Number of Micro BSs/operator	1 per building
Number of UEs	Poisson distributed with mean *N* per operator per the total area
Carrier Frequency	2.6 GHz
Total Bandwidth/ operator	30 MHz
Number of Component Carriers/ Operator	3
Spectrum pool size	4 Component carriers
Carrier Bandwidth	10 MHz
Transmission power in Femtocell	20 dBm
Transmission Power in Microcell	30 dBm
Scheduler	Proportional fair
Number of buildings	400
Inter-building distance	30 m
Building dimension	100 m X 100 m
Indoor Layout	Single Story
Number of Sub Areas	2
Sub Area dimension	50 m X 50 m
Path loss model	power law distance based path loss Cd^{-A}
Path loss exponent	A=3.7
Attenuation Constant	C= 8.435e-5
Wall Attenuation	17dB

The simulation results depict the following spectrum sharing scenarios:

- **Orthogonal spectrum sharing (Orthogonal-SS)**: The operators utilize their own spectrum orthogonally.
- **Non-Localized spectrum sharing (Non-Localized-SS)**: The sharing of the common spectrum pool agreed at the total geographic area level thus, both operators utilize the common spectrum pool jointly over the shared area.
- **Localized per building spectrum sharing (LocalizedBuilding-SS)**: The operators agree exchange of spectrum favor per building level *i.e.* operators exchange always a big favor.
- **Localized per half-building spectrum sharing (LocalizedHalfBuilding-SS)**: The exchange of spectrum usage favor is agreed per half building. The spectrum sharing favor consists in an option of either small or big favor.

In Figure 43 and Figure 44, the CDF of the user rate distribution of both operators with orthogonal-SS, Non-Localized-SS, localized per Building-SS and Localized per Half Building-SS with *asymmetric* mean number of users per operator is depicted.
In Figure 45, the CDF of the user rate distribution of operator 1 users with orthogonal-SS, Non-Localized-SS, localized per Building-SS and Localized per Half Building-SS with *symmetric* mean number of users per operator is depicted.

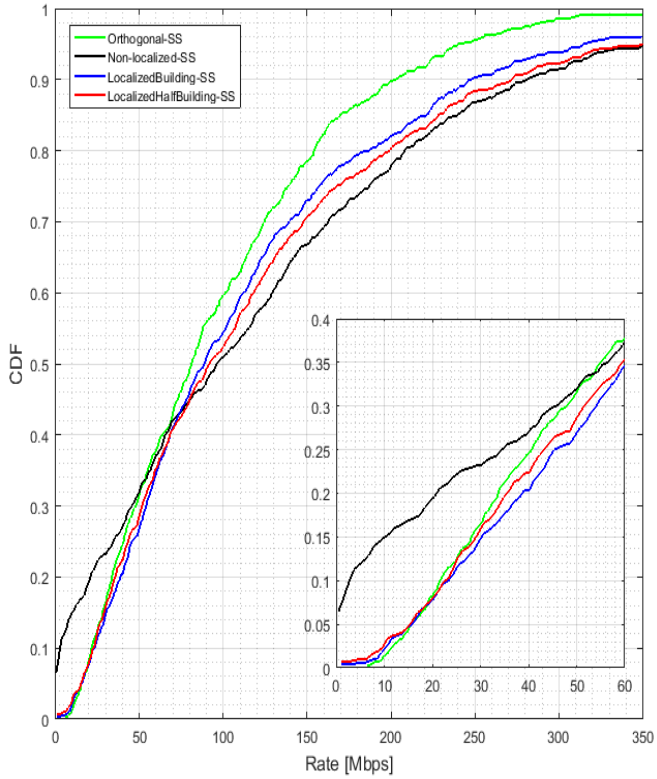

Figure 43. User rate distribution with asymmetric operator mean load (Operator 1 users).

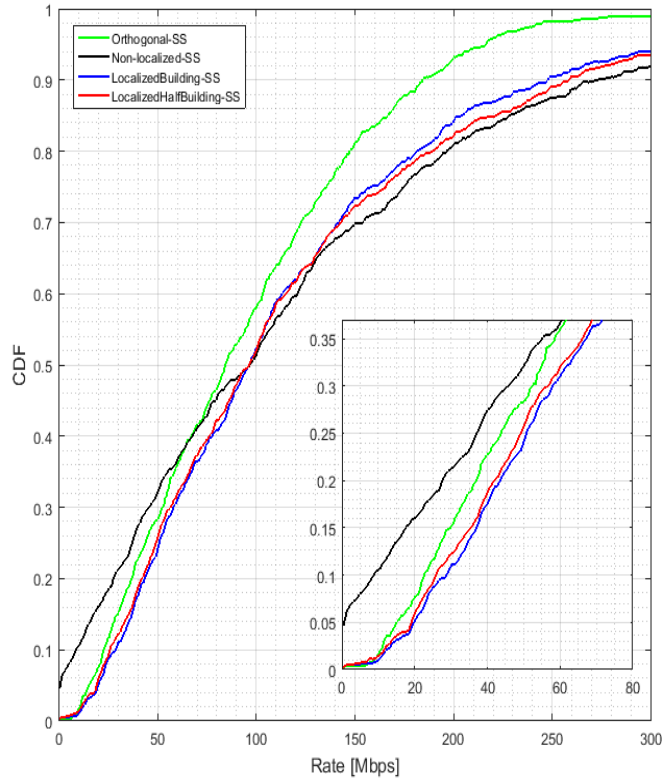

Figure 44. User rate distribution with asymmetric operator mean load (Operator 2 users).

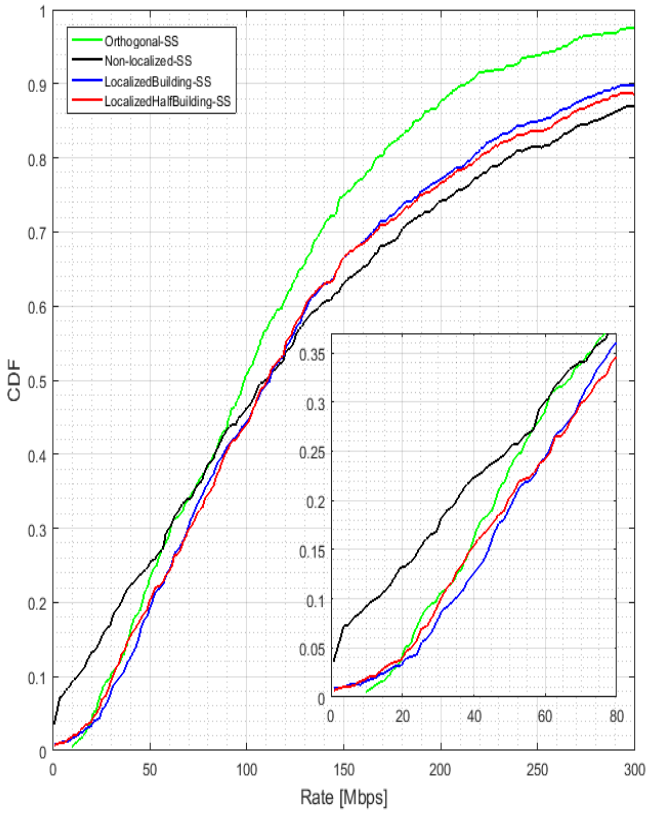

Figure 45. User rate distribution with symmetric operator mean load (operator 1 users).

From the results obtained we observe that the localized and non-localized spectrum sharing improves delivered throughput to the UEs. However, the non-localized spectrum sharing scheme in comparison to the orthogonal spectrum sharing introduces a performance loss for low data rate users. On the other hand, the localized spectrum sharing results a significant improvement to users' throughput when compared to the static orthogonal sharing scheme. We observe from the result that the localized per half building mechanism result dominates the localized per building sharing scheme result. Overall, we conclude that spectrum sharing at small scale level provides a better system performance improvement than sharing spectrum at a big geographic area.

7.5.4. Summary

Inter-operator co-primary spectrum sharing was investigated in a scenario where small-cell tiers of two operators share part of the bandwidth in local neighborhoods. Performance was evaluated in an environment with 100 houses, with a coverage micro tier of two operators, and spectrum sharing in a small-cell tier on a per-house or per half-house basis. A spectrum sharing protocol between the operators was modeled, based on requests presented to the opponent operators, and possibly granted. It was found that making local decisions about spectrum sharing can considerably improve the rates experienced by the users served by the two networks.

7.6. FDD Flexible Duplexing

Goal of the study and connection to the COHERENT architecture

We present a guideline to determine the downlink transmit power of a FDD flexible duplexing cell. We provide a closed form equation for the calculation of this power, proposing to make the flexible duplexing cell radiate in downlink, the equivalent mean uplink transmit power, considering a uniform distribution of users in the cell. For this case, the role of the SMA is to configure the downlink power in the flexible duplexing cell, implementing the proposed equation.

Task covered:

This work covers the activities undertaken within Task 4.3 (local spectrum sharing).

7.6.1. Introduction

Flexible Duplexing (FD) in Frequency Division Duplexing (FDD) is an important aspect for future networks to match traffic asymmetry by dynamically switching uplink and downlink transmission in a FDD uplink band. Flexible duplexing is being studied in 3GPP [LG_2014], [LG_2014_2], [Huawei_2014], and academia [Soh_2013], [Wan_2013], [Pirinen_2015], [Kliks_2016_2] and [Lembo_2017]. In addition, an introduction was reported in [COHERENT_D41]. In FDD-FD, a FD-cell may flexibly change the transmission direction from uplink (UL) to downlink (DL), using a FDD-UL band for downlink transmission. For example, in Figure 46, network operators 1 and 2 transmit in two neighbouring FDD-UL bands. Operator 1 uses band 1 for uplink or downlink transmission in a flexible duplexing cell, with Base Station (BS), BS_1. When BS_1 transmits in downlink, the Out-of-Band (OOB) emissions leaked from band 1, may become a strong Adjacent Channel Interference (ACI) to a BS_2 (victim) in band 2 [Lembo_2017] (Figure 47).

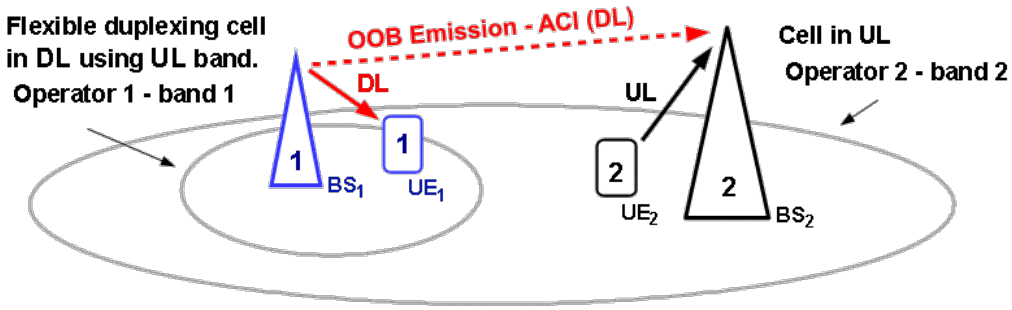

Figure 46. Two operators in UL-FDD neighbouring bands. OOB emission of Operator 1 interferes with Operator 2.

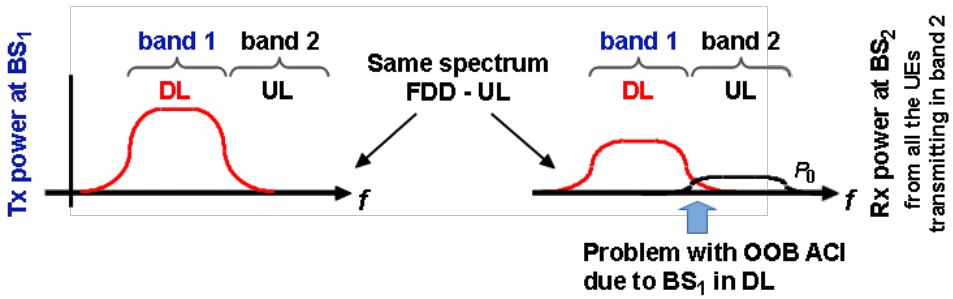

Figure 47. High OOB ACI in band 2, due to high DL transmit power of the FD-cell in band 1. Only two UEs are shown for simplicity. Ideal received power P_0 is assumed at BS_2.

7.6.2. Downlink Power Control for FDD Flexible Duplexing and Coexistence Results

A preliminary coexistence study of FDD flexible duplexing networks was reported in [COHERENT_D41] and [Lembo_2017]. In these studies, the uplink band is used for downlink transmission, considering the effect of ACI. In [Lembo_2017], we proposed to adopt downlink power control to make the cell implementing flexible duplexing behave, interference-wise, as an uplink cell. It is proposed that the flexible duplexing cell can radiate in downlink, the equivalent mean uplink

transmit power. For this purpose, the calculation of the expected uplink transmit power E[P], for the case of a uniform distribution of users in an annular cell, is presented with a closed form equation,

$$E[P] = \frac{2K_1 e^D}{A}\left[e^{\frac{A(A-4BC(R_2))}{4B^2}} - e^{\frac{A(A-4BC(R_1))}{4B^2}}\right] \quad (56)$$

where A,B, $C(.)$, D, and K_1, are variables defined in [Lembo_2017] that depend of the target received power, the path loss at the reference distance, the path loss exponent, shadow fading variance, and the distance between cells. R_1 and R_2 are the inner and outer radius of an annulus, representing the flexible duplexing cell.

Performance results are presented in terms of the cumulative distribution function (CDF) of the SINRs obtained in 2000 network instances obtained with Monte Carlo simulations. When switching the flexible duplexing cell from uplink to downlink transmission, the downlink transmit power is calculated with the formula reported above. Performance results for the SINR measured in the macro cell of operator 2 (victim), when the flexible duplexing cell is transmitting in uplink and downlink, are shown in Figure 48. Scenario, settings and additional results are detailed in [Lembo_2017]. We observe in the figure, that the effect in performance, when transmitting in downlink, is not worse than for the uplink case. Results indicate that, for the considered scenario, there is no coexistence problem. More details on flexible duplexing performance can be found in [Lembo_2017b,Chapter 4], and [Lembo_2017d].

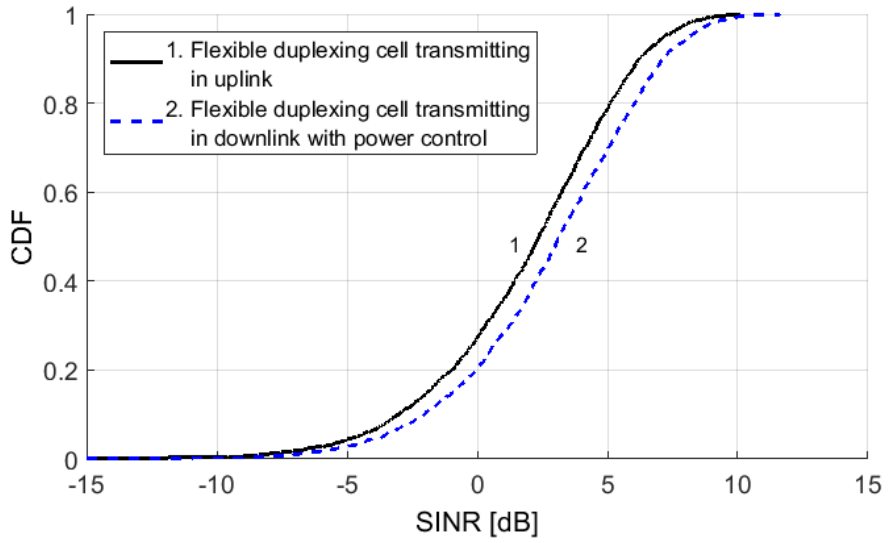

Figure 48. SINR measured in the macro cell of operator 2 (victim) operating in uplink, for the cases when the flexible duplexing cell is in: 1) uplink, and 2) downlink. (Power Control, -10.5 dBm / 10 MHz).

7.7. Multi-User Simultaneous Flexible Duplexing [2]

Goal of the study and connection to the COHERENT architecture

The problem of flexible duplexing focuses on specific aspects of small-scale spectrum management. In this chapter the ways for simultaneous and flexible uplink and downlink usage of uplink channel in frequency division duplexing mode is analysed. The key rules, to enable or not the opportunity of flexible duplexing is the role of SMA, whereas the rules are executed and controlled by C3. Information available in the network graphs (about the existing users, their transmission

[2] The content of this subchapter is a slightly modified version of the paper [Kliks_2017] published in an open access form, which assumes CC4, http://creativecommons.org/licenses/by/4.0/

parameters etc.) may allow for efficient calculation of the filter parameters that should be applied in the proposed scheme.

Task covered:

This work covers mainly the activities undertaken within Task 4.3 (local spectrum sharing), but are also extended to Task 4.1 and 4.2 (intra- and inter-operator spectrum sharing).

7.7.1. Introduction

As discussed in previous chapter, the problem of asymmetric traffic can be solved in various ways depending on the applied duplexing schemes between uplink (UL) and downlink (DL) data delivery. It is well known that in time division duplexing (TDD), a certain frequency channel is utilized in both directions (uplink and downlink), and the split between the direction is done in the time domain. In practice, more time slots can be assigned to that direction which needs to serve higher traffic. Contrarily, in the classical frequency division duplexing mode (FDD), the data between base station and mobile terminal can be delivered continuously in the time domain in both directions, and the split between UL and DL is realized in the frequency domain. It means that dedicated fragments of the frequency spectrum are assigned to each transmission direction. In such a case, the problem of asymmetric traffic can be solved by allowing data transmission in a selected direction in both bands. Following this approach, UL band can be utilized for DL transmission and vice-versa.

Here, we concentrate on FDD scheme with particular attention given to LTE/LTE-A systems (what entails that OFDMA and SC-FDMA will be used as a medium access scheme in DL and UL, respectively). Our motivation behind such a selection is to provide new technological solutions, while keeping the backward compatibility with current standards. It has been proposed to use the uplink bands in a highly flexible way, so that the split between uplink and downlink traffic depends mainly on the current user demands and assumed priorities. We consider simultaneous data transmission in both uplink and downlink directions, implementing advanced adaptive transmission/reception filtering for out-of-band attenuation. One may observe immediately that such a transmission scheme results in an interference rise observed inside the serving and all surrounding cells. Thus, in this work it has been evaluated what is the prospective impact of this scheme on the interference boost observed by other users (mobile terminals or base stations). Proposed solution is highly flexible and can be used as a way for advanced spectrum utilization in 5G networks guaranteeing backward compatibility with 4G systems. To fulfil this requirement the 4G-like HetNet scenario (Figure 49) has been modelled where uplink control data are transmitted at the edges of the uplink band as shown in Figure 50.

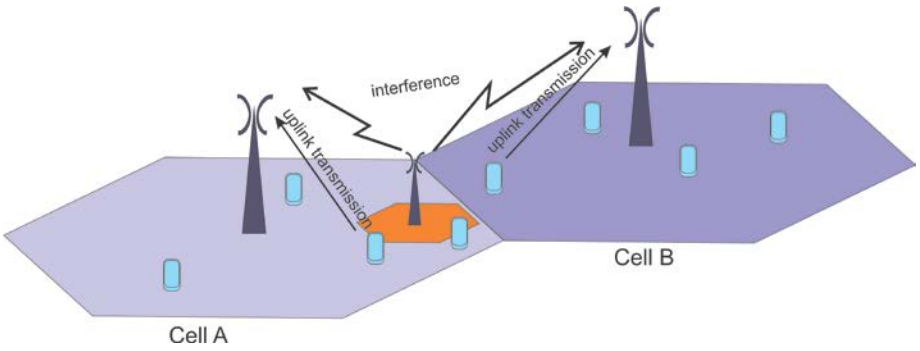

Figure 49. Considered scenario with two macrocells and one small cell

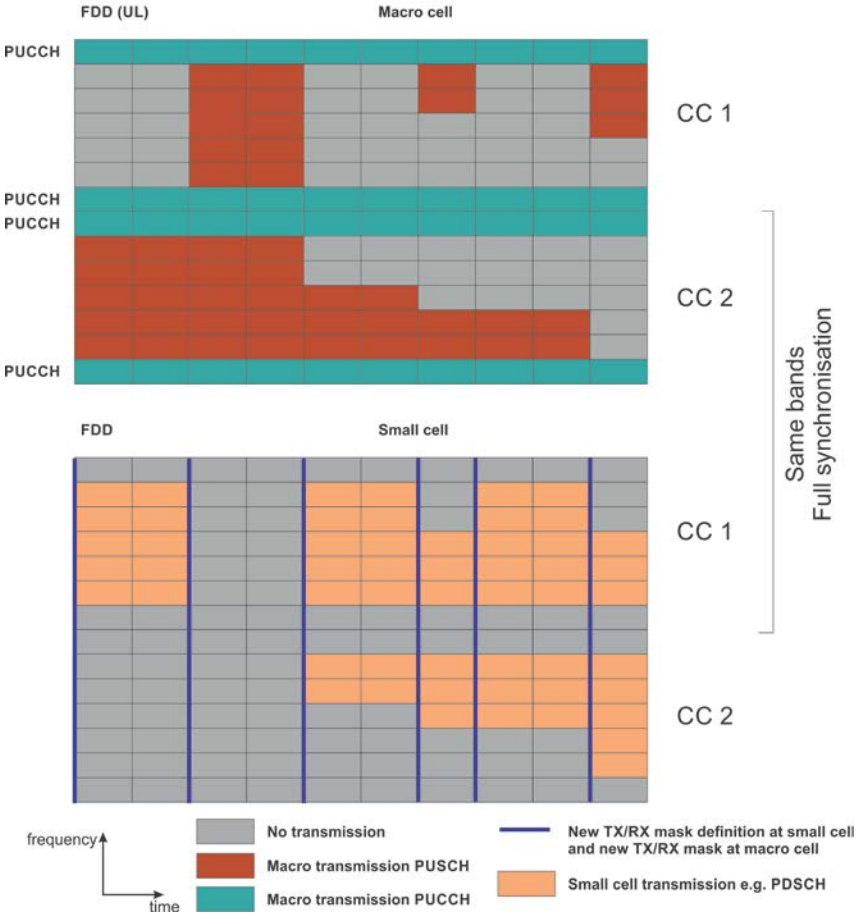

Figure 50. Proposed scheme with non-contiguous frequency usage- flexible duplexing FDD small cell

In the considered case an FDD-LTE-based system operates in both macro cells (hereafter denoted as cell A and cell B) with the frequency reuse factor close to unity. In that scenario, the uplink component carrier is used, broadly speaking, for user data delivery (realized in PUSCH, standing for physical uplink shared channel) and for uplink control information transmission (typically performed via PUCCH). It is important to notice that the PUCCH data are transmitted using small frequency segments located on the borders of the component carrier. The key concept that has been proposed is to apply advanced, adaptive spectrum shaping algorithms originally considered to be used in non-contiguous multicarrier transmission schemes [Bogucka_2015]. These solutions can guarantee a significant reduction of unwanted out-of-band emission even in a very narrow frequency band at a reasonable complexity. Moreover, these algorithms can be applied at the beginning of a frame, allowing for a pre-calculation of the required spectrum masks (filter shapes).

7.7.2. Sources of Interference in Non-Orthogonal OFDM/SC-OFDM Systems

The interference power in the considered scenario at the SC-OFDM receiver (cell B base station/eNodeB) comes from two sources: Out-of-band (OOB) radiation of the DL/UL transmitter, and limited selectivity of OFDM/SC-OFDM receiver.

The interference phenomenon existing between both systems can be described analytically. In the following, we provide the theoretical analysis of the interference phenomenon in considered simultaneous flexible duplexing scenario.

Let us assume that the SC-FDM/OFDM transceivers utilize the N point discrete Fourier transform with occupied subcarriers constituting set $\Im$. Each element of $\Im$ belongs to set of available subcarrier indexes $\{-N/2,\ldots, N/2-1\}$. In our analysis, we can consider only two consecutive symbols, i.e., 0th and -1st, without loss of generality. Each symbol has a cyclic prefix of the N_{CP} samples. The interfered receiver utilizes N point IDFT and as such can span samples out of maximally two consecutive OFDM symbols.

Most importantly, we will assume the signal is generated by SC-FDM transmitter and received by OFDM receiver. However, the shift in the transmitter by half of subcarrier spacing can be done at the receiver without causing differences in interference power. As such, the derived formula can be used to calculate interference power caused by OFDM transmitter to SC-FDMA receiver.

Let us note also that there is no need to consider here the DFT precoding applied normally at SC-FDMA transmitter. According to Parseval theorem, the interference power in the receiver after FFT block (applied as well in OFDM receiver) will be the same as after utilization of IFFT (specific for SC-FDMA). Having the above assumptions in mind, the *m*th sample of the 0th SC-FDMA symbol (where $m \in \{-N_{CP}, \ldots, N-1\}$) is defined as

$$s_m^{(0)} = \frac{1}{\sqrt{N}} \sum_{n \in \mathcal{I}} d_n^{(0)} e^{\jmath 2\pi \frac{m\left(n+\frac{1}{2}\right)}{N}}, \tag{57}$$

where $d_n^{(0)}$ is either QAM/PSK symbol (also after DFT precoding, if considered) transmitted at subcarrier indexed n, and the shift $n+1/2$ is due to the application of the legacy SC-FDMA scheme, where such a shift in frequency is introduced. Such a time-domain signal passes through the multipath channel of L taps with impulse response $h(l)$; the mobility of the users is also considered. The received signal normalized to subcarrier spacing is defined as:

$$r_m = \sum_{l=0}^{L-1} h(l) s_{m-l} e^{\jmath 2\pi \frac{m\nu}{N}}, \tag{58}$$

where ν stands for the Doppler shift. Let us denote the time instant of the beginning of the receiver DFT window as m', so the signal observed at n' th subcarrier is represented as

$$R_{n',m'} = \frac{1}{\sqrt{N}} \sum_{m=0}^{N-1} w_m r_{m+m'} e^{-\jmath 2\pi \frac{n'm}{N}}, \tag{59}$$

where w_m defines the reception window shape applied at the receiver side (e.g., rectangular, Hanning). Two cases are possible, first, when there is no inter-symbol interference (i.e., the receiver can be treated as to be symbol-synchronized and there is only one symbol within the reception window; it is denoted hereafter as case A); and second, when there is lack of synchronization and fragments of two consecutive symbols are observed within the duration of the reception window (denoted hereafter as case B). Following the detailed derivation showed in [Kliks_2017], the power on n' th subcarrier can be computed as:

- In Case A

$$E\left[\left|R_{n',m'}\right|^2\right] = \frac{1}{N^2} \sum_{n \in \mathcal{I}} \left|d_n^{(0)}\right|^2 \left|H\left(n+\frac{1}{2}\right)\right|^2 \times \left|\sum_{m=0}^{N-1} w_m e^{\jmath 2\pi \frac{m}{N}\left(n+\frac{1}{2}-n'+\nu\right)}\right|^2 \tag{60}$$

- In Case B

$$E\left[\left|R_{n',m'}\right|^2\right] = \frac{1}{N^2}\sum_{n\in\mathcal{I}}\left|d_n^{(-1)}\right|^2\left|H\left(n+\frac{1}{2}\right)\right|^2 \times\left|\sum_{m=0}^{-m'-1-N_{\mathrm{CP}}} w_m e^{J2\pi\frac{m}{N}\left(n+\frac{1}{2}-n'+\nu\right)}\right|^2 + \frac{1}{N^2}\sum_{n\in\mathcal{I}}\left|d_n^{(0)}\right|^2\left|H\left(n+\frac{1}{2}\right)\right|^2 \times\left|\sum_{m=-m'-N_{\mathrm{CP}}}^{N-1} w_m e^{J2\pi\frac{m}{N}\left(n+\frac{1}{2}-n'+\nu\right)}\right|^2. \quad (61)$$

7.7.3. Flexible Duplexing for 4G and 5G—Extension to Multiple Component Carrier Case

Let us now consider the case where the mobile network operator utilizes more than one component carrier in its wireless cellular network. In this context one may observe the presence to two adjacent component carriers, which are utilized in the FDD mode for flexible duplexing by applying the transmission scheme proposed in this work. Moreover, for the sake of clarity, the intra- and inter-cell interference phenomenon in a certain time slot is emphasised by indicating the resource blocks being the source of interference and the affected resource blocks.

Application of non-contiguous multicarrier transmission

Let us observe that from the perspective of the downlink transmission, it is a natural consequence that the consideration of more than one component carrier immediately entails the possibility of application of non-contiguous multicarrier schemes for data transmission [Bogucka_2015], [Kryszkiewicz_2016]. In such a scheme, the concatenation of two component carriers can be treated as a joint wide spectrum for multicarrier signal transmission, where selected subcarriers are not used to protect the present uplink signals. Such subcarriers cancelation (switch off) results in narrow gaps in the spectrum of the transmitted signal—in the considered case of flexible duplexing, these are the PUCCH channels that have to be protected.

Cooperation between base stations

As one of our goals is to guarantee backward compatibility (so there would be no need to modify existing legacy hardware, i.e., MT devices), it is also worth analysing the impact of radio access network on the performance of proposed flexible duplexing scheme. In the context of 4G networks, one may observe that the neighbouring base stations (eNodeBs) are connected via well-known X2 interface which allows for efficient coordination of these base stations and application of various advanced algorithms, e.g., inter-cell interference cancelation. For flexible duplexing, coordination between the base stations (eNodeBs, but in a broader sense also potentially between eNodeBs and small cells) entails accurate allocation of unused resource blocks for downlink transmission. If reliable communication between the eNodeBs will be guaranteed, then the dedicated radio resource management algorithms can be applied which will assign UL resources for DL transmission in such a way that the activity of MT located in a considered cell and in the neighbouring cells is taken into considerations.

7.7.4. Simulation Results

In order to evaluate the proposed scheme, we would like to measure the impact of the interference induced to other users due to the application of the proposed flexible duplexing scheme (i.e., when the advanced spectrum shaping is implemented) in both scenarios—when one or more component carriers are used in the system. We consider the presence of various receivers in the system, ones that are equipped with the proposed spectrum shaping algorithms, and others that can be treated as classical, legacy LTE devices (base stations or mobile terminals). The idea here is to guarantee backward compatibility with the existing devices.

Power spectral density analysis— a multichannel case

As the results for the single-component case are promising, let us now evaluate the effectiveness of the proposed solution when the non-contiguous multicarrier transmission is applied for two adjacent component carriers. For each component carrier, the details of the transmit signal are analogous to the setup of the signal described in [Kliks_2016_2] for single-component carrier case, as we again assume the compatibility with LTE standard. In particular, SC-OFDM (UL) and OFDM (DL) occupying a maximum of 2 component carriers (CCs), 20 MHz bandwidth each, are considered. It is assumed that both CCs are generated and received using a single processing chain utilizing 4096-point FFT/IFFT and spanning 61.44 MHz bandwidth (subcarrier spacing is equal to 15 kHz). This approach is advantageous over separate processing of each CC as it guarantees orthogonality between CCs. The frequency separation between both CCs is calculated to be 19.8 MHz. Both systems transmit their signals in dedicated time slots (0.5 ms duration each) composed of 7 OFDM/SC-OFDM symbols. While the first symbol in a slot utilizes 320 samples with CP, the rest are 288 samples long, each. It is assumed that there is no synchronization, neither in time, nor in frequency domain (as it is the most challenging scenario) between UL and flexible DL transmissions. The results were generated for 1000 OFDM/SC-FDMA frames shifted randomly in time. The frequency misalignment between both systems is 0.5 subcarrier spacing.

Let us remind that the maximal number of resource blocks (RBs) in the considered scheme is 100 per CC. In the case of no data transmission in UL, only PUCCH is transmitted on both ends of the available band, i.e., RBs indexed 50 and −50 in each CC. In the proposed scheme, unused resource blocks in between utilized UL channels can be used by cell A for its DL transmission. In Figure 51, normalized power spectral densities (PSDs) of UL and DL signals are shown using solid lines. While the top figure shows whole 61.44 MHz bandwidth, the bottom plot zooms the left edge of CC no. 1. Cell A transmission utilizes RBs with indexes {−48,…,−1,1,…,48} in both CCs, i.e., a contiguous band around the DC subcarrier (0th RB is not used). Signals are normalized to have equal received power per utilized RB. The OOB emission from the DL transmission in band of the uplink is at the level of around −25 dB. As these results are very close to the ones for single-component carrier case [Kliks_2016_2], one may conclude that the influence of adjacent channels (component carriers) is negligible for the outer (i.e., distant from adjacent component carrier centre frequency in frequency domain) PUCCH channels. However, also the impact of the adjacent component carriers on the inner PUCCHs is rather negligible. It is due to the most significant impact originating from the subcarriers closes to the edge of the DL signal spectrum.

Now, let us analyse the effective interference power observed at the SC-OFDM receiver, as we did in the single-component carrier scheme in [Kliks_2016_2]. Again, four combinations of transmitter-receiver settings have been verified, i.e., one where both the transmitter (in DL) and receiver (in UL) do not apply advanced spectrum filtering—this case is denoted by dashed blue line. Next, two cases where either transmitter apply dedicated method considered in [Kryszkiewicz_2013] (dashed black) or receiver apply 512-sample-long Hanning windowing (dashed blue with plus markers). Finally, the case where both, transmitter and receiver, apply dedicated algorithms for interference minimization (dashed black with plus signs). Again, as in the previous case with single-component carrier, the best results have been achieved in the situation when dedicated algorithms have been applied at both sides of the system. One may observe that again, the observed interference power is around −45 dB less than the observed power of the wanted PUCCH signal. It also shows that the impact of the additional component carriers is negligible and that the proposed FDD non-contiguous multicarrier scheme can be efficiently applied to flexible duplexing with carrier aggregation (i.e., when many component carriers are used). Most importantly, the analytical formula (derived in previous chapters) for received interference power was utilized for standard TX and standard RX case and it is aligned with simulation results. In order to obtain this result interference power observed at a given subcarrier $n\acute{}$ was averaged over all possible RX windows positions $m\acute{}$. Flat channel was assumed ($H(n)$ =1) and no carrier frequency offset other than standard shift by 0.5 subcarrier spacing.

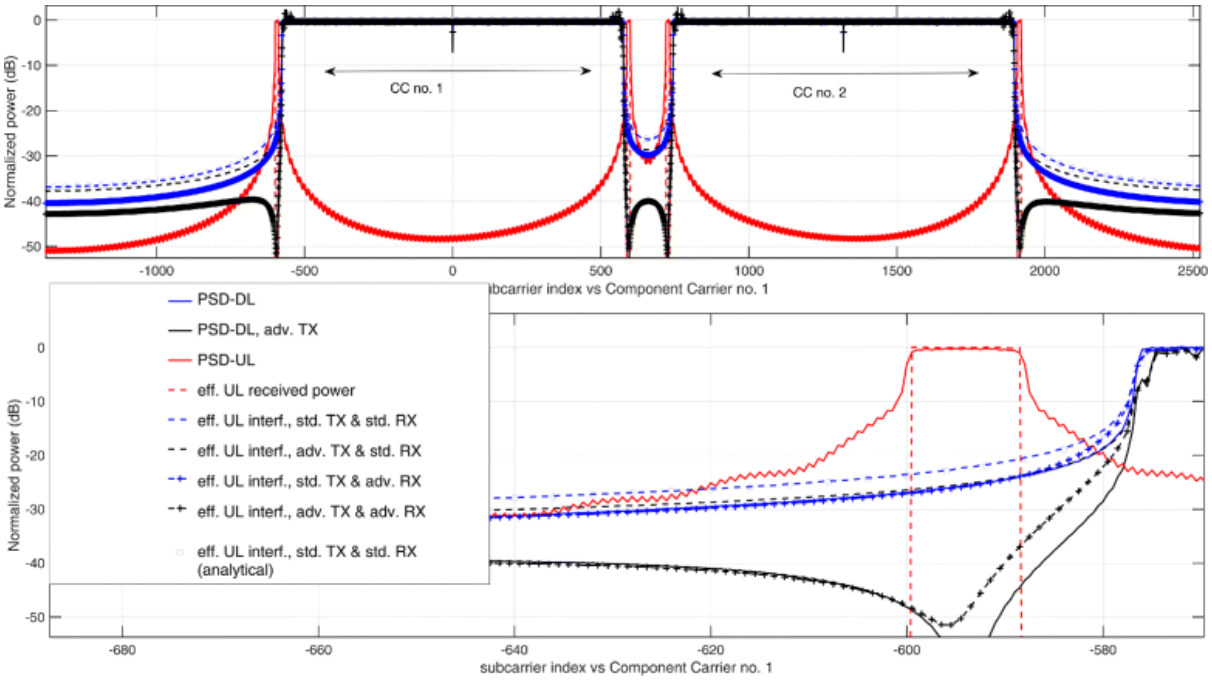

Figure 51. Normalized PSDs of UL and DL transmitted signals, effective interference/useful signal power at cell B base station (receiver)—multichannel case. Only lower frequency edge is shown at the bottom figure [Kliks_2016_2]

Adjacent channel interference ratio analysis—extension to multichannel case

In this section, we analyse the adjacent channel interference ratio (ACIR) as a good metric used for the assessment of the ratio of wanted power to the interference power from the other bands. Mathematically, ACIR is the function of the adjacent channel leakage ratio (ACLR, used to characterize the transmitter) and the adjacent channel selectivity (ACS, used to characterize the receiver). In our case, it is calculated as a ratio of FD signal power at the BS RX antenna to the summarized power of interfering signal observed over 12 subcarriers utilized by a given PUCCH channel at the output of FFT block in SC-OFDM receiver.

As it has been mentioned, another possibility to decrease interference power at the cell B receiver is to use guard subcarriers (GSs) [Bogucka_2015]. Turning off DL subcarriers closest to the utilized UL band increases both ACLR and ACS. Let us note that such an approach is compliant with the existing LTE TX/RX technology, although it decreases the achievable rate (as some subcarriers are not utilized). The efficiency of this approach is considered here. In Figure 52, ACIR values of the standard and advanced TX/RX technologies are shown as the functions of frequency separation between the UL and DL signals. Although this value addresses ACIR for a single PUCCH RB, differences between 4 observed PUCCH RBs were negligible. Results are shown only for one of these RBs.

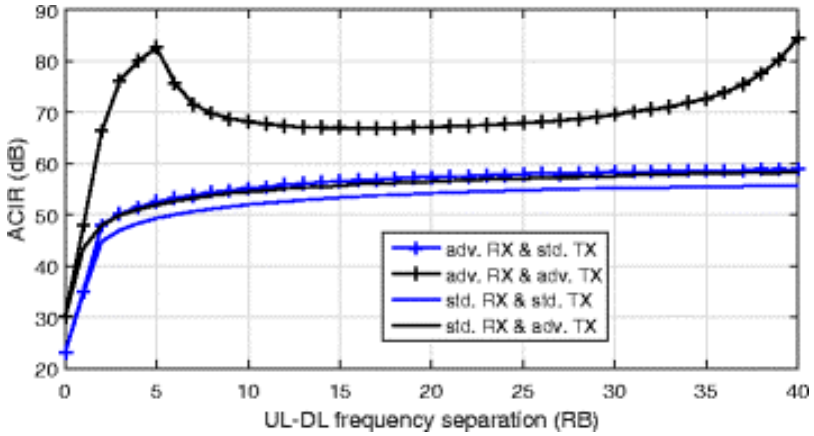

Figure 52. Adjacent Channel Interference Ratio for a single PUCCH RB vs UL-DL frequency separation (0 RBs mean that PUCCH and PDSCH overlap) with standard and advanced TX/RX

It is shown that when the PDSCH and PUCCH overlap (frequency separation equal 0), ACIR equals about 25–30 dB. The situation changes rapidly when guard subcarriers are used. Even in the case of a standard transmitter and receiver, the introduction of a single empty resource block between the UL and DL bands (frequency separation equal to 2, this is the case shown in Figure 51.) increases ACIR to 45 dB. In the case of advanced TX and RX utilization (with the spectrum shaping algorithms discussed previously), the frequency separation of 2 RBs results in ACIR equal to 66 dB. It means that by proper signal processing, e.g., spectrum shaping at the transmitter and windowing at the receiver together with the application of guard subcarriers, a significant ACIR increase can be achieved. It is worth explaining why the curve representing ACIR for an advanced transmitter and receiver rises steeply for low frequency separation, and then it falls down. Such behaviour is observed due to the specificity of the OCCS method [Kryszkiewicz_2013] that reduces the OOB most significantly in the adjacent subcarriers. For higher distance (in frequency) between modulated subcarriers and protected band, its performance is limited. Please notice also that for very high distance (in frequency), the performance increases again—it is due to the fact that the total number of used CCs relative to the considered number of data subcarriers is high, so the OOB in wide spectrum can be precisely minimized.

Influence on transmission opportunity in neighboring cell in multichannel scheme

In the most rigorous approach, the given base station (i.e., the one that applies proposed flexible duplexing scheme) can transmit according to the proposed scheme only if all other cells' transmissions are not deteriorated (in practice, some controlled deterioration should be acceptable). According to Table 8.2.1.1–6 in [3GPP_2014], the minimum SINR that should allow for PUSCH transmission using QPSK modulation and 1/3 coding rate is −0.4 dB. However, PUCCH reception should even be possible for lower SINR values, namely, −3.8 dB. Assuming the proposed FD scheme is used when only PUCCH is transmitted in all neighbouring cells UL (although in general, other scenarios can be considered as well—some assumption on allowed reception deterioration would have to be defined), it is visible that interference plus noise power can be increased by 3.4 dB without decreasing the effective standard cells radius. In order to evaluate this issue, the effective cell radius has been calculated using the COST 231 model for carrier frequency f = 2 GHz, base station antenna height HA = 30 m, mobile terminal antenna height h_{MT} = 1.5 m, and mobile terminal and BS gains G_{MT} = 0 dBi and G_{BS} = 18 dBi, respectively,. Assuming the mobile terminal transmit power is P_{MT} = 23 dBm and thermal noise power in 300 K increased by a noise figure (NF) of 5 dB, standard cell radius equals R_A = 0.83 km.

For the same system parameters, the interference plus noise power can be increased by 3.4 dB while transmitting PUCCH (instead of PUSCH), as discussed above. It can be calculated that the effective interference power from cell A to standard cell UL should be equal or lower than −93 dBm per a given PUCCH RB.

Let us now assume the case where the base stations are deployed according to the scheme presented in Figure 53. The considered system composes of 3 standard cells utilizing in a given time slot only PUCCH. We assume also the application of full-frequency reuse strategy, i.e., in every cell both

component carriers are used. Locations of standard base stations in [X,Y] coordinates are [0,0] km, [0,1.43] km and [1.24,0,72] km, i.e., the radius of the cell is set to R = 0.8275 km. In Figure 54, the maximal allowed power of FD transmission is calculated in 600 points between these BSs. For each location pathloss to each UL BS is calculated. For each case −93 dBm of effective interference power per PUCCH RB can be introduced, as derived above. The interference propagation between BSs is assumed to follow log-distance path loss model with pathloss exponent γ equal to 2 or 2.5. Although previously G_{BS} = 18 dBi was used, now it can be assumed that both BSs (i.e., interfered and interfering) are not directed at each other. G_{BS} equal to 10 dBi at both BSs is used.

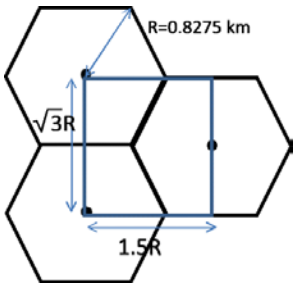

Figure 53. Fragment of the considered cellular network

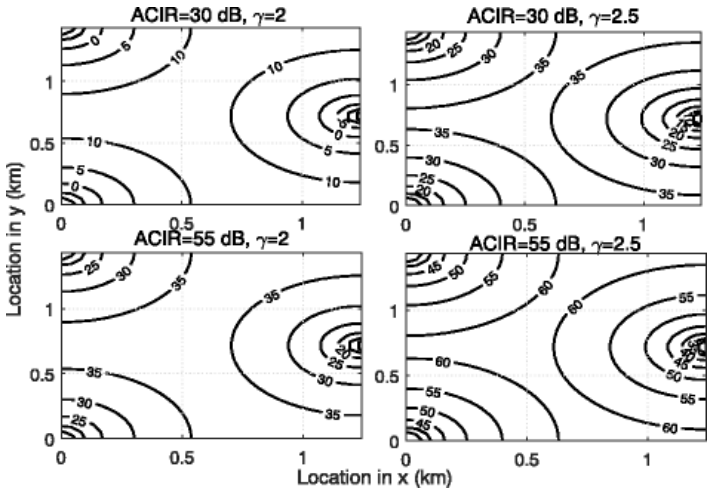

Figure 54. Maximal FD transmission power vs location in the presence of 3 PUCCH-receiving BSs

It is visible that the lowest allowed FD BS power is obtained for ACIR = 30 dB and γ = 2. In this case, interference propagates easily using line-of-sight propagation between both BS. ACIR value shows there are not many GSs between FD and UL transmission or advanced TX & RX is not used. Still 10 dBm FD transmission is possible if the BSs are distanced by more than 500 m. On the other hand, higher pathloss (γ = 2.5) or ACIR = 55 dB allows to use higher FD transmission power or to transmit in locations closer to UL-utilizing BSs. For ACIR = 55 dB and γ = 2.5, it is possible to place FD-utilizing BS about 50 m apart from PUCCH-receiving BS and transmit using 35 dBm power.

7.7.5. Conclusions

In this work, we have evaluated the possibility of simultaneous UL and DL data transmission in the flexible duplexing mode by the application of advanced spectrum shaping algorithms. Comparing to our previous work, we have considered more advanced scenario, where multiple component carriers utilized for uplink in the mobile wireless network are used for downlink transmission. In such a case, the non-contiguous transmission can be efficiently applied. Presented results proved the correctness of the proposed approach, as the proposed technical solutions guarantee that the assumed maximum level of allowable interference is not exceeded. In some cases (by the application of guard subcarriers), even backward compatibility can be achieved. It means that the unused frequency resources in the UL channel can be utilized simultaneously for DL transmission, leading to better spectrum utilization. As

the results are promising, one should consider investigating a situation where not only PUCCH is present in the UL band, but user data as well. Moreover, one may think on more advanced approaches where each component carrier is used independently, although both of them are used simultaneously, due to the utilization of some context information, such as position of the macro base stations.

7.8. Multi-User Small-Scale Spectrum Aggregation

Goal of the study and connection to the COHERENT architecture

The main goal of this study was to investigate the possibilities of small-scale (in terms of set of subcarriers) spectrum sharing and aggregation. In that context, this work is highly related to SMA, as the algorithm proposed here will be invoked for detection of new small-scale transmit opportunities. However, the rules for the spectrum sharing in real-time will be examined in lower layers of the COHERENT architecture.

Task covered:

This work covers mainly the activities undertaken within Task 4.1 and 4.2.

The goal of this section is to focus on flexible and efficient spectrum aggregation of licensed spectrum in multi-user scenario, as discussed in [Kryszkiewicz_2016, Kryszkiewicz_2017]. In the former paper, we concentrated on practical validation of the newly proposed interference model, limiting the discussions to the case, where only one narrowband link has to be protected by the 5G system. As the proposed model was successfully validated, the next step was to verify the applicability of the small-scale spectrum aggregation scheme in a more practical, multi-user scenario.

7.8.1. The Idea of the Non-Contiguous Multicarrier Schemes as the Small-Scale Spectrum Aggregation Mechanism

Let us now briefly summarize the key ideas of application of Non-Contiguous Multicarrier (NC-MC) schemes, such as NC orthogonal frequency division multiplexing, NC-OFDM, or filter bank based multicarrier, NC-FBMC. In a broader sense, spectrum aggregation refers to making use of discontinuous frequency bands, as in the carrier aggregation scheme standardised for 4G networks, where the co-called component carriers (CC) are considered. In a small scale spectrum aggregation, the frequency segments of arbitrary (possibly narrow) bandwidths can be assigned to particular users or systems. For example, an operator may share own-licensed spectrum among various technologies (e.g., GSM and 5G, LTE Release 8 and 5G, etc.). In that context, one may consider a generic NC-MC transmitter (TX), where the data bits are mapped to QAM/PSK complex symbols and fed to the dedicated transmit pulses. In the non-contiguous scheme, there may be some gaps in the signal spectrum, contrarily to the traditional multicarrier scheme, where the spectrum of the transmit signal composes a “solid” block.

7.8.2. Interference Analysis

In the analysis below, we focus on the downlink case, however the results may be easily adjusted to the uplink transmission. Thus, let us consider a generic scenario, where the 5G wireless system is deployed in the same area as other, already existing system that has to be protected from harmful interference. This situation is shown in Figure 55, where two systems, future and the traditional one, are presented. The user equipment j to be protected (PS UE$i,j$) receives the signal from its system base station BSi (with power attenuation $\alpha_{PSi-PSi,j}$ and frequency response $H_{PSi-PSi,j}(f)$). It observes also the interference signal from the coexisting system, for which the power attenuation α_{5G-PSi}, as well as the frequency response $H_{5G-PSi}(f)$), should be considered. Similarly, the 5G UE detects not only the wanted NC-MC signal from its BS, but also interfering signal from incumbent PS. In Figure 55, the wanted signal is denoted by solid line, whereas interference - by dotted line. Our goal was to maximize the rate in the 5G system while fully protecting the traditional users. What is important, in the analysis we also take into consideration the realistic model of the transmit and reception filters, expressed widely by the out-

of-band-emission - OOBE, adjacent channel selectivity metric, ACS, respectively. These two cases are presented graphically in Figure 56 and Figure 57, respectively for NC-MC and traditional systems.

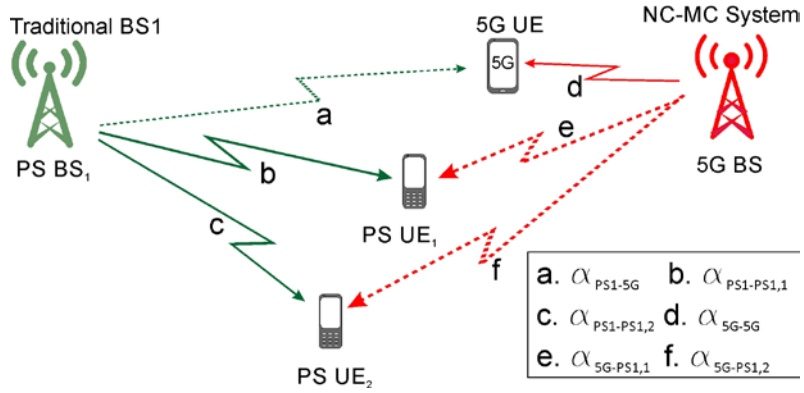

Figure 55. Considered coexistence scenario for small-scale spectrum aggregation

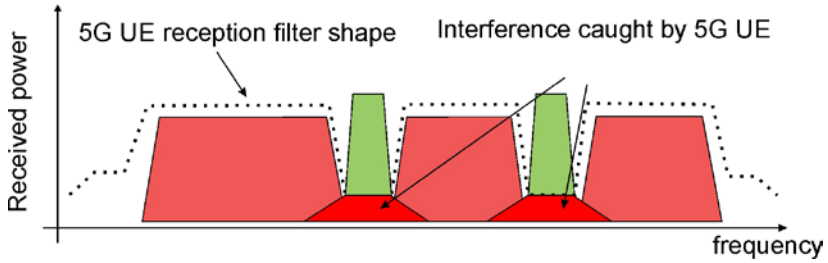

Figure 56. Illustration of the interference phenomenon present in the considered scenario – the perspective of the NC-MC receiver

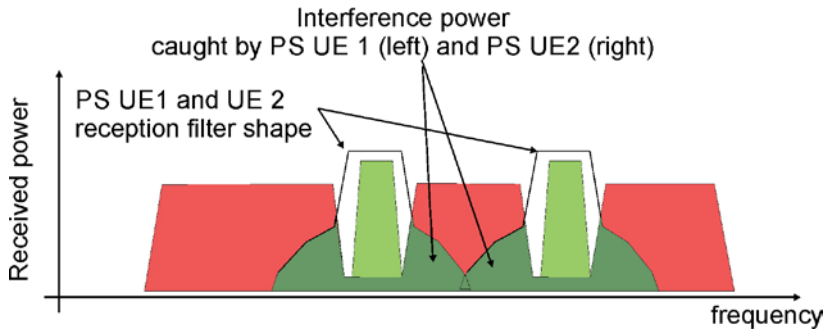

Figure 57. Illustration of the interference phenomenon present in the considered scenario – the perspective of the traditional receiver

In [Kryszkiewicz_2016, Kryszkiewicz_2017], the detailed mathematical analysis of the interference phenomenon has been presented together with the proposal of the algorithm that allows for maximization of the rate in 5G systems.

7.8.3. Simulation Results

In order to evaluate the correctness of the proposed solution, extensive computer simulation have been carried out. The scenario presented in Figure 58 has been modelled, where beside the 5G network operating at frequency 1850 MHz, the GSM network has been deployed. In that figure, the fragment of GSM network consisting of two base stations is shown. These base stations transmit with power equal to 40 and 37 dBm, are located 3 km away from each other, and operate at frequencies f_1 = 1849.6 MHz and f_2 = 1850.6 MHz. One may observe also the specific subset of GSM users which are mostly affected by the 5G base station. The transmit power of the 5G base station is intentionally set to high value, i.e, 37 dBm.

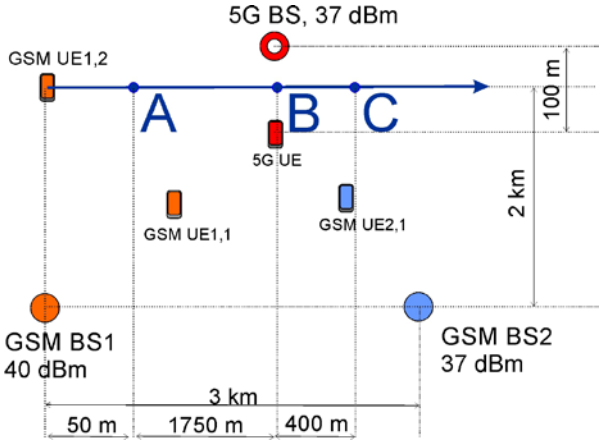

Figure 58. Scenario for the conducted experiment

There is also a blue route which shows the GSM mobile user moving from one cell to another. In our simulations we have assumed that the handover procedure starts when received power from GSM BS2 is higher than the power received from GSM BS1. Three points have been marked on its route: A - the PS UE1,2 is served by the first GSM base station (orange) at arbitrarily selected frequency f_1, B – the GSM mobile user is very close to the high power 5G base station, and C, second base station serves the mobile user at the new centre frequency f_2. The path loss is calculated using the Log-distance model (path loss exponent was set to 3), and antenna gains equal 15 dBi and 0 dBi at BS and UE, respectively. 12 dB noise figure was assumed. Moreover, the minimum value of signal-to-interference noise ratio at the GSM receiver was set to SIR_{min} = 9 dB. We have assumed the IFFT size of 256 subcarriers, from this set the subcarriers indexed $\{-90, ...,-1\} \cup \{1, ..., 90\}$ were available for 5G system for power allocation. As discussed in [Kryszkiewicz_2016] and [Kryszkiewicz_2017], three NC-MC schemes have been tested, mainly the NC-OFDM with the cyclic prefix of 16 samples, NC-OFDM with windowing (each symbol extended by 16 window samples), and NC-FMBC with the *K* factor of the PHYDYAS filter set to 2 and 4. Additionally, perfect case with rectangular TX/RX filter is considered. In Figure 59 one may observe the mean throughput as the function of the GSM UE location. Only in the worst case (when the GSM UE is close to the 5G BS) the achieved throughput is low, whereas in in all other cases the adaptive algorithm proposed in [Kryszkiewicz_2016] and [Kryszkiewicz_2017] efficiently allocates the power across the available subcarriers in non-contiguous mode.

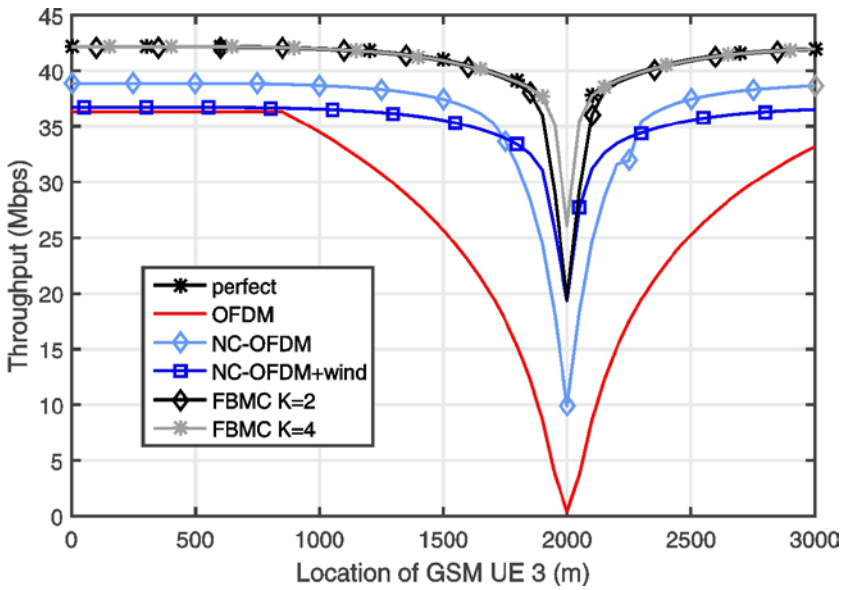

Figure 59. Observed mean throughput as function of GSM UE location

7.8.4. Conclusions

The feasibility of the small scale spectrum aggregation concept in a multi-user scenario has been examined in this work. It was claimed that such a non-contiguous nature of the utilized spectrum entails the natural selection of various multicarrier transmission schemes. The achieved results show that the 5G network can achieve reasonable throughput while protecting the coexisting legacy systems. The key issue, however, is that the proposed algorithm assumes the knowledge to both transmit and reception filter characteristics

8. Towards Experimentation

8.1. Evaluation Platforms

Experimental evaluation is an important part of research and a foundation for innovation. Within the domain of research projects such as COHERENT, experimental evaluations are carried out using sophisticated simulation tools as well as practical experimentation using test equipment and software tools in lab environments. In either case, the sophistication of the simulation or experimentation platforms plays a significant role in determining the relevance of the achieved results to a real system implementation and performance. Therefore, it is very important that the evaluation platforms are realistic enough to capture the necessary details of real systems and that they also provide support e.g. through extensions, APIs etc., for implementing and testing new solutions to relevant research problems.

The capabilities of the experimentation and evaluation platforms to support a wide range of use-cases, apart from the physical limitations of the platforms, also depends on a precise description of the necessary inputs and outputs that will be considered during experimentation. In COHERENT, these requirements map to the details of the abstraction and control flows that the platform need to support. For the implementation of spectrum management and sharing use-cases considered in WP4, the abstraction and control flows associated with these tasks have to be supported by the evaluation platforms.

To this end, a clear description of the necessary inputs has to be provided in order to develop and utilize the necessary APIs in the COHERENT evaluation platforms for the management and/or exchange of RF spectrum among candidate network elements (e.g., base stations). Below we provide the brief summary of the architecture of selected platforms, knowing that the detailed description is available in [DELIVERABLE_D61].

8.1.1. OpenAirInterface 5G

The OAI platform offers an open-source software-based implementation of the LTE system spanning the full protocol stack of 3GPP standards both in E-UTRAN and evolved packet core, EPC [OAI_2017], [Nikaein_2014], [Nikaein_2014_2]. It can be used to build and customize an LTE base station and core network on a PC and connect a commercial UE to test different configurations and network setups and monitor the network and mobile device in real-time. OAI is based on a PC-hosted software radio frontend architecture. With OAI, the transceiver functionality is realized via a software radio front-end connected to a host computer for processing. This approach is similar to other software-defined radio (SDR) prototyping platforms in the wireless networking research community such as SOftware Radio (SORA) [Tan_2011].

Other similar approaches combining PCs and FPGA-based processing make use of NI LabVIEW software or using the WARP [Amiri_2007] architecture. To our best knowledge, OpenAirInterface is the only fully x86-based SDR open-source solution, providing UE, eNodeB, and core-network functionality. A similar closed-source development commercialized by Amarisoft (LTE 100) which targets several USRP platforms provides eNodeB and core-network functionality on standard Linux-based PCs. OAI is written in standard C for several real-time Linux variants optimized for x86 and released as free software under the terms of version 3 of the GNU General Public License (GPLv3). OAI provides a rich development environment with a range of built-in tools such as highly realistic emulation modes, soft monitoring and debugging tools, protocol analyser, performance profiler, and configurable logging system for all layers and channels.

Currently, the OAI platform includes a full software implementation of the 4th generation mobile cellular systems compliant with 3GPP LTE standards in C under real-time Linux optimized for x86.

8.1.2. 5G-EmPOWER

5G-EmPOWER is an open Mobile Network Operating System for SDN/NFV research and experimentation in mobile networks. Its flexible architecture and the high-level programming APIs allow for fast prototyping of novel services and applications. 5G-EmPOWER blurs the line between radio and core network introducing the concept of Programmable Data Plane which abstracts the radio

and packet processing resources available in a network and exposes them to network service developers via a high level intent driven application framework.

5G-EmPOWER natively supports multi-tenancy allowing MVNOs to specify radio resource management policies (e.g. scheduling, modulation and coding scheme (MCS) selection, or HARQ) separately for each slice while ensuring performance isolation between slices and efficient spectrum utilization.

The 5G-EmPOWER platform consists of three components:

- Data-plane, Multi-technology Programmable Data Plane: in 5G-EmPOWER everything is a Virtual Network Function (including radio access). The current supported technologies are 802.11a/b/g/n and LTE/LTE-A. Future technologies will include Low-Power Wide-Area Network (LPWAN) technologies such as LORA and 802.11ah.
- Management-plane. Complex network services can be implemented by chaining different packet processing functions. A domain specific language can be used to specify custom packet processing function over a specific portion of the flow space.
- SDK. Data and management plane abstractions are exposed as high-level programming primitives by the 5G-EmPOWER SDK runtime.

8.1.3. Capabilities of the Evaluation Platforms for Spectrum Management and Sharing

OpenAirInterface 5G

The OAI is a flexible platform for advanced research on LTE-like solutions. In that sense, it does not allow flexible change for many transmit parameters, as these options have been not allowed in the LTE standards. Investigation on the ways of effective Spectrum Management Application implementation on OAI (being the subject of WP6 work) resulted in the following conclusions:

- It is impossible to implement full functionality envisaged for SMA in OAI due to the hardware and software limitations; mainly, it is impossible to change transmit parameters in real time, thus some indirect solution should be proposed;

- In order to demonstrate the SMA functionality, a dedicated application has been implemented within the WP6. The role of WP4 was to identify the functional split between the SMA and other, already implemented applications in the OAI platform.

- It has been decided that the SMA functionality will be limited to the detection, analysis (processing) and selection of the best transmit opportunities based on the available transmit policies. The SMA algorithm will take into account the preferences of the operator, and select in a dynamic way the list of most promising transmit opportunities. Such a list will be delivered to the FlexRAN application which will be in charge of applying the new transmission rules.

5G-EmPOWER Platform

The 5G-EmPOWER natively supports the multi-tenancy concept in the radio access network segment which is very important for demonstrating spectrum management and sharing among tenant networks that utilize the same network infrastructure and radio resources. The multi-tenancy support and the programmable APIs make the 5G-EmPOWER platform well suited to experimenting with spectrum sharing models and techniques. The 5G-EmPOWER platform fully supports the abstraction and control flows in the COHERENT architecture. For spectrum management and sharing, the abstraction flow constitutes converting technology specific sensing parameters into composite/abstract representation (graphs) that are to be used by the spectrum management application for implementing spectrum management and sharing algorithms. Table 2, (reproduced from deliverable D4.1 [COHERENT_D41]) shows the standard parameters/information collected in LTE and Wi-Fi networks and are the primitive inputs for supporting the abstraction flows. A subset of these, particularity parameters related to channel quality, resource availability and load statistics are also relevant for spectrum management and sharing

use-cases. The main features provided by 5G-EmPOWER that can be a part of the abstraction and control flow for any particular spectrum management and sharing use-case are detailed below.

1. **Spectrum Availability**: Spectrum availability is a fundamental input to the SMA for supporting its decision-making algorithms regarding allocation/distribution of radio resources. Fundamentally, every network/slice is associated with a chunk of radio spectrum which it can share with *others* at different times and/or locations per the agreed sharing model and applicable policies. In the spectrum sharing context, this implies an abstraction flow where a network/slice exposes spectrum availability information to the SMA. As 5G-EmPOWER support multi-tenancy in the radio access domain, this information can be collected per slice and exposed via the controller to the SMA. The SMA can keep a track of the overall spectrum availability in the controlled spectrum bands and use this information for accommodating the spectrum needs of its managed networks/slices. The spectrum availability can be monitored proactively or be exposed by the networks/slices at different intervals.

2. **Resource Granularity**: The specification of the resource granularity is tied with the availability of the spectrum. Radio resources are characterized by both the time and frequency domain specification. In addition, radio frequency bands are also tied to a specific or set of radio access technologies. In the spectrum sharing context, the granularity of exposed spectrum in time and frequency domains must be exposed to the SMA which can be technology specific (e.g. Physical Resource Blocks) or technology agnostic (metrics defined at higher abstractions than MAC and PHY). The 5G-EmPOWER platform currently supports Wi-Fi and LTE networks which use different radio access technologies. With each of these technologies however, a controller agent in the 5G-EmPOWER platform can expose the radio resource of any specific granularity tied with the two supported network types.

3. **Frequency/Band Information**: The specific frequency/band information is important as untying the radio access technology from a specific frequency/band is not an easy process. The SMA needs this information to target the subset of the network that can benefit from the specific radio resources exposed by a managed network/slice. An LTE network for example (eNB and UEs) operate on pre-defined wireless channels and cannot change to any arbitrary frequency. In the COHERENT architecture, multiple RATs are managed within the domain of a single operator which implies that the SMA should maintain the frequency/band information for managing the exchange of radio resources among different networks/tenants using heterogeneous radio access technologies. The collection of this information is trivial in 5G-EmPOWER platform as this information is part of the operational parameters which an eNB or Wi-Fi Access Point needs to function.

4. **Network/Cell Load**: While the network load can be characterized at different abstraction levels in a network, for SMA, the load metric of interest is the utilization of radio resources in individual cells or network/slice as a whole. This information may be tied with the spectrum availability information described above, but could also be maintained separately for example, for developing a proactive spectrum management and sharing approach where the offers and demands are addressed proactively. Further, the network load can be segmented into different classes reflecting not only the potential availability but also the upcoming spectrum requests.

5. **Spectrum Requests**: Whereas in a proactive approach, the network/cell load information can be used to predict the needs for additional spectrum, in a reactive approach, the networks/slices need to expose requests for additional spectrum to the SMA. These requests can be in an aggregated form exposed by a network to the SMA (collective required spectrum from all cells) or cell-specific real-time requests. As individual cells are also characterized by the specific radio access technology, the spectrum requests must be a composite data structure specifying, among others, the required granularity in time and frequency domains. The full set of information that a spectrum request must constitute can be pre-determined per policy or requirements of SMA algorithms. The 5G-EmPOWER platform also facilitates this requirement.

6. **Spectrum Quality**: The quality of the shared resource is directly proportional to the effective value of the spectrum to a candidate buyer in terms of the amount of data that can be transmitted using that additional resource. This is particularly important in the multi-tenancy/RAN sharing context where the observed parameters such as RSSI, channel quality indicator CQI etc., in one slice may also be valid for other slices in the same cell. The quality of the spectrum/shared resource can be expressed with the existing technology specific parameters e.g, CQI or be aggregated over pre-defined time intervals into some composite parameter. The 5G-EmPOWER platform provides this possibility.

7. **Network Roles/Priority**: Many spectrum sharing models associate different roles with the involved networks which in turn may dictate the spectrum sharing decisions taken by the SMA. For example, in some sharing models, the concept of primary and secondary networks are kept and associated priorities are different for each role. The SMA must take these network roles and priorities into consideration for example, with requests for additional spectrum needs. In 5G-EmPOWER, these roles/priorities can be expressed in associating different labels/classes to the networks/slices managed under the COHERENT control architecture.

8. **Location Information**: Spectrum sharing may be restricted to certain segments of the involved network for many reasons. At a higher abstraction, the applicable policy or regulations may enforce the SMA to consider spectrum sharing only in certain geographical parameters and therefore, the network must expose spectrum information within those geographical parameters. At more granular level, the offered resource may exist in a small network segment e.g., a specific small cell and therefore its location must be identifiable from the rest of the network to consider allocation within that proximity. The location information can be maintained with actual coordinates or with network-specific identifiers such as cell-Ids.

8.2. Spectrum trials

Poznan pilot network consists of three different networks, which share the same frequency range in time, frequency, and space. The networks are: Night-time (NT) primary point-to-multipoint network serving consumers, Day-time (DT) primary point-to-point network serving business customers, and Opportunistic secondary network taking the advantage of unused spectrum resources, see Figure 60. Night-time and day-time primary networks are managed by independent network management systems. Opportunistic secondary networks are independent single base station networks, which operate as Citizen's Broadband Radio Service (CBRS) General Authorized Access (GAA) users. The network management system of the primary networks and the base stations, which are called CBRS Devices (CBSD) a CBRS system, are connected to spectrum management system.

Spectrum management system controls the centre frequencies and bandwidths of Night-Time and Day-Time primary networks so that the Night-time network has a wider bandwidth in the evening and during the night, and the Day-time network has a wider bandwidth during the day time. The transitions between the settings are pre-programmed in the spectrum management system, and triggered by the system clock. The opportunistic secondary network requests from the Spectrum management a possibility for radio transmission in its location. When the propagation model estimates and measurements from the primary networks allow, Spectrum management system allows the secondary network transmission. A spectrum domain of sharing can be found in Figure 61.

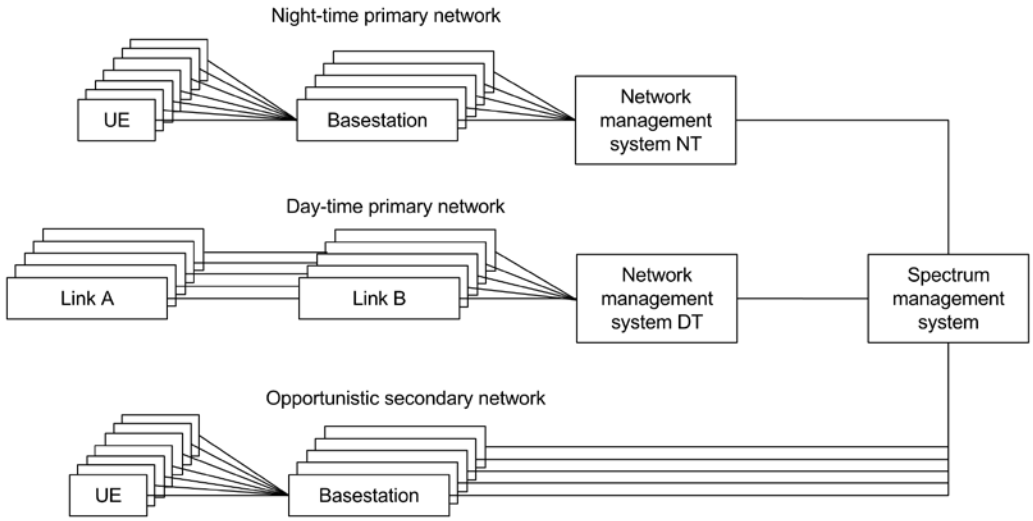

Figure 60. Network setup in Poznan spectrum sharing trial

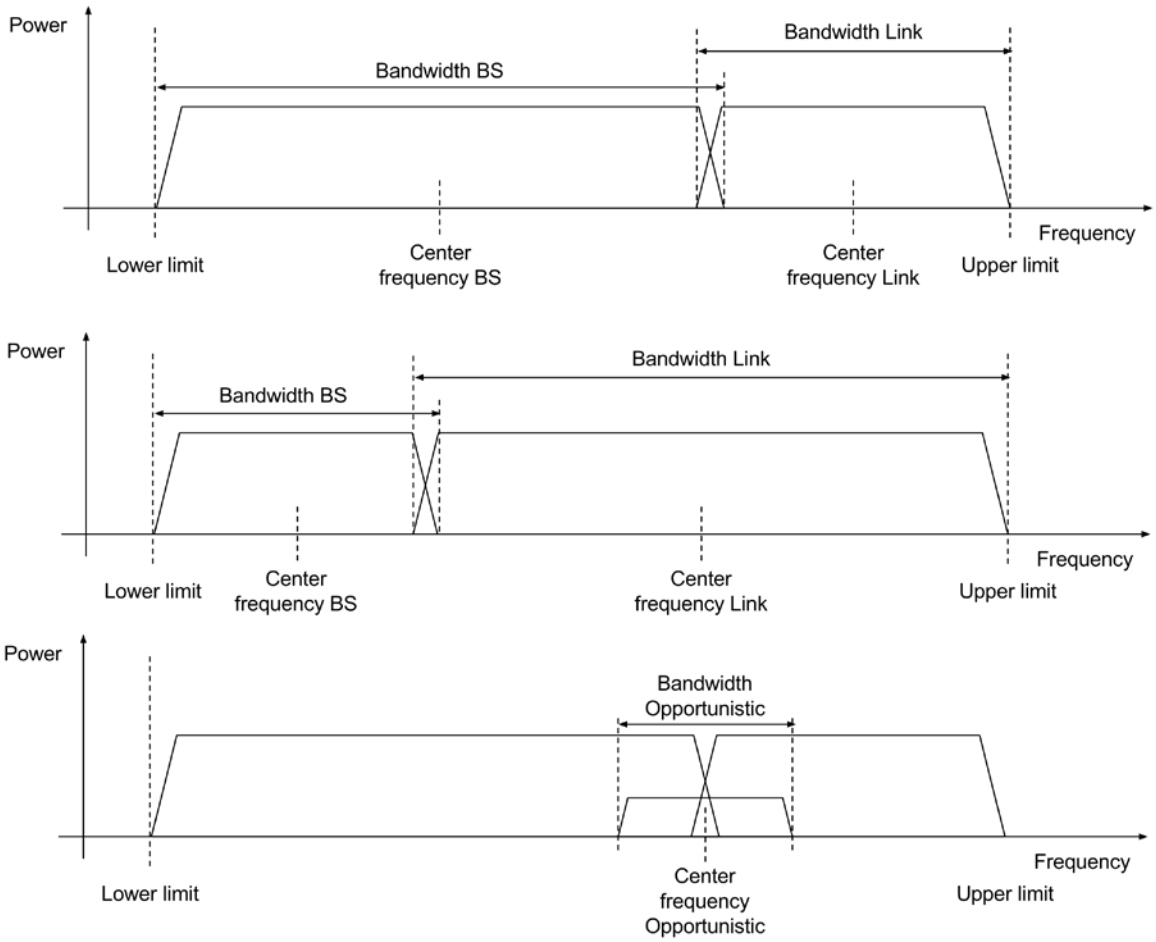

Figure 61. Frequency domain illustration of Poznan trial

Network management systems of the Night-time and Day-time primary networks act as SNMP servers. Spectrum management system has a SNMP client, which has rights to read and write to SNMP MIBs of the network management systems. The network management system contains the information of all base stations and links. The write operations are used to change the centre frequency, and bandwidth of the primary networks and to execute the changes. The read functions are for the current settings of centre frequency, bandwidth, and performance measurements including for example, bitrate and CNIR.

The control protocol between Spectrum management system and opportunistic network is SAS-CBSD protocol specified in WINNF-16-S-0016, see Figure 62. For spectrum management tasks, the system uses registration, spectrumInquiry, grant, and heartbeat procedures. The spectrum management combines the propagation model estimates and performance measurements from the primary networks for controlling the transmissions of the opportunistic networks.

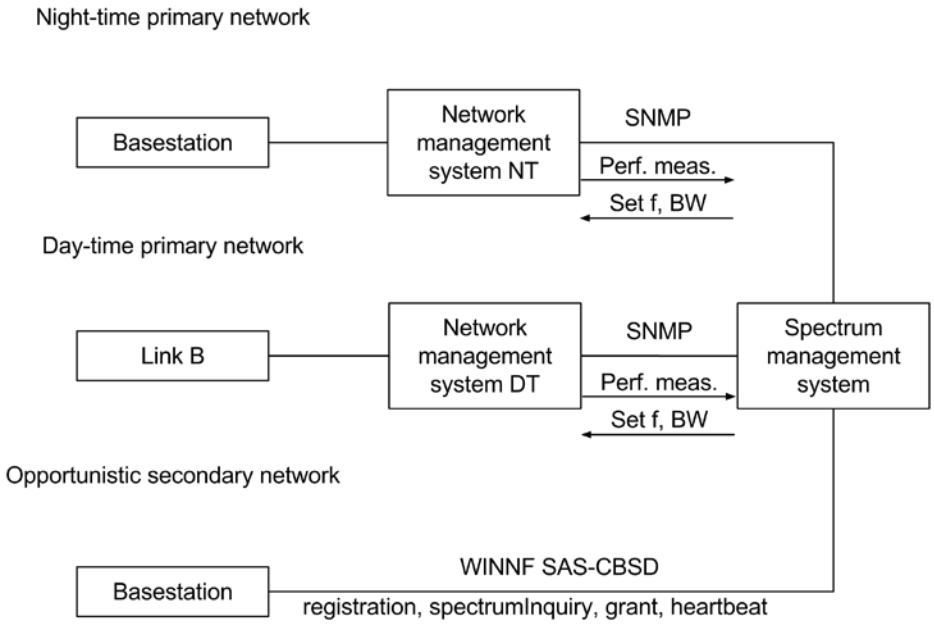

Figure 62. Spectrum management control plane in Poznan trial

8.2.1. Considered Scenario

In practice the sharing scheme described above is exemplified to the one shown graphically in Figure 63. There are two business networks operating in the 3.6-3.8 GHz band, mainly the WiMAX system and the point-to-point microwave line. The WiMAX base station and the associated CPEs are illustrated here in form of black circles, whereas the transceivers of the microwave links are presented in form of white squares. These two business systems correspond to the highest tiers of the CBRS model. The lowers priority users (GAA users constituting the lowest layer), are denoted graphically as white base stations.

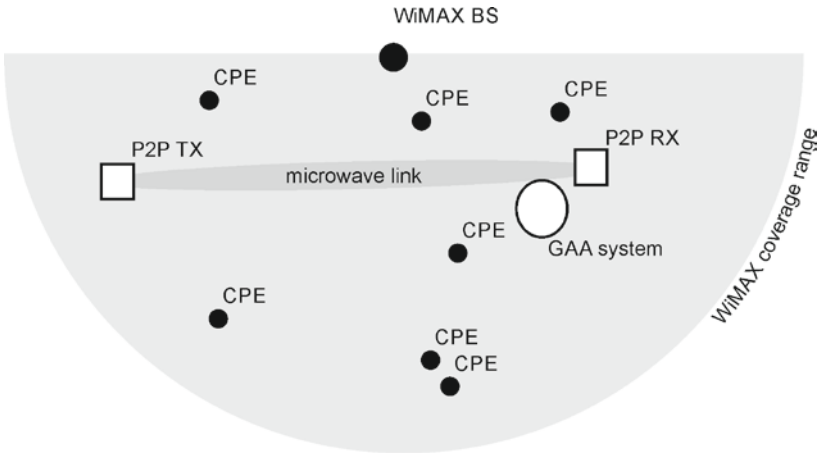

Figure 63. Considered scenario of the planned experiment

8.2.2. Database Structure

The spectrum management system consists of a database, protocol implementation, and logic software. The protocol to communicate with WiMAX and Microwave Link Network Management systems is SNMP in a Virtual Private Network (VPN) tunnel. The spectrum management system acts as a SNMP client. The information obtained from the devices using SNMP is stored in a Structured Query Language (SQL) database. The logic has a time-based control to change the center frequency and bandwidth allocation for WiMAX and Microwave links, so that Microwave links have more spectrum resources during the office hours and WiMAX at the other times. The spectrum management system communicates with General Authorized Access (GAA) Citizens Broadband radio Service Devices (CBSD) using the Wireless Innovation Forum (WInnF) SAS-CBSD protocol. The spectrum management system is the server in SAS-CBSD protocol communication and supports Registration, Spectrum Inquiry, Grant, and Heartbeat procedures. The performance measurements, especially uplink and downlink Carrier to Interference and Noise Ratio (CINR), carried out by WiMAX and Microwave links and communicated to the spectrum management system with SNMP are used to control the power levels of the GAA devices. If the performance decreases in the WiMAX or Microwave links, the spectrum management system decreases the maximum allowed power level of the relevant GAA devices using the SAS-CBSD protocol. The functional architecture of the spectrum management system can be found in Figure 64.The detailed version of the logic applied in the database for controlling third-tier of users is shown in [Kliks_2017_2].

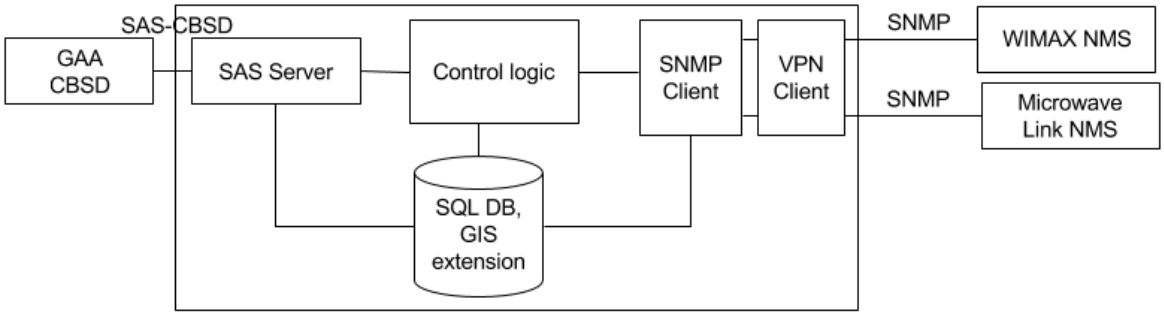

Figure 64. Structure of Spectrum Management System database

At the same time the GAA subsystem, i.e., USRP device in our case, applies the following algorithm for accessing the spectrum:

1. First, the GAA transmitter sends the registration request (following the implemented CBRS protocol), where it asks for registration in the whole system. As a response it receives a dedicated device identification number. The coordinates of the devices are also delivered to the system.

2. After registration, the GAA subsystem inquires the database for a set of parameters defining its transmit opportunities (like maximum EIRP value) for a list of selected subbands, e.g., it may ask for these sets of parameters for three 2 MHz wide frequency subbands with center frequency of 3.64 GHz, 3.70 GHz and 3.75 GHz. As a response the GAA subsystem receives the limits of the allowed parameters.

3. The GAA transmitter sends the request for granting transmission by the controller at the database side, where the proposed transmit parameters are defined. The controller either grants the transmission with the proposed parameters (see Step 5 then), or blocks the request (see Step 4).

4. If the GAA device does not receive a positive grant response, it may either modify the transmit parameters (e.g., proposed transmit power) in the considered frequency band or switch to other band of interest. In both cases the new grant request is sent to the database with new set of parameters.

5. The device will start transmission (please note that until now there was no wireless activity in the GAA subsystem, as the communication with remote database was guaranteed via external control channel). After agreed transmission time, the device will analyze the so-called heartbeat response, where the database informs if the transmission can be continued (then repeat Step 5) or the transmission has to be stopped (then the algorithm goes back to Step 3)

6. Once the device has no data to send it will deregister from the system, releasing the device identification number. The algorithm presented above is fully adaptive and tries to maximize the rate of the GAA link in the transmission regime defined by the database.

8.2.3. Field Tests

Extensive laboratory and field tests have been carried out to verify the efficiency of the proposed theoretical model (an outcome of WP4, which will be showed in WP6 as the result of the conducted experiment). Their main idea was to apply the dynamic spectrum access schemes described above in a fully automated scheme in real life. In Figure 65 we show the exemplary screen shot from the R&S FSL6 spectrum analyser, where the spectrum of the WiMAX and RADWIN links (middle spectra) are visible jointly with the two signals generated by the GAA devices following the rules defined by the database. The transmit parameters (such as centre frequency of the GAA devices and their transmit power), as well as the current location of WiMAX and RADWIN have been monitored and managed by the dedicated C3 and SMA entity, respectively. The entire management process took into account the requirements, defined by the network operator, regarding the performance of each type of the transmission. In all cases, this Dynamic Spectrum Access scheme worked correctly guaranteeing the fulfilment of all necessary requirements.

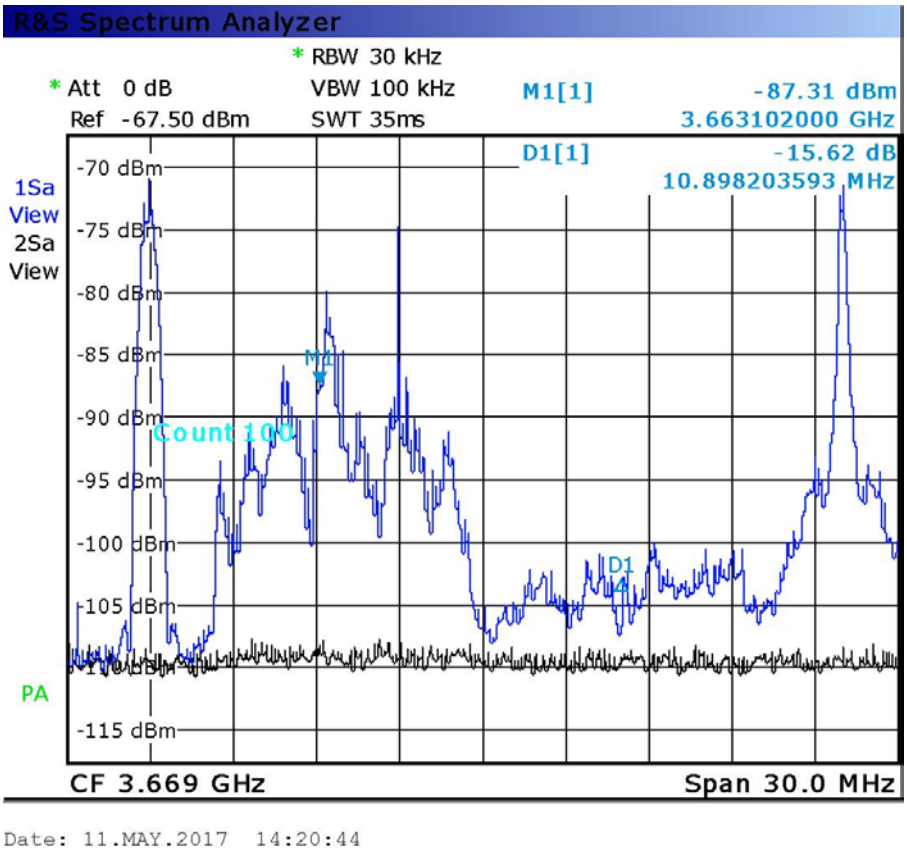

Figure 65. Screen shot from the Rohde&Schwarz FSL6 spectrum analyser

8.2.4. Relation to C3

Finally, let us briefly analyze the whole field trials from the perspective of COHERENT architecture. In this case, the role of the SMA and the central coordinator has been played by dedicated software

associated with the advanced databases (located in Finland). The distributed scheme has been applied, meaning that some intelligence of SMA (used for spectrum reasoning and negotiating) has been implemented on the network side guaranteeing fast access to the set of repositories The goal of the SMA at the network side was to analyze requirements related to the WiMAX and RADWIN part, and to provide the guidelines in order to allow efficient spectrum access. On the second side, the SMA module (i.e., the SMA agent) has been instantiated in the small-cell transmitter, and its role was to negotiate the new transmit opportunities with the SMA instance from the network domain. Once these are agreed, the logically central controller monitors the true execution of these rules.

9. Summary

The whole WP4 within the COHERENT project was focused on development of new solutions for flexible spectrum sharing and management, particularly considering their application in fully virtualized wireless networks. Practical realization of the virtualization concept in the context of radio access networks has to take into account various limitations and restrictions originated from the spectrum management domain. As the key target of Work Package 4 was to concentrate the work around the "spectrum utilization in a virtualized scenario", other aims defined in this project pointed the need for development of new spectrum sharing paradigms for future wireless networks. These interesting research problems have been analyzed within three tasks, where dynamic spectrum aspects, spectrum sharing and management have been discussed with reference to intra- and inter-operator spectrum sharing as well as to so-called small-scale scenarios. This logical spit resulted in significant achievements, which constitute the main outcomes of this Work Package, and are called pillars. These are briefly characterized below:

- The first key outcome is the proposal of the solid architecture for the flexible spectrum management, which was analyzed in details with the reference to the wireless network virtualization. Being a part of entire COHERENT architecture, this solution allows for effective representation of various transmit policies in form of annotated network graph. All of the key existing spectrum sharing schemes have been mapped to this architecture. In that respect, WP4 contributed to WP2 and WP3, and it also took into consideration the findings in those respective Work Packages.

- The second outcome is strictly related to the development of dedicated SDKs, being at the same time contribution towards WP5 and partially to WP6. In particular, set of simulation tools, functions and methods (just to mention some of them) have been developed by COHERENT partners, allowing for efficient simulation of spectrum sharing solutions in various aspects. Dedicated implementations have been made on both hardware platforms, i.e., the EmPOWER and OpenAirInterface. The developed SDKs are part of the WP6 demonstrator, where the ways for spectrum management in virtualized networks is considered for presentation.

- The third pillar is constituted by numerous achievements being the results of the work of the WP4 partners in all three tasks. Various research topics have been investigated in the project lifetime, including inter-tier resource allocation in heterogeneous networks, scheduling aspects of multi-tenant radio access network, coexistence between LTE and Wi-Fi networks, location-based spectrum sharing, FDD flexible duplexing, and multi-user small scale spectrum aggregation. All of these outcomes provide new solutions towards better resource utilization in next generations of wireless communication systems.

- Finally, the last pillar is built upon the spectrum trials done in Poland, being the practical, real-time and area-wide verification of the dynamic spectrum access concept, where the proposed architecture for spectrum management has been applied. In particular, two existing legacy networks have been dynamically managed by the Spectrum Management Application module (realized in a distributed manner) and controlled by the centralized controlling entity. In addition to this, the third network was subject to deployment in this scenario. Field-test trials have proved the correctness of such approach.

All of the results mentioned above have been discussed in this final summary report of WP4. Taking into account all of these aspects we claim that main WP4 objectives have been achieved.

References

[3GPP TR32.855] 3GPP TR 32.855, Study on OAM support for Licensed Shared Access (LSA), V14.0.0 (2016-03).

[802_11n_2009] "Part 11: Wireless LAN Medium Access Control (MAC) and Physical Layer (PHY) Specifications, Amendment 5: Enhancements for Higher Throughput," IEEE Standard for Information Technology – Telecommunications and Information Exchange between Systems – Local and metropolitan Area networks, 2009.

[3GPP_2014] 3GPP: TS 36.104 V12.5.0 (2014-09) - Technical Specification Group Radio Access Network; Evolved Universal Terrestrial Radio Access (E-UTRA): base station (BS) radio transmission and reception (release 12) (2014). 3GPP

[Amiri_2007] K. Amiri et al. WARP, a Unified Wireless Network Testbed for Education and Research. In Proceedings of IEEE MSE, 2007.

[Andras_2017] Andras Varga, "OMNeT++: Discrete Events Simulator" Online: http://omnetpp.org: Accessed: July 9th, (2017)

[Andrews_2011] J. G. Andrews, F. Baccelli and R. K. Ganti, "A Tractable Approach to Coverage and Rate in Cellular Networks," IEEE Transactions on Communications, vol. 29, n0. 11, pp. 3122 - 3134, November 2011.

[Atapattu_2011] S. Atapattu, C. Tellembura, H. Jiang, "Energy Detection Based Cooperative Spectrum Sensing in Cognitive Radio networks," IEEE Transactions on Wireless Communications, vol. 10, no. 4, April 2011.

[Bogucka_2015] H Bogucka, P Kryszkiewicz, A Kliks, "Dynamic spectrum aggregation for future 5G communications", IEEE Commun. Mag. 53(5), 35–43, 2015

[CEPT 56] CEPT Report 56, Technological and regulatory options facilitating sharing between Wireless broadband applications (WBB) and the relevant incumbent services/applications in the 2.3 GHz band, March 2015.

[CEPT 58] CEPT Report 58, Technical sharing solutions for the shared use of the 2300-2400 MHz band for WBB and PMSE, July 2015.

[CISCO_2016] CISCO: The Mobile Economy, whitepaper, GSMA, (2016) https://www.gsma.com/mobileeconomy/archive/GSMA_ME_2016.pdf

[COHERENT_D22] COHERENT, "System Architecture and Abstractions for Mobile Networks", Deliverable D2.2 within H2020 COHERENT project (Coordinated Control and Spectrum Management for 5G Heterogeneous Radio Access Networks), Grant Agreement No. : 671639, Call: H2020-ICT-2014-2

[COHERENT_D31] COHERENT, "First report on physical and MAC layer modelling and abstraction", Deliverable D3.1 within H2020 COHERENT project (Coordinated Control and Spectrum Management for 5G Heterogeneous Radio Access Networks), Grant Agreement No. : 671639, Call: H2020-ICT-2014-2

[COHERENT_D32] COHERENT, "Final report on Physical and MAC layer modelling and abstraction", Deliverable D3.2 within H2020 COHERENT project

(Coordinated Control and Spectrum Management for 5G Heterogeneous Radio Access Networks), Grant Agreement No. : 671639, Call: H2020-ICT-2014-2

[COHERENT_D41] COHERENT, "Report on enhanced LSA, intra-operator spectrum-sharing and micro-area spectrum sharing", Deliverable D4.1 within H2020 COHERENT project (Coordinated Control and Spectrum Management for 5G Heterogeneous Radio Access Networks), Grant Agreement No. : 671639, Call: H2020-ICT-2014-2

[COHERENT_D61] COHERENT, "Draft report on technical validation", Deliverable D6.1 within H2020 COHERENT project (Coordinated Control and Spectrum Management for 5G Heterogeneous Radio Access Networks), Grant Agreement No. : 671639, Call: H2020-ICT-2014-2

[COM(2016) 588] Communication from the Commission to the European Parliament, the Council, the European Economic and Social Committee and the Committee of the Regions: "5G for Europe: An Action Plan". COM(2016) 588. Brussels, 14.9.2016

[Dai_2012] Z. Dai, J. Liu and K. Long, "Improved Energy Detection with Interference Cancellation in heterogeneous Cognitive Wireless Networks," in proc. of the IEEE Global Communications Conference (Globecom), December 2012.

[Davies_1973] R. B. Davies, "Numerical Inversion of a Characteristic Function," Biometrika, vol. 60, no. 2, pp. 415-417, 1973.

[Digham_2007] F. F. Digham, M.-S. Alouini and M. K. Simon, "On the Energy Detection of Unknown Signals Over Fading Channels," IEEE Transactions on Communications, vol. 55, no. 1, pp. 21-24, January 2007.

[DigitalEurope] DigitalEurope. 5G Spectrum options for Europe. October 2017. Available at: http://www.digitaleurope.org/DesktopModules/Bring2mind/DMX/Download.aspx?EntryId=2534

[EC_2012] Standardisation Mandate to CEN, CENELEC and ETSI for Recon-figurable Radio Systems. European Commission, M/512, 2012.

[EC_2014] Mandate to CEPT to develop harmonised technical conditions for the 2300-2400MHz ('2.3GHz') frequency band in the EU for the provision of wireless broadband electronic communication services. European Commission, DG CONNECT/B4, 2014.

[EC_2015] A Digital single market strategy for Europe. Communication from the Commission to the European Parliament, the Council, the European Economic and Social Committee and the Committee of the Regions, European Commission. COM(2015) 192 final, 2015.

[EC_2016] 5G action plan from EC. Communication from the Commission to the European Parliament, the Council, the European Economic and Social Committee and the Committee of the Regions. European Commission. COM(2016) 588 final, 2016.

[EC_2016_2] Mandate to CEPT to develop harmonised technical conditions for spectrum use in support of the introduction of next-generation (5G) terrestrial wireless systems in the Union, European Commission. RSCOM16-40rev3, 2016.

[EC_2016_3] Communication from the Commission to the Parliament, the Council, the European Economic and Social Committee and the Committee of the Regions.

Connectivity for a Competitive Digital Single Market - Towards a European Gigabit Society. European Commission. COM (2016) 587 final, 2016.

[ECC_2014] Harmonised frequency arrangements for mobile/fixed communications networks (MFCN) operating in the bands 3400-3600 MHz and 3600-3800 MHz. Electronic Communications Committee, ECC Decision (11)06, 2014.

[ECC/DEC/(15)01] ECC/DEC/(15)01. Harmonised technical conditions for mobile/fixed communications networks (MFCN) in the band 694-790 MHz including a paired frequency arrangement. Implementation. Available at: http://www.ecodocdb.dk/doks/implement_doc_adm.aspx?docid=2651

[ElSawy_2016] H. Elsawy, A. Sultan-Salem, M.-S. Alouini and M. Z. Win, "Modeling and Analysis of Cellular Networks Using Stochastic Geometry: A Tutorial," IEEE Communications Surveys & Tutorials, vol. 19, no. 1, pp. 167-203, First Quarter 2017.

[ETSI TR 103 113] Electromagnetic compatibility and Radio spectrum Matters (ERM); System Reference document (SRdoc); Mobile broadband services in the 2 300 MHz – 2 400 MHz frequency band under Licensed Shared Access regime, V1.1.1 (2013- 07).

[ETSI TS 103 379] Reconfigurable Radio Systems (RRS); Information elements and protocols for the interface between LSA Controller (LC) and LSA Repository (LR) for operation of Licensed Shared Access (LSA) in the 2300 MHz-2400 MHz band, ETSI TS 103 379, V0.0.5 (2016-03).

[EU/2014/276] Commission Implementing Decision of 2 May 2014 on amending Decision 2008/411/EC on the harmonisation of the 3400 – 3800 MHz frequency band for terrestrial systems capable of providing electronic communications services in the Community (notified under document C(2014) 2798). Available at: http://eur-lex.europa.eu/legal-content/EN/TXT/PDF/?uri=CELEX:32014D0276&from=EN

[EU_2012] Decision No 243/2012/EU of the European Parliament and of the Council of 14 March 2012 establishing a multiannual radio spectrum policy programme. Official Journal of the European Union.

[EU_2014] Directive 2014/53/EU of the European Parliament and of the Council of 16 April 2014 on the harmonisation of the laws of the Member States relating to the making available on the market of radio equipment and repealing Directive 1999/5/EC. 2014/53/EU.

[FCC_2002] Federal Communications Commission Spectrum Policy Task Force, "FCC report of the spectrum efficiency working group," November 15, 2002.

[FCC 2012] In the Matter of Expanding the Economic and Innovation Opportunities of Spectrum Through Incentive Auctions. Federal Communications Commission, FCC 12-118, 2012.

[FCC_2016] Amendment of the Commission's Rules with Regard to Commercial Operations in the 3550-3650 MHz Band, Order of Reconsiderations and Second Report and Order. Federal Communications Commission, FCC-16-55, 2016.

[Fette_2009] B. A. Fette, ``Cognitive Radio Technology", 2nd Ed. Elsevier Press 2009

[Giorgetti_2005] A. Giorgetti and D. Dardari, "The Impact of OFDM Interference on TH-PPM/BPAM Transmission Systems," in proc. of the IEEE 61st Vehicular Technology Conference (VTC 2005-Spring), June 2005.

[Haenggi_2009] M. Haenggi, G. Andrews, F. Baccelli, O. Dousse and M. Franceschetti, "Stochastic geometry and random graphs for the Analysis and Design of Wireless Networks," IEEE Journal on Selected Areas in Communications, vol. 27, no. 7, August 2009.

[Huawei_2014] Huawei, HiSilicon, China Telecom, Unicom, and CATR, "Motivation of new SI proposal: Evolving LTE with flexible duplex for traffic adaptation," Tech. Rep. 3GPP TSG-RAN 63 RP-140426, 2014.

[IEEE 1900.5] IEEE Std 1900.5™-2011, IEEE Standard for Policy Language Requirements and System Architectures for Dynamic Spectrum Access Systems.

[IETF RFC 6953] A. Mancuso, Ed., Protocol to Access White-Space (PAWS) Databases: Use Cases and Requirements, IETF RFC 6953, May 2013.

[IETF RFC 7545] V. Chen, Ed., Protocol to Access White-Space (PAWS) Databases, IETF RFC 7545, May 2015.

[INET_2017] INET-Framework: An open-source OMNeT++ model suite for wired, wireless and mobile networks" Online: https://inet.omnetpp.org/ Accessed: July 9th, (2017)

[ITU-R M.2135] ITU, "ITU-R M.2135 (2009). guidelines for evaluation of radio interface technologies for IMT-advanced," ITU-R, 2009. Available: http://www.itu.int/pub/R-REP-M.2135

[ITU-R RR16] ITU-R Radio Regulations, No. 119-16, Geneva, 15 July 2016.

[ITU-R WRC-19] ITU-R Preparatory studies for WRC-19. Available at: http://www.itu.int/en/ITU-R/study-groups/rcpm/Pages/wrc-19-studies.aspx

[ITU-R_2011] Introduction to cognitive radio systems in the land mobile service. Report ITU-R M.2225. International Telecommunications Union Radiocommunication sector, 2011.

[ITU-R_2011_2] Cognitive radio systems specific for International Mobile Telecommunications systems. Report ITU-R M.2242. International Telecommunications Union Radiocommunication sector, 2011.

[ITU-R_2012] Studies on the implementation and use of cognitive radio systems. ITU-R Resolution 58. International Telecommunications Union Radiocommunication sector, 2012.

[ITU-R_2014] Cognitive radio systems in the land mobile service. Report ITU-R M.2330. International Telecommunications Union Radiocommunication sector, 2014.

[ITU-R_2015] Studies on frequency-related matters for International Mobile Telecommunications identification including possible additional allocations to the mobile services on a primary basis in portion(s) of the frequency range between 24.25 and 86 GHz for the future development of International Mobile Telecommunications for 2020 and beyond. ITU-R Resolution 238. International Telecommunications Union Radiocommunication sector, 2015.

[ITU-R_2015_2] Railway radiocommunication systems between train and trackside. ITU-R Resolution 236. International Telecommunications Union Radiocommunication sector, 2015.

[ITU-R_2015_3] Intelligent Transport Systems applications. ITU-R Resolution 237. International Telecommunications Union Radiocommunication sector, 2015.

[ITU-R_2015_4] Urgent studies required in preparation for the 2019 World Radiocommunication Conference. ITU-R Resolution 958. International Telecommunications Union Radiocommunication sector, 2015.

[ITU-R_2015_5] Studies concerning Wireless Access Systems including radio local area networks in the frequency bands between 5 150 MHz and 5 925 MHz. ITU-R Resolution 239. International Telecommunications Union Radiocommunication sector, 2015.

[ITU-R_2015_6] Alternative methods of national spectrum management. ITU-R Question 208-1/1. International Telecommunications Union Radiocommunication sector, 2015.

[ITU-R_2017] Regulatory tools to support enhanced shared use of the spectrum. Report SM.2404. International Telecommunications Union Radiocommunication sector, 2017.

[ITU-R_2017_2] Spectrum management principles, challenges and issues related to dynamic access to frequency bands by means of radio systems employing cognitive capabilities. Report SM.2405. International Telecommunications Union Radiocommunication sector, 2017.

[JRC 5G] European Commission. Montenegro Villacieros Belen. JRC Technical Reports. Implications of WRC-15 on spectrum and 5G. 2016. Available at http://publications.jrc.ec.europa.eu/repository/bitstream/JRC102401/jrc102401_jrc%20technical%20report%20-deliverable_i_5g_fv-6.pdf

[Khan_2017] S. N. Khan, A. Kliks, Tao Chen, M. Mustonen, R. Riggio and L. Goratti, "Virtualization of spectrum resources for 5G networks," 2017 European Conference on Networks and Communications (EuCNC), Oulu, 2017, pp. 1-5.

[Kliks_2016] A. Kliks, L. Goratti, T. Chen, “REM: Revisiting a Cognitive Tool for Virtualized 5G Networks”, in *23rd International Conference on Telecommunications (ICT)*, 16-18 May 2016, Thessaloniki, Greece

[Kliks_2016_2] A. Kliks and P. Kryszkiewicz, “Simultaneous uplink and downlink transmission scheme for flexible duplexing,” in proc. 11th International Conference Cognitive Radio Oriented Wireless Networks, CROWNCOM 2016, Grenoble, France, May 30 - June 1, 2016, Proceedings, D. Noguet, K. Moessner, and J. Palicot, Eds. Springer International Publishing, 2016, pp. 192–203.

[Kliks_2016_3] A. Kliks, B. Bossy, S. N. Khan, R. Riggio and L. Goratti, "An architecture for spectrum management and coordinated control in 5G heterogeneous networks," 2016 International Symposium on Wireless Communication Systems (ISWCS), Poznan, 2016, pp. 648-652.

[Kliks_2017] A. Kliks, P. Kryszkiewicz, “Multichannel simultaneous uplink and downlink transmission scheme for flexible duplexing”, EURASIP Journal on Wireless Communications and Networking, December 2017, 2017:111, Open-access: https://link.springer.com/article/10.1186/s13638-017-0884-5

[Kliks_2017_2] A. Kliks, P. Kryszkiewicz, Ł. Kulacz, K. Kowalik, M. Kołodziejski, H. Kokkinen, J. Ojaniemi, A. Kivinen, “Application of the CBRS model for wireless systems coexistence in 3.6-3.8 GHz band”, in proc. of 12th International Conference Cognitive Radio Oriented Wireless Networks, CROWNCOM 2017, Lisbon, Portugal, September 20–21, 2017

[Kryszkiewicz_2013] P Kryszkiewicz, H Bogucka, “Out-of-band power reduction in NC-OFDM with optimized cancellation carriers selection”. IEEE Commun. Lett. 17(10), 1901–1904, 2013

[Kryszkiewicz_2016] P Kryszkiewicz, A Kliks, H Bogucka, “Small-scale spectrum aggregation and sharing”, IEEE J. Sel. Areas Commun. 34(10), 2630–2641, 2016

[Kryszkiewicz_2017] P. Kryszkiewicz, A. Kliks and H. Bogucka, "Multi-user small-scale spectrum aggregation," 2017 IEEE International Conference on Communications (ICC), Paris, 2017, pp. 1-6., doi: 10.1109/ICC.2017.7997226

[Kwon_2016] H-J Kwon et al., “Licensed-Assisted Access to Unlicensed Spectrum in LTE Release 13,” IEEE Communications Magazine, vol. 55, no. 2, pp. 201-207, Dec. 2016

[LG_2014] LG Electronics and IAESI, “Discussion on dynamic traffic adaptation for LTE FDD system,” Tech. Rep. 3GPP TSG-RAN 63 RP-140414, 2014.

[LG_2014_2] LG Electronics, “Discussion on flexible resource utilization for LTE FDD system,” Tech. Rep. 3GPP TSG-RAN 64 RP-140757, 2014.

[Lembo_2017] S. Lembo, O. Tirkkonen, M. Goldhamer, and A. Kliks, “Coexistence of FDD flexible duplexing networks,” in European Conf. on Networks and Comm. (EuCNC), Jun. 2017, pp. 1–6.

[Lembo_2017b] S. Lembo, “Functions and Abstractions for Radio Access Network Softwarization”, Ph.D. thesis, Aalto University, Nov. 2017.

[Lembo_2017c] S. Lembo, Sergio Lembo, Alexis A. Dowhuszko, Olav Tirkkonen, “Network Functions for Inter Cell Interference Coordination in Heterogeneous Networks”, submitted to IEEE/ACM Transactions on Networking, 2017.

[Lembo_2017d] S. Lembo, Olav Tirkkonen, “Interference analysis for FDD Flexible Duplexing Networks”, submitted to IEEE Trans. Vehic. Techn, 2017.

[Liang_2015_1] C. Liang, F. R. Yu and X. Zhang, “Information-centric network function virtualization over 5g mobile wireless networks”, *IEEE Network*, vol. 29, no. 3, pp. 68-74, May-June 2015, doi: 10.1109/MNET.2015.7113228

[Liang_2015_2] C. Liang and F. R. Yu, "Wireless Network Virtualization: A Survey, Some Research Issues and Challenges," in *IEEE Communications Surveys & Tutorials*, vol. 17, no. 1, pp. 358-380, First Quarter 2015, doi: 10.1109/COMST.2014.2352118

[Liu_2008] E. Liu, and K. K. Leung. "Proportional fair scheduling: Analytical insight under rayleigh fading environment." *Wireless Communications and Networking Conference, 2008. WCNC 2008. IEEE*. IEEE, 2008.

[MET_DEL] METIS-II, “Enablers to secure sufficient access to adequate spectrum for 5G”, Deliverable D3.2, 30 June 2017, EU project: *Mobile and wireless communications Enablers for the Twenty-twenty Information Society-II*, contract no: 671680 https://metis-ii.5g-ppp.eu/wp-content/uploads/deliverables/METIS-II_D3.2_V1.0.pdf

[Mohammad_2015] Mohammad S.O, Tuncer O., Janusz K., Joaquim F., “Simulation and Modeling Methodologies, Technologies and Applications” Springer International Publishing Switzerland 2015

[Monserrat _2015] J. F Monserrat, G. Mange, V. Braun, H. Tullberg, G. Zimmermann and Ö. Bulakci, “METIS research advances towards the 5G mobile and wireless system definition”, in *EURASIP Journal on Wireless Communications and Networking* 2015, 2015:53, DOI: 10.1186/s13638-015-0302-9, 10 March 2015

[Mustonen_2014] M. Mustonen, M. Matinmikko, D. Roberson and S. Yrjola, ``Evaluation of recent spectrum sharing models from the regulatory point of view," 1st International Conference on 5G for Ubiquitous Connectivity, Akaslompolo, 2014, pp. 11-16

[Nikaein_2014] N. Nikaein, R. Knopp, F. Kaltenberger, L. Gauthier, C. Bonnet, D. Nussbaum, and R. Ghaddab. Demo: OpenAirInterface: an open LTE network in a PC. In MOBICOM 2014, 20th Annual International Conference on Mobile Computing and Networking, 2014.

[Nikaein_2014_2] N. Nikaein, M. Marina, S. Manickam, A. Dawson, R. Knopp, and C. Bonnet. Openairinterface: A flexible platform for 5G research. ACM Sigcomm Computer Communication Review, 2014

[OAI_2017] The OpenAirInterface Initiative. http://www.openairinterface.org/

[Ofcom 5G] Ofcom Statement. Update on 5G spectrum in the UK. Feb 8, 2017. Available at: https://www.ofcom.org.uk/__data/assets/pdf_file/0021/97023/5G-update-08022017.pdf.

[Pirinen_2015] P. Pirinen, "Challenges and possibilities for flexible duplexing in 5G networks," in Computer Aided Modelling and Design of Communication Links and Networks (CAMAD), 2015 IEEE 20th International Workshop on, Sept. 2015, pp. 6–10.

[Rabbachin_2007] A. Rabbachin, T. Q. S. Quek, P. C. Pinto, I. Oppermann and M. Z. Win, "UWB Energy Detection in the Presence of Multiple Narrowband Interferers," in proc. of the IEEE International Conference on Ultra-Wideband (ICUWB 2007), September 2007.

[Rabbachin_2011] A. Rababchin, T. Q. S. Quek, S. Hyundong and M. Z. Win, "Cognitive Network Interference," IEEE Journal on Selected Areas in Communications, vol. 29, no. 2, pp. 480-493, Feb. 2011.

[RSPG_2011] Final RSPG Report on Cognitive Technologies. European Commission, Radio Spectrum Policy Group. RSPG10-348.

[RSPG_2011_2] Report on Collective Use of Spectrum (CUS) and other spectrum sharing approaches. European Commission, Radio Spectrum Policy Group. RSPG11-392.

[RSPG_2013] RSPG Opinion on Licensed Shared Access. European Commission, Radio Spectrum Policy Group. RSPG13-538.

[RSPG_2016] Strategic roadmap towards 5G for Europe, Opinion on spectrum related aspects for next-generation wireless systems (5G). European Commission, Radio Spectrum Policy Group. RSPG16-032.

[RSPG_BEREC_2011] BEREC-RSPG report on infrastructure and spectrum sharing in mobile/wireless networks. Body of European Regulators for Electronic Communications & European Commission, Radio Spectrum Policy Group. BoR (11)16, RSPG11-374.

[Stine_2015] J. A. Stine and C. E. Caicedo Bastidas, Enabling Spectrum Sharing via Spectrum Consumption Models, in IEEE Journal on Selected Areas in Communications, vol. 33, no. 4, pp. 725-735, April 2015.

[Sewda_2017] B. Sewda, "Location-Specific spectrum sharing in Heterogeneous networks," M.S. thesis, Dept. Commn.Net., Aalto Univ., Espoo, Finland, 2017.

[Sesia_2011] S. Sesia, I. Toufik and M. Baker, "LTE The UMTS Long Term Evolution: From Theory to Practice," John Wiley & Sons, 2011.

[Singh_2015] B. Singh, et al. "Repeated spectrum sharing games in multi-operator heterogeneous networks." *Dynamic Spectrum Access Networks (DySPAN), 2015 IEEE International Symposium on*. IEEE, 2015.

[Singh_2015_2] B. Singh, et al. "Co-primary inter-operator spectrum sharing over a limited spectrum pool using repeated games." *Communications (ICC), 2015 IEEE International Conference on*. IEEE, 2015.

[Soh_2013] Y. S. Soh, T. Q. S. Quek, M. Kountouris, and G. Caire, “Cognitive hybrid division duplex for two-tier femtocell networks,” IEEE Transactions on Wireless Communications, vol. 12, no. 10, pp. 4852–4865, Oct. 2013.

[Stoyan_2008] D. Stoyan, W. S. Kendall and J. Mecke, “Stochastic geometry and its Applications,” John Wiley & Sons, Second Edition, 2008.

[Tan_2011] K. Tan et al. Sora: High-Performance Software Radio Using General-Purpose Multi-Core Processors. Communications of the ACM, 54(1):99–107, Jan 2011

[Teng_2014] Y. Teng, Y. Wang, and K. Horneman, “Co-primary spectrum sharing for denser networks in local area,” in Cognitive Radio Oriented Wireless Networks and Communications (CROWNCOM), 2014 9th International Conference on, pp. 120–124, IEEE, 2014.

[Wan_2013] L. Wan, M. Zhou, and R. Wen, “Evolving LTE with Flexible Duplex,” in 2013 IEEE Globecom Workshops (GC Wkshps), Dec 2013, pp. 49–54

[Win_2009] M. Z. Win, P. C. Pinto and L. A. Shepp, “A Mathematical Theory of Network Interference and its Applications,” Proceedings of the IEEE, Special Issue on Ultra-Wide bandwidth (UWB) technology & Emerging Applications, vol. 97, no. 2, pp. 205-2039, February 2009.

[Yang_2004] J. Yang, “Spatial channel characterization for cognitive radios, master’s thesis,”University of California, Berkeley, 2004.

[Yang_2016] C. Yang, J. Li, M. Guizani, A. Anpalagan and M. Elkashlan, "Advanced spectrum sharing in 5G cognitive heterogeneous networks," IEEE Wireless Communications, vol. 23, no.2, pp.94-101, 2016